Fundamentals of MICROFABRICATION

Marc Madou

CRC Press
Boca Raton New York

Development Editor: Marleen Madou
Publisher: Ron Powers
Project Editor: Paul Gottehrer
Prepress: Gary Bennett, Kevin Luong, Carlos Esser, Walt Cerny, Greg Cuciak
Cover design: Denise Craig

Library of Congress Cataloging-in-Publication Data

Madou, Marc J.
Fundamentals of microfabrication / Marc Madou.
p. cm.
Includes bibliographical references and index.
ISBN 0-8493-9451-1 (alk. paper)
1. Microelectronics—Design and construction. 2. Machining.
3. Microelectronic packaging. 4. Lasers—Industrial applications.
I. Title.
TK7836.M33 1997
621.3815'2—dc20 96-43344
CIP

International Standard Book Number 0-8493-9451-1
Library of Congress Card Number 96-43344
Printed in the United States of America 1 2 3 4 5 6 7 8 9 0
Printed on acid-free paper

Resist Stripping

Wet Stripping

Photoresist stripping means, in slightly oversimplified terms, organic polymer etching. The primary consideration is complete removal of the photoresist without damaging the device under construction. To place stripping in its proper context in a typical process flow we are recapping in Figure 1.22 some of the fundamental processes introduced so far.[23] For reasons of simplicity, baking steps of the photoresist are not detailed in this figure. An oxidized wafer (a) is first coated with a 1-μm thick photoresist coat (b). After exposure (c), the wafer is rinsed in a developing solution or sprayed with a spray developer, removing either the exposed areas (positive tone) or the unexposed areas of photoresist (negative tone), leaving a pattern of bare and photoresist-coated oxide on the wafer surface (d). The photoresist pattern is either the positive or negative image of the pattern on the photomask. In a typical next process step after the development, the wafer is placed in a solution of HF or HF + NH_4F, meant to attack the oxide but not the photoresist or the underlying silicon (e). The photoresist protects the oxide areas it covers. Once the exposed oxide has been etched away, the remaining photoresist can be stripped off with a strong acid such as H_2SO_4 or an acid-oxidant combination such as $H_2SO_4 - Cr_2O_3$ attacking the photoresist but not the oxide or the silicon (f). Other liquid strippers are organic solvent strippers and alkaline strippers (with or without oxidants). Acetone can be used if the postbake was not too long or happened at not too high a temperature. With a post-bake of 20 min at 120°C acetone is still fine. But with a post-bake at 140°C, the resist develops a tough 'skin' and has to be burned away in an oxygen plasma.

The oxidized Si wafer with the etched windows in the oxide (f) now awaits further processing. This might entail a wet anisotropic etch of the Si in the oxide windows with SiO_2 as the etch mask.

Dry Stripping

Dry stripping or oxygen plasma stripping (also ashing) has become more and more popular as it poses fewer disposal

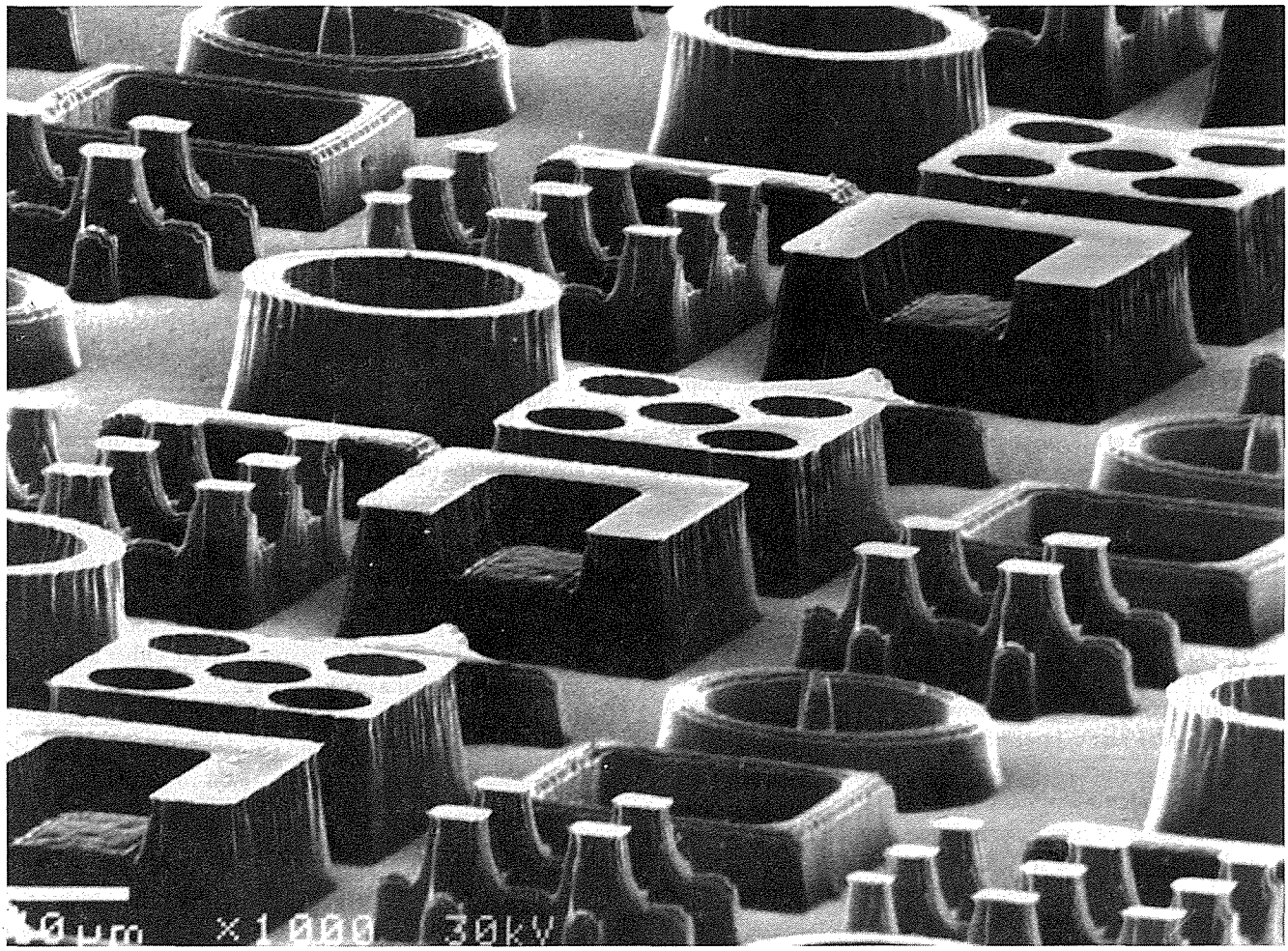

C

Figure 1.21 (Continued)

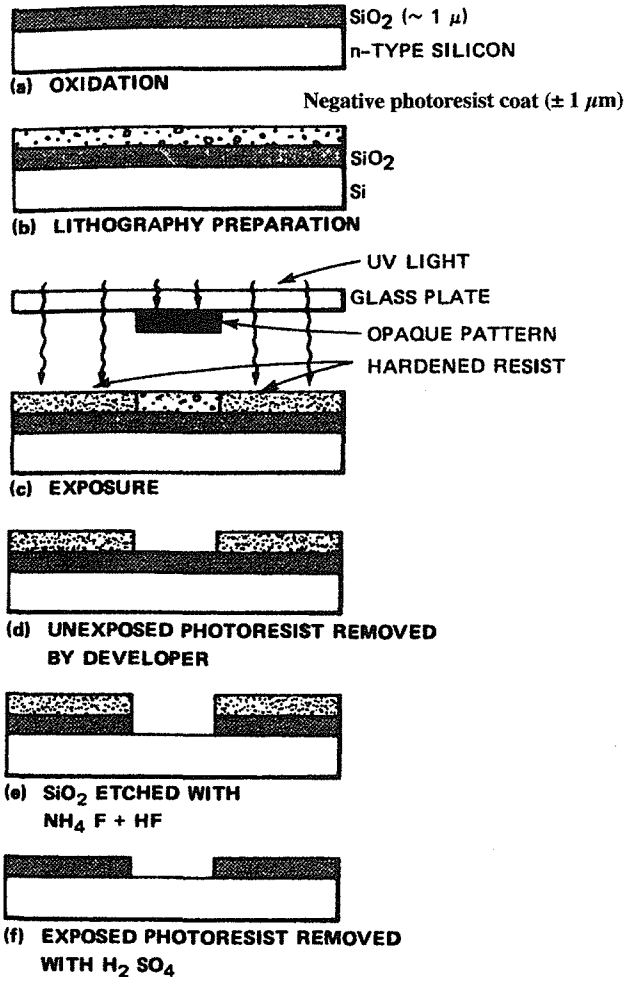

Figure 1.22 Basic IC process steps on an oxidized Si wafer; photolithography (with a negative-tone resist), including exposure, development, oxide etching, and resist stripping. (From Brodie. I. and J. J. Muray, The Physics of Microfabrication, Plenum Press, New York, 1991. With permission.)

problems with toxic, flammable, and dangerous chemicals. Wet stripping solutions also lose potency in use, causing stripping rates to change with time. Accumulated contamination in solutions can be a source of particles, and liquid phase surface tension and mass transport tend to make photoresist removal difficult and uneven. Also dry stripping is more controllable than liquid stripping, less corrosive with respect to metal features on the wafer, and, importantly, under the right conditions it leaves a cleaner surface. Finally, it causes no undercutting and broadening of photoresist features as wet strippers do.

In solid-gas resist stripping, a volatile product forms either through reactive plasma stripping (e.g., with oxygen), gaseous chemical reactants (e.g., ozone), and radiation (UV) or a combination thereof (e.g., UV/ozone-assisted). Plasma stripping employs a low pressure electrical discharge to split molecular oxygen (O_2) into its more reactive atomic form (O). This atomic oxygen converts an organic photoresist into a gaseous product that may be pumped away. This type of plasma stripping belongs to the category of chemical dry stripping and is isotropic in nature (see Chapter 2 on Pattern Transfer with Dry Etching). In ozone strippers, ozone, at atmospheric pressure, attacks the resist. In UV/ozone stripping, the UV helps to break bonds in the resist, paving the way for a more efficient attack by the ozone. Ozone strippers have the advantage that no plasma damage can occur on the devices in the process. Reactive plasma stripping currently is the predominant commercial technology due to its high removal rate and throughput. Some different stripper configurations* are barrel reactors, downstream strippers, and parallel plate systems. These prevalent stripping systems are reproduced in Figure 1.23.[51] In Chapter 2 more details about these different plasma strippers will be provided.

Dry stripping of resist has been so successful that it accelerated the use of plasmas in other lithography steps such as etching, development, and even deposition of resist. For example, the study of the attack of oxygen on polymers led to the development of dry resists as used in the DESIRE process (see Figure 1.19). Such dry resists are vital for future submicron lithography where underetching and broadening of features are most critical. So far dry resists have not been applied to the field of micromatching, as submicron features have not yet gained enough importance.

For more detailed information on multilayer resists, resist monitoring, dry resists, surface imaging resists (SIR), and other resist aspects not touched upon here or mentioned only briefly, we refer to Moreau.[6] Also *Solid State Technology*, *Semiconductor International*, and *Microlithography World* carry excellent tutorials on these topics.

Expanding the Limits of Photolithography Through Improved Mask Technology

Background

Control of the deposition of films in the z-direction can be achieved with remarkable precision, down to 20 Å. The x,y dimensions are more difficult to control and depend on the lithography as described in the preceding sections. The minimum x,y feature size feasible on a substrate in IC and microfabrication technology is determined primarily by the precise focus of the energy source that allows discrimination between areas of exposed resist and nonexposed resist. Other key factors are the tolerances on the mask itself, the ability to align the mask to the wafer and to align subsequent layers of masks to create the proper vertical geometry, and the ability to control the rate

* For a further comparison of the stripping systems shown in Figure 1.23 we refer to the August 1992 issue of *Solid State Technology*, pp. 37–39.[51] A listing of leading manufacturers of plasma stripping equipment can be found in the October 1992 issue of *Solid State Technology*, pp. 43–48.[52] Finally, in *Semiconductor International*, February 1992, pp. 58–64, a review on how to strip resists toughened through processing and difficult to remove with regular techniques is presented.[53] A lot of the proposed techniques are combinations of wet and dry etching techniques.

2

Pattern Transfer with Dry Etching Techniques

Introduction

Lithography steps precede a number of subtractive and additive processes. Materials either are removed from or added to a device, usually in a selective manner, using thin and/or thick film manufacturing processes, transferring the lithography patterns into integrated circuits (ICs) or three-dimensional micromachines. This chapter deals with material removal by dry etching processes. Chapter 3, Pattern Transfer with Additive Techniques, focuses on additive technologies.

Table 2.1 lists the most important subtractive processes encountered in micromachining, including mask-based wet and dry etching, and maskless processes such as focused ion-beam etching (FIB), laser machining, ultrasonic drilling, electrochemical discharge machining (EDM), and traditional precision machining. Examples (mostly involving Si), typical material removal rates, relevant reference(s), and some remarks on the techniques supplement the list. One of the most important subtractive techniques for micromachining listed in Table 2.1 is etching. Etching can be described as pattern transfer by chemical/physical removal of a material from a substrate, often in a pattern defined by a protective maskant layer (e.g., a resist or an oxide). From the etching processes listed in Table 2.1, the mask-based dry etching processes including chemical, physical, and physical-chemical etching will be analyzed in the current chapter. Etching in the liquid phase is analyzed separately in Chapter 4, Wet Bulk Micromachining. Maskless material removing technologies, such as focused ion beam (FIB), precision machining, and laser and ultrasonic drilling, will be discussed in Chapter 7, Comparison of Micromachining Techniques.

When introducing resist stripping in Chapter 1, we learned that the popularity of dry stripping of resists (ashing) and the need for better control of critical dimension (CD) precipitated a major research and development effort in all types of dry etching processes based on plasmas. The preference of dry stripping over wet stripping methods is based on a variety of advantages: fewer disposal problems, less corrosion problems for metal features in the structure, and less undercutting and broadening of photoresist features, i.e., better CD control (nanometer dimensions!) and, under the right circumstances, a cleaner resulting surface. Also, with the current trend in IC manufacture leading towards sub-half-micron geometries, surface tension might preclude a wet etchant from reaching down between photoresist features, whereas dry etching, characterized as selective stripping, precludes any problem of that nature. As in IC manufacture, dry etching evolved into an indispensable technique in micromachining.

Dry Etching: Definitions and Jargon

Dry etching covers a family of methods by which a solid state surface is etched in the gas phase, physically by ion bombardment, chemically by a chemical reaction with a reactive species at the surface, or combined physical and chemical mechanisms. The plasma-assisted dry etching techniques are categorized according to the specific set-up as either glow discharge techniques (diode set-up) or ion-beam techniques (triode set-up). Using the glow discharge techniques, the plasma is generated in the same vacuum chamber where the substrate is located, whereas when using ion-beam techniques the plasma is generated in a separate chamber from which ions are extracted and directed towards the substrate by a number of grids. Figure 2.1 represents the relation between the various dry etching diode and triode techniques.[14] In sputter/ion etching and ion-beam milling or ion-beam etching, the etching occurs as a consequence of a physical effect, namely momentum transfer between energetic Ar^+ ions and the substrate surface. Some chemical reaction takes place in all the other dry etching methods. In the physical/chemical case, impacting ions, electrons, or photons either induce chemical reactions or, in sidewall-protected ion-assisted etching, a passivating layer is cleared by the particle bombardment from horizontal surfaces only. As a result, etching occurs almost exclusively on the cleared planar surfaces. In Table 2.2, the most common dry etching methods are reviewed and the associated jargon clarified. From the methods listed, plasma etching and reactive ion etching are the most widely used techniques in IC manufacture and micromachining.

In selecting a dry etching process, the desired shape of the etch profile and the selectivity of the etching process require careful consideration. In Figure 2.2, different possible etch profiles are shown. Depending on the etching mechanism, isotropic, directional, or vertical etch profiles are obtained. In dry etching anisotropic etch profiles, directional or vertical, can be generated

TABLE 2.1 Partial List of Subtractive Processes Important in Micromachining (For More Details See Chapter 7)

Subtractive Technique	Applications	Typical Etch Rate	Remark	Ref.
Wet chem. etch. (iso. and anis.)	Iso.: Si spheres, domes, grooves Anis.: Si angled mesas, nozzles, diaphragms, cantilevers, bridges	Iso.: Si polishing at 50 μm/min with stirring (RT, acid) Anis.: etching at 1 μm/min on a (100) plane (90°C, alkaline)	Iso.: Little control, simple Anis.: With etch-stop more control, simple.	1, Chapter 4
Electrochem. etch.	Etches p-Si and stops at n-Si (in n-p junction), etches n-Si of highest doping (in n/n^+).	p-Si etching 1.25–1.75 μm/min. on a (100) plane, 105–115°C (alkaline)	Complex, requires electrodes	2,3, Chapter 4
Wet photoetch.	Etches p-type layers in p-n junctions	Etches p-Si up to 5 μm/min (acid)	No electrodes required	4, Chapter 4
Photoelectrochem. etch.	Etches n-Si in p-n junctions, production of porous Si	Typical Si etch rate: 5 μm/min (acid)	Complex, requires electrodes and light	5, Chapter 4
Dry chem. etch.	Resist stripping, isotropic features	Typical Si etch rate: 0.1 μm/min (but with more recent methods up to 6 μm/min)	Resolution better than 0.1 μm, loading effects	6, 7, Chapter 2
Phys./Chem. etch.	Very precise pattern transfer	Typical Si etch rate: 0.1 to 1 μm/min (but with more recent methods up to 6 μm/min)	Most important of dry etching techniques	7, 8, Chapter 2
Phys. dry etch., sputter etch., and ion milling	Si surface cleaning, unselective thin film removal	Typical Si etch rate: 300 Å/ min	Unselective and slow, plasma damage	8, Chapter 2
Focused ion-beam (FIB) milling	Microholes, circuit repair, microstructures in arbitrary materials	Typical Si etch rate: 1 μm/min	Long fabrication time: >2 h including set-up	9, Chapter 7
Laser machining (with and without reactive gases)	Circuit repair, resistor trimming, hole drilling, labeling of Si wafers	Typical rate for drilling a hole in Si with a Nd: YAG(400W laser): 1 mm/sec (3.5 mm deep and 0.25 mm dia.)	Laser beams can focus to a 1-μm spot, etch with a resolution of 1 μm^3	10, Chapter 7
Ultrasonic drilling	Holes in quartz, silicon nitride bearing race rings	Typical removal rate of Si: 1.77 mm/min	Especially useful for hard, brittle materials	11, Chapter 7
Electrostatic discharge machining (EDM)	Drilling holes and channels in hard brittle metals	Typical removal rate for metals: 0.3 cm^3/min	Poor resolution (>50 μm), only conductors, simple, wire discharge machining resolution much better	12, Chapter 7
Mechanical turning, drilling and milling, grinding, honing, lapping, polishing, and sawing	Almost all machined objects surrounding us	Removal rates of turning and milling of most metals: 1 to 50 cm^3/min; for drilling: 0.001 to 0.01 cm^3/min	Prevalent machining technique	13, Chapter 7

Note: Boldface type indicates techniques reviewed in Chapter 2, RT = room temperature, chem. etch. = chemical etching, iso. = isotropic, anis. = anistropic.

in single crystalline as well as in polycrystalline and amorphous materials. The anisotropy is not a result of the anisotropy of single crystals as in the case of anisotropic wet chemical etching (Chapter 4); rather, the degree of anisotropy is controlled by the plasma conditions. Selectivity of a dry etch refers to the difference in etch rate between the mask and the film to be etched, again controllable by the plasma conditions.

At low pressures, in the 10^{-3}- to 10^{-4}-Torr range (see Figure 2.1), obtaining anisotropic etching is easy, but accomplishing selectivity is difficult. At higher pressures (1 Torr) in plasma etching, chemical effects dominate, leading to better selectivity than in the case of ion beams, but etched features are isotropic. In the extreme case of anisotropic etching, vertical sidewalls result (no lateral undercut) with perfect retention of the CD (see Figure 2.2).

To ensure a uniform etch rate over the whole wafer and between wafers, overetching may be required. The drawing in Figure 2.3 illustrates the etch profile for a 25% overetch. Making the initial lithography smaller compensates for the loss of dimensionality incurred by overetching.

A sharp vertical sidewall does not always agree with the desired edge profile. For example, with line-of-site deposition methods such as resistive evaporation (see Chapter 3), a tapered sidewall is easier to cover than a vertical wall. Another example where a nonvertical process has the advantage is illustrated in Figure 2.4. To take away the layer on the vertical walls shown, an anisotropic etchant would require extensive overetching, whereas an isotropic etchant will remove the material quickly. The resulting etching patterns associated with all the possible different dry etching mechanisms are illustrated in Figure 2.5.[6]

Plasmas or Discharges

Most dry etching systems find their common base in plasmas or discharges, areas of high energy electric and magnetic fields that will rapidly dissociate any gases present to form energetic

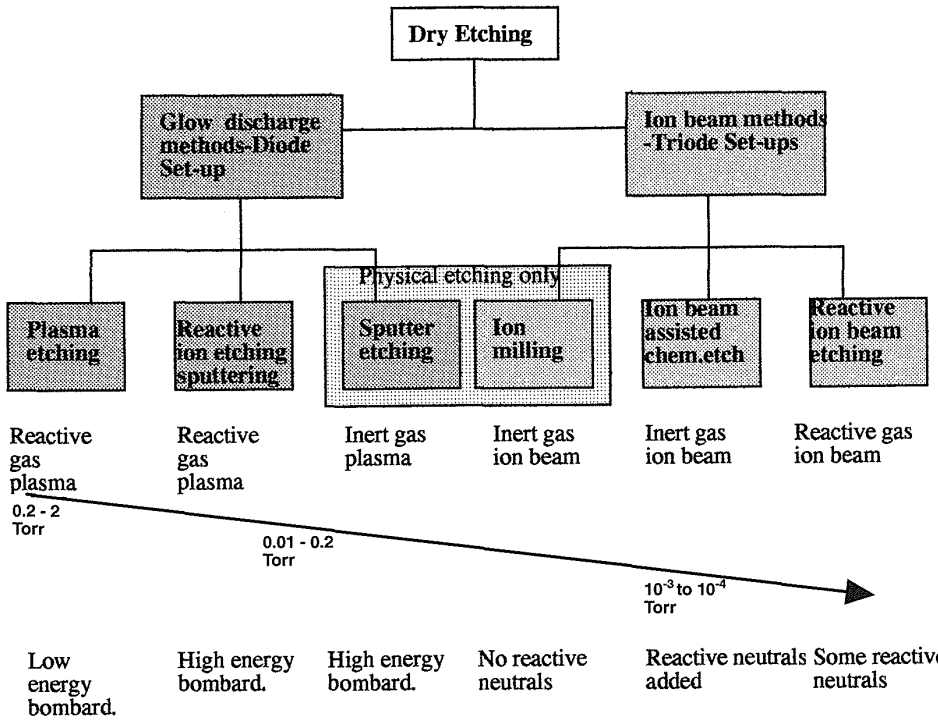

FIGURE 2.1 Relationship between the various dry etching techniques. (Adapted from Lehmann, H. W., in *Thin Film Processes II,* Vossen, J. L. and Kern, W., Eds. Academic Press, Boston, 1991.)

TABLE 2.2 Some Popular Dry Etching Systems[a]

	CAIBE	RIBE	IBE	MIE	MERIE	RIE	Barrel Etching	PE
Pressure (Torr)	$\sim 10^{-4}$	$\sim 10^{-4}$	$\sim 10^{-4}$	10^{-3}–10^{-2}	10^{-3}–10^{-2}	10^{-3}–10^{-1}	10^{-1}–10^{0}	10^{-1}–10^{1}
Etch mechanism	Chem./phys.	Chem./phys.	Phys.	Phys.	Chem./phys.	Chem./phys.	Chem.	Chem.
Selectivity	Good	Good	Poor	Poor	Good	Good	Excellent	Good
Profile	Anis. or iso.	Anis.	Anis.	Anis.	Anis.	Iso. or anis.	Iso.	Iso. or anis.

Note: CAIBE = Chemically assisted ion beam etching; MERIE = Magnetically enhanced reactive ion etching; MIE = Magnetically enhanced ion etching; PE = Plasma etching; RIBE = Reactive ion beam etching; RIE = Reactive ion etching.[15,16]

[a] Many of the more recent dry etching techniques are not listed here. For more information on inductively coupled plasmas (ICP), electron cyclotron plasmas (ECR), microwave multipolar plasmas (MMP), and introductory material on helicon plasma sources, helical resonators, rotating field magnetrons, hollow cathode reactors, etc., refer to References 16–22.

ions, photons, electrons, and highly reactive radicals and molecules. We will start our foray into the physics and chemistry of plasmas by looking at the simplest plasma set-up, i.e., a DC-diode glow discharge.

Physics of DC Plasmas

The simplest plasma reactor may consist of opposed parallel plate electrodes in a chamber maintainable at low pressure, typically ranging from 0.001 to 1 Torr. The electrical potentials established in the reaction chamber filled with an inert gas such as argon at a reduced pressure determine the energy of ions and electrons striking the surfaces immersed in the discharge. Using the set-up shown in Figure 2.6A and applying 1.5 kV between the anode and cathode, separated by 15 cm, results in a 100-V/cm field. Electrical breakdown of the argon gas in this reactor will occur when electrons, accelerated in the existing field, transfer an amount of kinetic energy greater than the argon ionization potential (i.e., 15.7 eV) to the argon neutrals. Such energetic collisions generate a second free electron and a positive ion for each successful strike. Both free electrons reenergize, creating an avalanche of ions and electrons that results in a gas breakdown emitting a characteristic glow. Avalanching requires the ionization of 10 to 20 gas molecules by

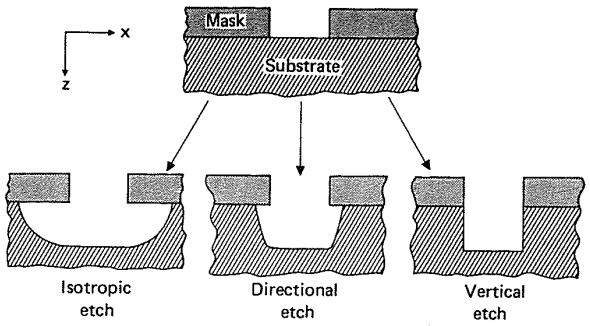

FIGURE 2.2 Directionality of etching processes.

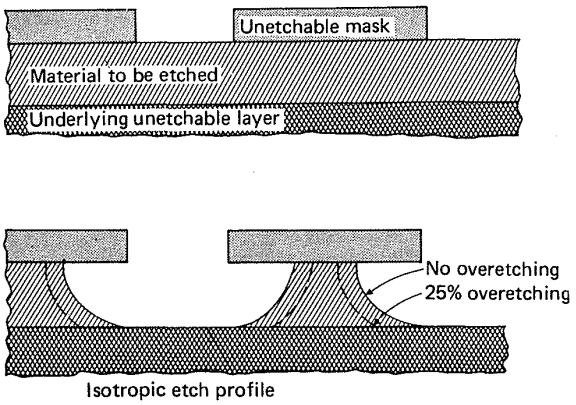

FIGURE 2.3 Example illustrating the loss of dimensionality incurred by an isotropic etch when the etch depth is of the order of the lateral dimensions involved. Making the initial lithography smaller compensates for the loss of dimensionality by overetching.

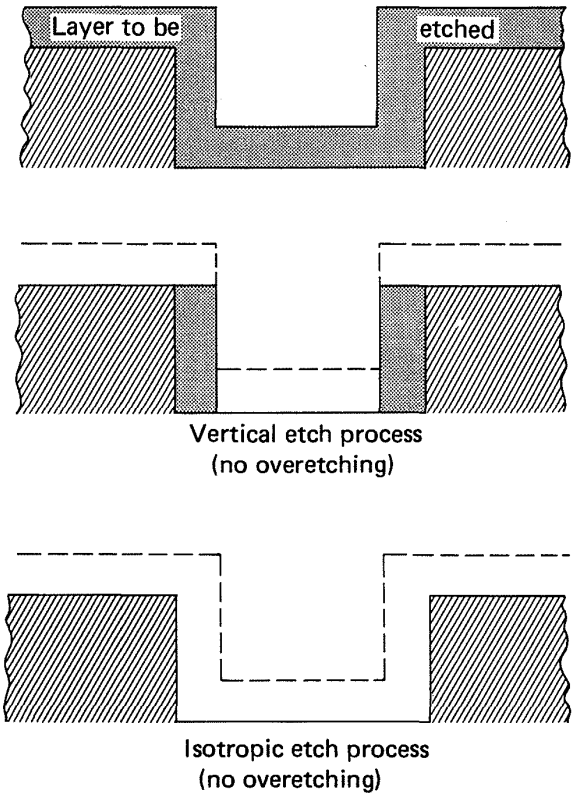

FIGURE 2.4 An example of dry etching illustrating a case where an isotropic etch is preferred to a vertical etch process. To clear the layer on the vertical walls, an isotropic etch only requires a minimal overetch while an anisotropic etch requires a substantial amount of overetching.

one secondary electron. At the start of a sustained gas breakdown, a current begins flowing and the voltage between the two electrodes drops from 1.5 kV to about 150 V. The discharge current builds up to the point where the voltage drop across a current limiting resistor is equal to the difference between the supply voltage (1.5 kV) and the electrode potential difference (150 V). To sustain a plasma, a mechanism to generate additional free electrons must exist after the plasma-generating electrons have been captured at the positively charged anode. Plasma-sustaining electrons are generated at the cathode which emits secondary electrons (Auger electrons) when struck by ions. The continuous generation of those 'new' electrons prompts a sustained current and a stable plasma glow. It is easy to understand why plate (electrode) separation and gas pressure are critical. Plates positioned too closely prevent ionizing collisions, but plates separated too far cause too many inelastic collisions of ions which lose energy. Once equilibrium is reached, the glow region of the plasma, being a good electrical conductor, hardly sustains a field and its potential is almost constant. The potential drop resides at electrode surfaces where electrical double layers are formed in so-called sheath fields, counteracting the loss of electrons from the plasma (Figure 2.6B). The plasma sheaths coincide with the plasma dark spaces (the dark space in front of the cathode is called the Crookes dark space). The dark spaces develop because the higher energy electrons in those spaces are more likely to cause ionization than light-generating excitation.

The permanent positive charge of a plasma with respect to the electrodes is a striking characteristic and is a result of the random motion of the electrons and ions. The positive charge of a plasma can be understood from kinetic theory which predicts that for a random velocity distribution the flux of ions, j_i, and electrons, j_e, upon a surface is given by:

$$j_{i,e} = \frac{n_{i,e}\langle v_{i,e}\rangle}{4} \qquad 2.1$$

where n and $\langle v \rangle$ are the densities and average velocities, respectively. Because ions are heavier than electrons (typically 4000 to 100,000 times as heavy), the average velocity of electrons is larger. Consequently, the electron flux (according to Equation 2.1) is larger than the ion flux, and the plasma loses electrons to the walls, thereby acquiring a positive charge. The bombarding

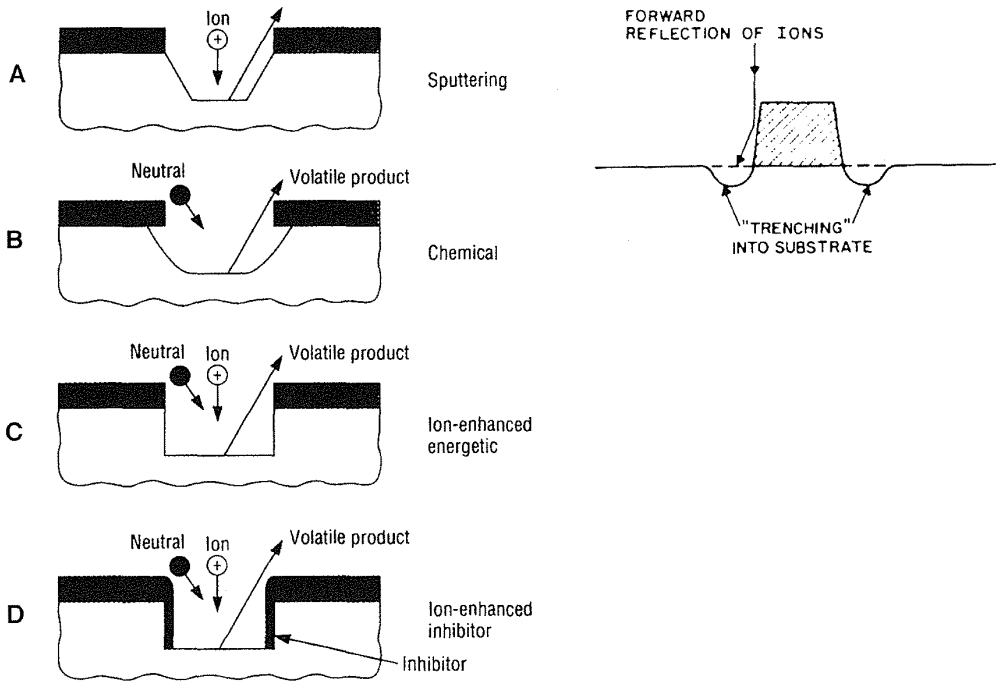

FIGURE 2.5 Important dry etching profiles associated with the different dry etching techniques. (A) Sputtering and the formation of trenches (ditches) in physical ion etching. The mask is etched most rapidly in the neighborhood of the mask corner. The slope becomes less steep and not all ions are arriving at the etch bottom parallel to the sides any more. Some of them collide with the sides of the mask or substrate before arriving at the etch surface. Consequently, an increase in the number of incident ions close to the edges occurs, locally increasing the etch rate forming ditches. (B) Chemical etching in a plasma at low voltage and relative high pressure leads to isotropic features and lateral undercuts. (C) Ion-enhanced etching: physical-chemical, is the most perfect image transfer, as the undercutting is limited by the combined action of physical and chemical etching. The low pressure and high voltage lead to directional anisotropy. (D) Ion-enhanced inhibitor. Sidewalls are protected from undercutting by a surface species (e.g., a polymer) which starts etching when hit by a particle such as an ion, a photon, or an electron. Since very few particles hit the sidewalls (high voltage and high pressure), undercutting is suppressed. (Left side of figure is from Flamm, D. L., *Solid State Technol.*, October 49–54 (1993). With permission.)

energy of ions is proportional to the potential difference between the plasma potential and the surface being struck by ions. In equilibrium, the plasma potential V_p (see Figure 2.6) averages a few times the electron energy $\langle v_e \rangle$ and typically reaches 2 to 10 volts. The rationale behind the asymmetric voltage distribution at the anode and cathode as seen in Figure 2.6 is as follows: electrons near the cathode rapidly accelerate away from it due to their relatively light mass. The ions, being more massive, accelerate towards the cathode in a slower tempo. Thus, on average, ions spend more time in the Crookes dark space, and at any instant their concentration is greater than that of electrons. The net effect is a very large field in front of the cathode in comparison with the field in front of the anode or in the glow region itself. Consequently, the greatest part of the voltage between the anode and the cathode, V_c, is dropped across the Crookes dark space where charged particles (ions and electrons) experience their largest acceleration. We will analyze the voltage distribution in a glow discharge in more detail when introducing RF discharges below.

The degree of ionization in a plasma depends on a balance between the rate of ionization and the rate at which particles are lost by volume recombination and by losses to the walls of the apparatus. Wall losses generally dominate over volume recombination. Accordingly, the occurrence of a breakdown in a given apparatus depends on the gas pressure (particle density), the type of gas, electric field strength (electron velocity), and on surface-to-volume ratio of the plasma. Figure 2.7 represents the Paschen curve and illustrates the gas breakdown voltage required to initiate discharge as a function of the product of the pressure, P, and the electrode spacing, d. The sharp rise in the breakdown voltage at the left side in Figure 2.7 (low Pxd side) occurs because the electrode spacing is too small, or the gas density is so low that electrons are lost to walls without colliding with gas atoms to produce ionization. On the right hand side of this plot (high Pxd side), the slow rise in the required voltage occurs because the electron energy is too low to cause ionization. This occurs at high pressures, because electron collisions with gas atoms become so frequent that the electrons cannot gather sufficient energy to overcome the ionization potential of the inert gas. Different gases exhibit similar 'Paschen' behavior, with the curves more or less shifted from the air-curve depending on the mean free path of the gas molecules involved.

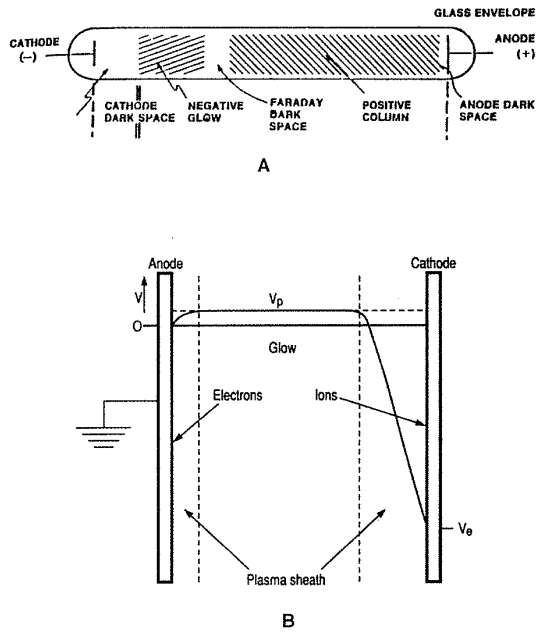

FIGURE 2.6 Glow discharge in a DC diode system. (A) Structure of the glow discharge in a DC diode system. (B) Voltage distribution in a DC diode discharge in equilibrium.

To better understand the implication of a Paschen curve, another way of introducing this plot might be of use. At constant pressure (say at 1 atmosphere), on the right side of the minimum in the Paschen curve, the breakdown voltage increases as the distance between the two parallel plane electrodes increases. Based on intuition about electrical breakdown, we predict higher voltages for larger electrode distances. Interestingly and counter intuitively, on the left side of the Paschen curve, i.e., at very short distances between anode and cathode (below 5 μm at atmospheric pressure in air), the breakdown voltage suddenly increases for shorter electrode distances because the electrode distances are too short for avalanche to take effect. We will see in Chapter 9 that a wide variety of electrostatic micromachines such as motors, switches, and gas sensors can operate in air without sparking as they operate on the left side of the Paschen curve. Microstructures, with dimensions of a few microns, operate in air as if surrounded by a reduced pressure environment. This typifies how linear scaling might be misleading when predicting the behavior of microdevices.

All glow discharges are nonequilibrium as the average electron energy ($\langle v_e \rangle = kT_e$, see Equation 2.2) is considerably higher than the average ion energy ($\langle v_i \rangle = kT_i$, see Equation 2.3), so a discharge or plasma cannot be described adequately by one single temperature (T_e (electrons)/T_i(ions) = 10 to 100). High temperature electrons in a low temperature gas occur due to the small mass of electrons (m_e) compared to ions and neutrals. In collisions between electrons and argon atoms (M_A), the ratio m_e/M_A is only $1.3^{*}10^{-5}$. Thus, in collisions, electrons have a poor energy transfer and stay warmer longer than the heavier ions and neutrals. Electrons can attain a high average energy, often many electron volts (equivalent to tens of thousands of degrees above the gas temperature), permitting electron-molecule collisions to excite high temperature type reactions which form free radicals in a low temperature neutral gas. Generating the same reactive species without a plasma would require temperatures in the ~10^3 to 10^4 K range, destroying resists and damaging most inorganic films.

Also important to note is that a plasma typically is weakly ionized: the number of ions is very small compared to the number of reactive neutrals such as radicals. The ratio between ionized and neutral gas species in a glow discharge plasma is of the order of 10^{-6} to 10^{-4}. This fact is crucial in understanding which entities are responsible for the actual etching of a substrate placed in a glow discharge.

Of the different dry etching techniques, the choice of technique depends on the efficiency or 'strength' of a particular plasma evaluated by parameters such as the average electron energy, $\langle v_e \rangle$, also called electron temperature, i.e.,

$$\langle v_e \rangle = kT_e \left(\text{e.g., } 1 - 10\,\text{eV}\right) \qquad 2.2$$

the average ion energy, i.e.,

$$\langle v_i \rangle = kT_i \left(\text{e.g., } 0.04\,\text{eV}\right) \qquad 2.3$$

the electron density (e.g., between 10^9 and 10^{12} cm^{-3}), plasma ion density (e.g., 10^8 to 10^{12} cm^{-3}), neutral species density (e.g., 10^{15} to 10^{16} cm^{-3}), and the ion current density (e.g., 1 to 10 mA/cm^2). A quantity of particular use in characterizing a plasma's average electron or ion energy is the ratio of the electrical field to the pressure:

$$kT_{i,e} \sim \frac{E}{P} \qquad 2.4$$

With increasing field strength, the velocity of free electrons or ions increases because of acceleration by the field (~E) but velocity is lost by inelastic collisions. Since an increase in pressure decreases the electron or ion mean free path, there being more collisions, the electron or ion energy decreases with increasing pressure (~1/P).

How do we use the described DC plasmas for dry etching? In one of the arrangements the substrate to be etched is placed on the cathode (target) in an argon plasma, while sufficiently energetic ions (between 200 and 1000 eV) induce physical etching, i.e., ion etching or sputtering in which atoms are billiard ball-wise ejected from the bombarded substrate (see Figure 2.8). Externally applied voltages concentrate across the cathode plasma sheath and ions are accelerated in that field before hitting the cathode. Each ion will collide numerous times with other gas species before transversing the plasma sheath, as the sheath thickness is larger than the mean free path. As a result of these collisions, the ions lose a lot of their energy and move across the sheath with a drift velocity that is less than the 'free fall' velocity. But these vertical velocities are still very large compared to the random thermal velocities discussed above. The resulting bombarding ion flux, j_i, is given by:

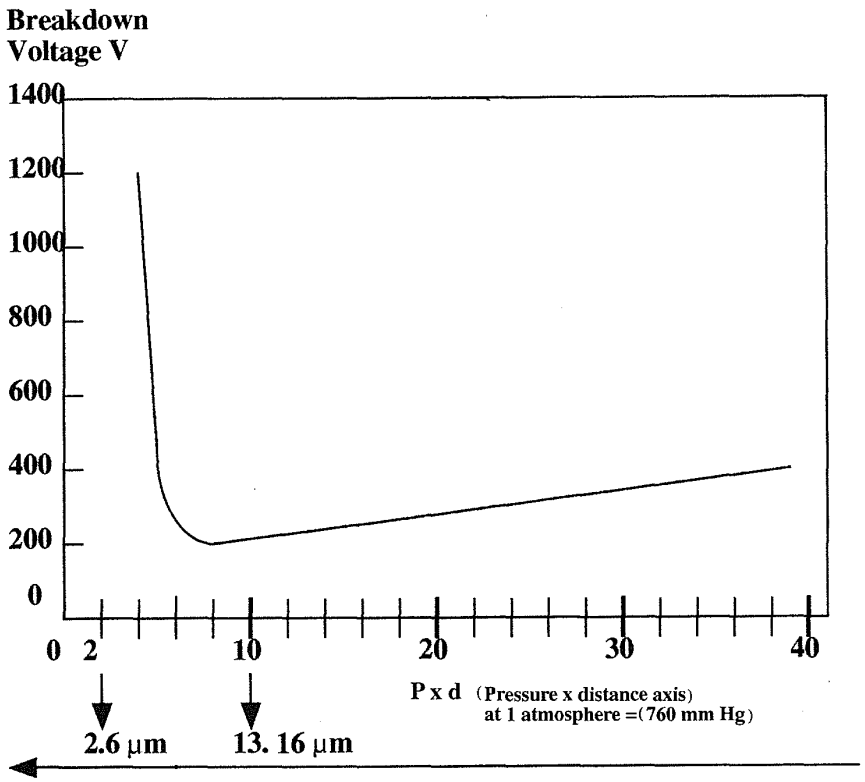

FIGURE 2.7 The DC breakdown voltage as a function of the gas pressure P and the electrode spacing d for plane parallel electrodes in air. Such curves are determined experimentally and are known as Paschen curves.

$$j_i = qn_i\mu_i E \qquad 2.5$$

with E, the electric field, n_i, the ion density, μ_i, the ion mobility, and q the charge. Reducing the pressure in the reactor increases the mean free path. Consequently, ions accelerated towards the cathode at lower pressures can gain more energy before a collision takes place. In an alternate mode, reactive species generated by the DC plasma may combine with the substrate to form volatile products that evaporate, chemically etching the substrate.

Physics of RF Plasmas

In an RF-generated plasma, a radio frequency voltage applied between the two electrodes causes the free electrons to oscillate and to collide with gas molecules leading to a sustainable plasma. RF-excited discharges can be sustained without relying on the emission of secondary electrons from the target. Electrons pick up enough energy during oscillation in an RF field to cause ionization, thus sustaining the plasma at lower pressures than in a DC plasma (e.g., 10 vs. 40 mTorr). Another asset RF has over DC sputtering is that RF allows etching of dielectrics as well as metals. The RF breakdown voltage of a plasma shows the Paschen behavior of a DC plasma, i.e., a minimum in the required voltage as a function of the pressure with the mean free path of the electrons substituting the spacing, d, between the electrodes.

In the simplest case of RF ion sputtering, the substrates to be etched are laid on the cathode (target) of a discharge reactor, for example, a planar parallel plate reactor as shown in Figure 2.8. The reactor consists of a grounded anode and powered cathode or target, enclosed in a low-pressure gas atmosphere (e.g., 10^{-1} to 10^{-2} Torr of argon). An RF plasma, formed at low gas pressures, again consists of positive cations, negative anions, radicals, vibrationally excited polyatomic species, and photons (the UV photons create the familiar plasma glow). As with a DC plasma, the neutral species greatly outnumber the electrons and ions; the degree of ionization only being on the order of 10^{-4} to 10^{-6} for parallel plate gas discharges. The RF frequency typically employed is 13.56 MHz (a frequency chosen because of its non-interference with radio-transmitted signals). The RF power

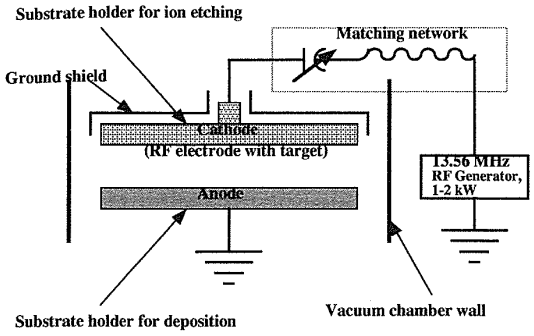

FIGURE 2.8 Two electrode set-up (diode) for RF ion sputtering or sputter deposition. For ion sputtering, the substrates are put on the cathode (target); for sputter deposition, the substrates to be coated are put on the anode.

supply rates between 1 and 2 kW. With one of the two electrodes capacitively coupled to the RF generator, the capacitively coupled electrode automatically develops a negative DC bias and becomes the cathode with respect to the other electrode (see Figure 2.9A). This DC bias (also called 'self-bias' V_{DC}) is induced by the plasma itself and is established as follows. When initiating an AC plasma arc, electrons, being more mobile than ions, charge up the capacitively coupled electrode; since no charge can be transferred over the capacitor, the electrode surface retains a negative DC bias.

The energy of charged particles bombarding the surface in a glow discharge is determined by three different potentials established in the reaction chamber: the plasma potential, V_p, i.e., the potential of the glow region; the self bias, V_{DC}; and the bias on the capacitively coupled electrode, $(V_{RF})_{pp}$ (see also Figure 2.9B). The following analysis clarifies how these potentials relate to one another and how they contribute to dry etching.

The voltage build-up, V_{DC}, on an insulating electrode by the electron flux (Equation 2.1) is given by:

$$V_{DC} = \frac{kT_e}{2e} \ln \frac{T_e m_i}{T_i m_e} \qquad 2.6$$

where T_e and T_i are the electron and ion temperatures defined by Equations 2.2 and 2.3 and m_e and m_i are the electron and ion masses, respectively.[22]

The electron loss creates an electric sheath field in front of any surface immersed in the plasma, counteracting further electron losses. This sheath or dark space also forms a narrow region (typically 0.01 to 1 cm depending on pressure, power, and frequency) between the conductive glow region and the cathode (Crookes dark space) where most of the voltage (V_{DC} in Figure 2.9A) is dropped as in the DC plasma case (the cathode being capacitively coupled acts effectively as an insulator for DC currents). The other electrode is grounded and conductive (no charge build-up and no voltage build-up) and automatically becomes the anode with respect to the capacitively coupled electrode.

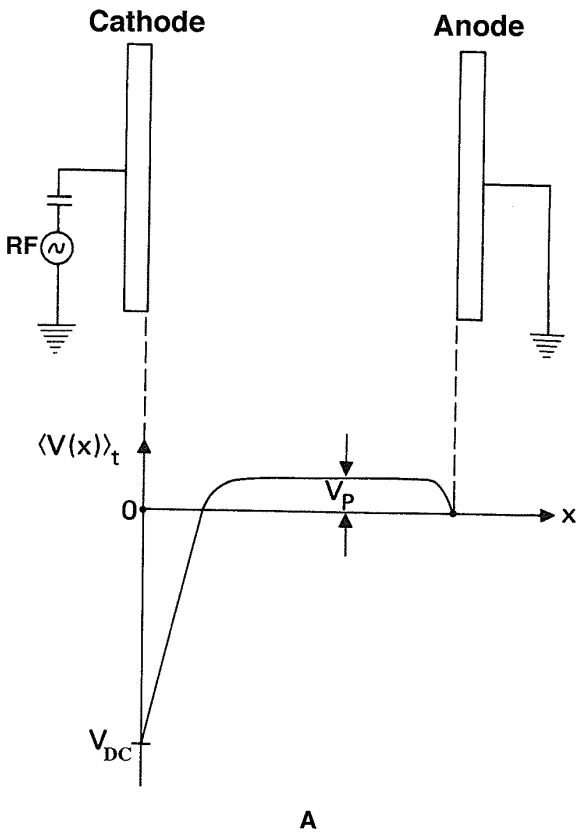

FIGURE 2.9 RF plasma: (A) Approximate time-averaged potential distribution for a capacitively coupled planar rf discharge system. (B) Potential distribution in glow discharge reactors. V_p: plasma potential, V_{DC}: self-bias of cathode electrode, $(V_{RF})_{pp}$: peak-to-peak RF voltage applied to the cathode. (C) Equivalent electrical circuit of an RF plasma.

The time-average of the plasma potential, V_p, the DC cathode potential (self-bias potential,) V_{DC}, and the peak-to-peak RF voltage $(V_{RF})_{pp}$, applied to the cathode are approximately related as (see Figure 2.9B):

$$2V_p \sim \frac{(V_{RF})_{pp}}{2} - |V_{DC}| \qquad 2.7$$

Clearly the magnitude of the self-bias depends on the amplitude of the RF signal applied to the electrodes. In the RF discharge the time-averaged RF potential of the glow region, referred to as the plasma potential, V_p, is more significantly positive with respect to the grounded electrode than in the case of a DC plasma.

Positive argon ions from the plasma are extracted by the large field at the cathode and are sputtering that electrode at near-normal incidence with energies ranging from a few to several electronvolts, depending on the plasma conditions and the chamber construction. One of the most important parameters determining the plasma condition is the total reactor pressure. As pressure is lowered below 0.05 to 0.1 Torr, the total ion energy, E_{max}, rises as both the self-bias voltage and the mean

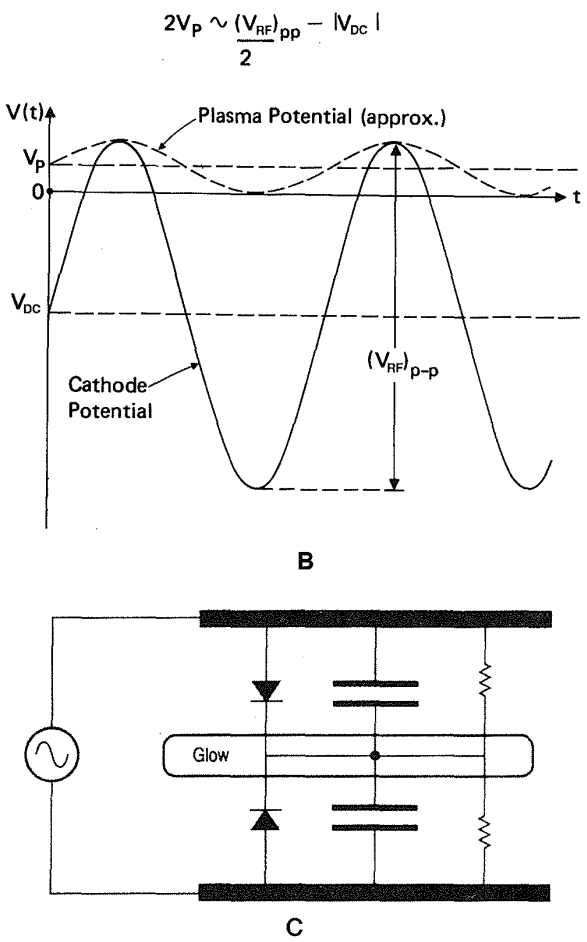

FIGURE 2.9 (Continued)

free path of the bombarding ions increase. Subsequently, ion-substrate bombardment energy rises sharply with decreasing pressure. The maximum energy of positive ions striking a substrate placed on the cathode is proportional to:

$$E_{max} = e\left(|V_{DC}| + V_p\right) = eV_T \qquad 2.8$$

with $V_T = |V_{DC}| + V_p$, whereas the maximum energy for a substrate on the grounded electrode (i.e., the anode) is proportional to:

$$E_{max} = eV_p \qquad 2.9$$

Equations 2.8 and 2.9 can be deduced from an inspection of Figure 2.9A. The situation where the wafers are put on the cathode is referred to as 'reactive ion etching' or 'reactive sputter etching'.

The chamber construction, especially the ratio of anode to cathode area, influences the rates of V_T/V_p and, consequently, as calculated from Equations 2.8 and 2.9, the energy of the sputtering ions on these respective electrodes. Usually one wants to avoid etching of the anode, i.e., one tries to make V_p small. To deduce the influence of the geometry of the anode and cathode on dry etching, we compare the sheath voltages in front of the anode and cathode, using the Child-Langmuir equation, expressing the relationship between the ion-current flux, j_i, the voltage drop, V, over the sheath thickness of the dark-space, d; and the mass of the current carrying ions, m_i. The relation can be deduced from Equation 2.5 assuming the presence of a space-charge limited current:

$$j_i = \frac{KV^{3/2}}{\sqrt{m_i}\,d^2} \qquad 2.10$$

in which K is a constant.[23] The current density of the positive ions must be equal on both the anode and cathode, resulting in the following relation for the sheath-voltages:

$$\text{(cathode)}\ \frac{V_T^{3/2}}{d_T^2} = \frac{V_p^{3/2}}{d_p^2}\ \text{(anode)} \qquad 2.11$$

The plasma behaves electrically as a diode (large blocking voltage drop towards the capacitively coupled cathode and small voltage drop on the anode/plasma interface) in parallel with the sheath capacitance. As soon as any electrode tends to become positive relative to the plasma, the current rises dramatically, causing the plasma to behave as if a diode were present in the equivalent electrical circuit of the plasma. Hence, a planar, parallel set-up also is called a diode set-up. The equivalent electrical circuit representing an RF plasma is represented in Figure 2.9C. The dark spaces in a plasma are areas of limited conductivity and can be modeled as capacitors, i.e.,

$$C \sim \frac{A}{d} \qquad 2.12$$

The plasma potential is determined by the relative magnitudes of the sheath capacitances which in turn depend on the relative areas of anode and cathode. An RF voltage will split between two capacitances in series according to:

$$\frac{V_T}{V_p} = \frac{C_p}{C_T} \qquad 2.13$$

Using Equations 2.12 and 2.13, we can write:

$$\frac{V_T}{V_p} = \left(\frac{A_p}{d_p}\right)\left(\frac{d_T}{A_T}\right) \qquad 2.14$$

and substituting into Equation 2.11, we obtain:

$$\frac{V_T}{V_p} = \left(\frac{A_p}{A_T}\right)^4 = R^4 \qquad 2.15$$

where A_p is the anode area and A_T the cathode area. If there were two symmetric electrodes, both blocked capacitively, sputtering would occur on both surfaces. If the area of the cathode were significantly smaller than the other areas in contact with the

discharge, the plasma potential would be small and little sputtering would occur on the anode, whereas the cathode would sputter very effectively. Since the cathode, in a set-up such as that represented in Figure 2.8, usually is quite large (> 1 m^2), allowing many silicon wafers or other substrates to be etched simultaneously, the grounded area needs to be larger yet. In actual sputtering systems, the larger grounded electrode consists of the entire sputtering chamber, creating a very small dark space, where there is hardly any sputtering taking place from these dark spaces. The exponential in Equation 2.15 in practical systems usually is less than 2, rather than 4.[23]

Higher ion energies (V_T large), translate into lower etch selectivity and can be a cause of ***device damage.*** Consequently, a key feature for good ***etch performance*** is effective ionization to turn out very high quantities of low energy ions and radicals at low pressures. In answer to this need, equipment builders have come up with low-energy, high-density plasmas, for example, magnetrons, ICPs (inductively coupled plasmas)[19] and ECRs (electron cyclotron resonance)[16] (see below).

Physical Etching: Ion Etching or Sputtering and Ion-Beam Milling

Introduction

Bombarding a surface with inert ions, such as argon ions, in a set-up as shown in Figure 2.8, translates into ion etching or sputter etching (DC or RF). With ions of sufficient energy, impinging vertically on a surface, momentum transfer (sputtering) causes bond breakage and ballistic material ejection, throwing the bombarded material across the reactor to deposit on an opposing collecting surface, provided the surrounding pressure is low enough. The kinetic energy of the incoming particles largely dictates which events are most likely to take place at the bombarded surface, i.e., physisorption, surface damage, substrate heating, reflection, sputtering, or ion implantation. At energies below 3 to 5 eV, incoming particles are either reflected or physisorbed. At energies between 4 and 10 eV, surface migration and surface damage results. At energies >10 eV (say, from 5 to 5000 eV), substrate heating, surface damage, and material ejection, i.e., sputtering or ion etching, takes place. At yet higher energies >10,000 eV, ion-implantation, i.e., doping, takes place. The energy requirements for these various processes are summarized in Table 2.3.

Device damage

Device damage comes in many "flavors" including:

- alkali (sodium) and heavy metal contamination
- catastrophic dielectric breakdown
- current-induced oxide aging
- particulate contamination
- UV damage
- temperature excursions which can activate metallurgical reactions
- "rogue" stripping processes which simply do not remove all the residue
- plasma-induced charges, surface damage, ion implantation

Etch performance

Etch Performance

Etch performance is being judged in terms of etch rate, selectivity, uniformity (evenness across one wafer and from wafer to wafer), surface quality, reproducibility, residue, microloading effects, device damage, particle control, post-etch corrosion, CD, and profile control. Selectivity as high as 40:1 might be required in the future for ICs and even more for micromachines. It is generally believed that 'radiation' damage of a plasma can be minimized by keeping ion energies low. It is also generally believed that a lot of the radiation damage can be annealed out. In reality, very little is understood of the damage a plasma can do. The higher the etch rate, the better the wafer throughput. Good selectivity, uniformity, and profile control are more easily achieved at lower etch rates. Trenches of various depths are made in Si in the manufacture of MOS devices. Shallow trenches (0.5 to 1.5 μm) are used to aid in reducing the effects of lateral diffusion during processing and to make flat structures (planarization). Deeper trenches (1.5 to 10 μm) are used to create structures that become capacitors and isolation regions in integrated circuits. For the shallowest trenches, photoresist is adequate as a mask. For deeper etching, a silicon dioxide mask may be needed. In micromachining one would like to obtain aspect ratios of 100 and beyond, so the degree of difficulty in masking keeps mounting. With aspect ratios above 2:1 or 2.5:1, the etching action at the bottom of a trench tends to slow down or stop altogether.

TABLE 2.3 Energy Requirements Associated with Various Physical Processes

Ion Energy (eV)	Reaction
<3	Physical adsorption
4–10	Some surface sputtering
10–5000	Sputtering
10–20 K	Implantation

The deposition phenomenon mentioned above can be used to deposit materials in a process called sputter deposition (Chapter 3). A low pressure and a long mean free path are required for material to leave the vicinity of the sputtered surface without being backscattered and redeposited.

In what follows, we shall consider two purely physical dry etching techniques at energies >10 eV, i.e., sputtering and ion-beam milling.

Sputtering or Ion-Etching

The gradient in the potential distribution around the target in Figure 2.8 accelerates the ions prompting them to impinge on the substrate in a direction normal to the surface, and the etch rate in the direction of the impinging ions (V_z) becomes a strong function of E_{max} (Equation 2.8). The impinging ions erode or sputter etch the surface by momentum transfer. This offers some advantages: volatility of the etch products is not critical as for dry chemical etching (only a billiard ball effect plays a role in physical etching), consequently the method does not lead to large differences in etch rates for different materials (sputter yields for most materials are within a factor of three of each other), and the method entails directional anisotropy. Physical etching is inherently material nonselective because the ion energy required to eject material is large compared to differences in chemical bond energy and chemical reactivity. When no reactive etching processes are available for a given material, physical etching always offers an option. The directional anisotropy remains as long as the dimensions of the surface topographical structures are small compared to the thickness of the sheath between the bulk plasma and the etched surface. However, etch rates are slow, typically a hundred to a few hundred angstroms per minute. The use of a magnetron can help improve upon the speed of the etch rate. In both DC and RF diode sputtering, most electrons do not cause ionization events with Ar atoms. They end up being collected by the anode, substrates, etc., where they cause unwanted heating. A magnetron adjusts this situation by confining the electrons with magnetic fields near the target surface; consequently, current densities at the target can increase from 1 mA/cm² to 10–100 mA/cm².

As sputter etching is nonselective, it introduces a masking problem. Another hurdle to overcome is the need for rather high gas pressure to obtain large enough ion currents, resulting in a short mean free path, λ_i, of the ions. With a mean free path smaller than the interelectrode spacing, considerable redeposition of sputtered atoms on the etching substrate laying on the cathode can occur. Electrical damage from ion bombardment also needs watching when critical electronic components reside on the substrate.

Ion-Beam Etching or Ion-Beam Milling

When the plasma source for ion etching is decoupled from the substrate which is placed on a third electrode, one practices ion beam milling (IBM). The equipment needed is called a triode set-up. In a typical DC triode set-up, as shown in Figure 2.10, control of the energy and flux of the ions to the substrate happens independently. The sample being etched can be rendered neutral by extracting low-energy electrons from an auxiliary thermionic cathode (i.e., a hot filament neutralizer), thus making this DC equipment usable for sputtering insulators as well as conductors. In ion-beam milling, as in ion etching, one generally uses noble gases as they exhibit higher sputtering yields (heavy ions!) and avoid chemical reactions. The argon pressure in the upper portion of the chamber can be quite low, 10^{-4} Torr, resulting in a large mean free ion path. Electrons are emitted by a hot filament (typically tantalum or tungsten) and accelerated by a potential difference between the cathode filament and an anode. The discharge voltage must be larger than the gas ionization potential (15.7 eV for argon) and typically is operated at several times this value, about 40 to 50 V, in order to establish a glow discharge. Ions are extracted from the upper chamber by the sieve-like electrode, formed into a beam, accelerated, and fired into the lower chamber where they strike the substrate. Typical etch rates with argon ions of 1-keV energy and an ion current density of 1.0 mA/cm² are in the range of 100 to 3000 Å/min for most materials such as silicon, polysilicon, oxides, nitrides, photo-resists, metals, etc. Inert ion-beam etching (IBE) is, in principle, capable of very high resolution (<100 Å) but aspect ratios are usually less than or equal to unity.

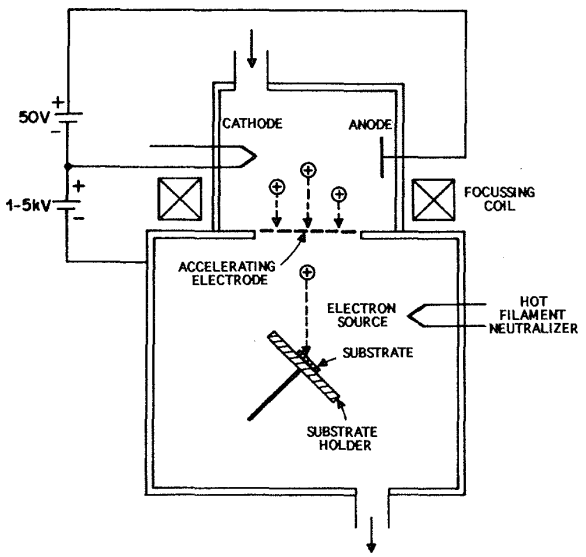

FIGURE 2.10 Ion-beam etching (IBE) apparatus (triode). In an ion beam apparatus, the beam diameter is approximately 8 cm. The substrates are mounted on a moveable holder allowing etching of large substrates. The coils focus the ion beam and densify the ion flux in magnetically enhanced confined ion etching (MIE).

In magnetically enhanced ion etching (MIE) the plasma is guided and made dense by an applied magnetic field (see coils in Figure 2.10). A magnetic field is applied to the extent that electrons cannot pass directly from the anode to the cathode, but follow helical paths between collisions, greatly increasing their path length and ionization efficiency. The cyclotron radius of a 100-eV electron in a field of 0.01 Tesla (T) (100 Gauss (G)) is 3.2 mm, making relatively low field strengths adequate. This results in an increased etch rate due to a denser ion plasma. When plasma density is increased with magnetic confinement, the degree of ionization is between 10^{-2} and 10^{-4}, compared to 10^{-4} to 10^{-6} for simple plate discharges.

When the inert argon ions, in a triode set-up as shown in Figure 2.10, are replaced with more reactive ions, one refers to reactive ion beam etching (RIBE). The ions not only transfer momentum to the surface, but they also react directly with the surface, i.e., a chemical and physical mechanism is involved. Direct reactive ion etching of a substrate is the exception rather than the rule. We will learn further that the chemical reactions at the surface usually are dominated by radicals.

Ion-beam etching typically involves an ion source energy of up to 1.5 keV and a current density of 25 mA/cm^2 covering a diameter of 3 to 8 cm. This also is referred to as showered ion etching. A second type of ion beam etching, a maskless technique called focused ion beam (FIB), in which the beam is made extremely narrow and used as a direct writing tool, will be discussed in more detail in Chapter 7.

Etching Profiles in Physical Etching

The ideal result in dry or wet etching is usually the exact transfer of the mask pattern to the substrate, with no distortion of the critical dimensions. Isotropic etching (dry or wet) always enlarges features and thus distorts the critical dimensions. Chemical anisotropic wet etching is crystallographic. As a consequence, critical dimensions can be maintained only if features are strategically aligned along certain lattice planes (see Chapter 4, Wet Bulk Micromachining). With sputtering the anisotropy is controllable by the plasma conditions.

As can be deduced from Figure 2.5A, ion etching and ion milling do not lead to undercutting of the mask but the walls of an etched cut are not necessarily vertical. A variety of factors contribute to this loss of fidelity in pattern transfer, and they are either caused by involatile sputtering reaction products or by special ion-surface interactions. We shall briefly review these dry physical etching problem areas.

Faceting Due to Angle-Dependent Sputter Rate

Even when starting out with a vertical mask side wall, ion sputtering exhibits a tendency to develop a facet on the mask edge at the angle of maximum etch rate. This corner faceting is detailed in Figure 2.11A. The corner of the mask, always a little rounded even when the mask walls are very vertical, etches faster than the rest and is worn off. Faceting at the mask corner arises because the sputter yield for materials usually is a function of the angle at which ions are directed at the surface. The sputter-etch rate of resist, for example, reaches a maximum at an

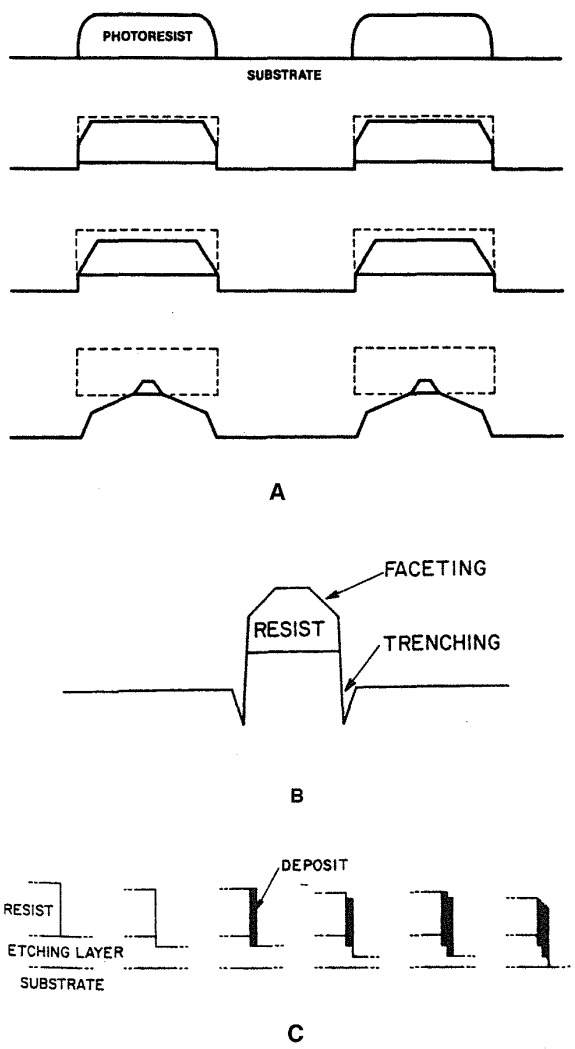

FIGURE 2.11 Limitations of dry physical etching. (A) Faceting. Sputtering creates angled features. An angled facet (~60°) in the resist propagates as the mask is eroded away. Sloped walls may also be created in the underlying substrate. (B) Ditching due to glancing incidence of ions. (C) Redeposition of material sputtered from the bottom of a trench. (B and C from Shutz, R. J. in *VLSI Technology*, Sze, S. M., Ed., McGraw-Hill, New York, 184–232, 1988. With permission.)

incidence angle of about 60°, more than twice the rate at normal incidence.[8] Sloped mask sidewalls may eventually be followed by sloped etch steps in the substrate. The faceting of the substrate itself will proceed along its own preferred sputtering direction angle. The faceting is more pronounced with an applied bias due to the increased electric field at corners. Usually the faceting affects only the masking pattern, and its influence on the fidelity of the pattern transfer process can be minimized by making the mask sufficiently thick. The faceting can also be minimized or eliminated by a more ideal resist profile, with very little rounding of the mask corners. In the case of a resist mask, post-bake temperatures must be controlled so the reflow does not induce rounding of the resist features, leading to faceting.

It should be noted, though, that some of the disadvantages of physical etching, such as resist corner faceting, can sometimes be exploited. For example, a gently sloping edge is advantageous to facilitate metal coverage or planarization because a tapered sidewall is easier to cover than a vertical wall, especially when using line-of-site deposition methods. The method most often used to obtain such a taper is a controlled resist failure, i.e., ***erodible or sacrificial masks.*** In other words, the 'negative effect' described in connection with Figure 2.11A is put to good use.

Ditching

When the slope of the side of the mask is no longer vertical, some ions will collide at a glancing angle with the sloping edges before they arrive at the etch surface. This gives a local increase in etch rate leading to ditches (Figures 2.5A and 2.11B). For this mechanism to be active there must be a sizable fraction of ions with at least slightly off-vertical trajectories, or the sidewall must have a slight taper as shown in Figure 2.5A and 2.11B.[24] The taper of the sidewall could result, for example, from redeposition (see next section) or faceting (see above). Since ditching is a small effect (say, 5%), it often goes unnoticed unless thick layers are etched.

Off-vertical ion trajectories could also be caused by sheath scattering and field nonuniformities. Most ions impinge perpendicularly on the substrate. Scattering of a small fraction of ions in the sheath causes a distribution of impinging angles. This scattering in the sheath is responsible for hourglass-shaped etch profiles that have been observed in trench etching of silicon.[14] Besides sheath scattering, there is a second mechanism active which may lead to skewing of ion directionality; namely, inhomogeneities in the electrical field at the substrate surface. When etching conductors, the bending of electric field lines due to surface topography has the effect of enhancing ion flux at feature edges and leads to ditching. On the other hand, when etching insulators, charging effects may cause appreciable ion fluxes to the sidewalls of a trench and contribute to lateral etching. The latter will again lead to hourglass-shaped trenches. The importance of the effect is very much related to the electrical conductivity of the masking and etching surfaces, with the greatest significance for strongly insulating materials.[25]

Redeposition

Another sputtering limitation, already alluded to, is the ***redeposition*** of involatile products on step edges (Figure 2.11C). Redeposition involves sputtered involatile species from the bottom of the trench settling on the sidewalls of the mask and etched trench. The phenomenon manifests itself mainly on sloped sidewalls.

By ***tilting and rotating*** the substrate during etching, etch profiles can be improved. The reasons for tilting and rotating improvements are a combination of shadowing the bottom of the step (to reduce trenching), partially etching the sidewalls of the mask (to reduce redeposition), and gaining more nearly vertical edges on the etched profiles in the substrate.[8] Especially with aspect ratios exceeding unity, redeposition becomes problematic, and reactive gas additives are necessary to generate volatile etch products. With aspect ratios above 2:1 or 2.5:1, the etching action at the bottom of too fine features tends to slow down or stop altogether. Reactive additives bring us into the realm of chemical-physical etching (discussed further below). For micromachining, tilting and rotating of substrates is a recurring topic. It is one of the desirable modifications of standard

Erodible or sacrificial masks

Comparison of the control of etch profiles by the use of erodible (sacrificial) and nonerodible mask materials.

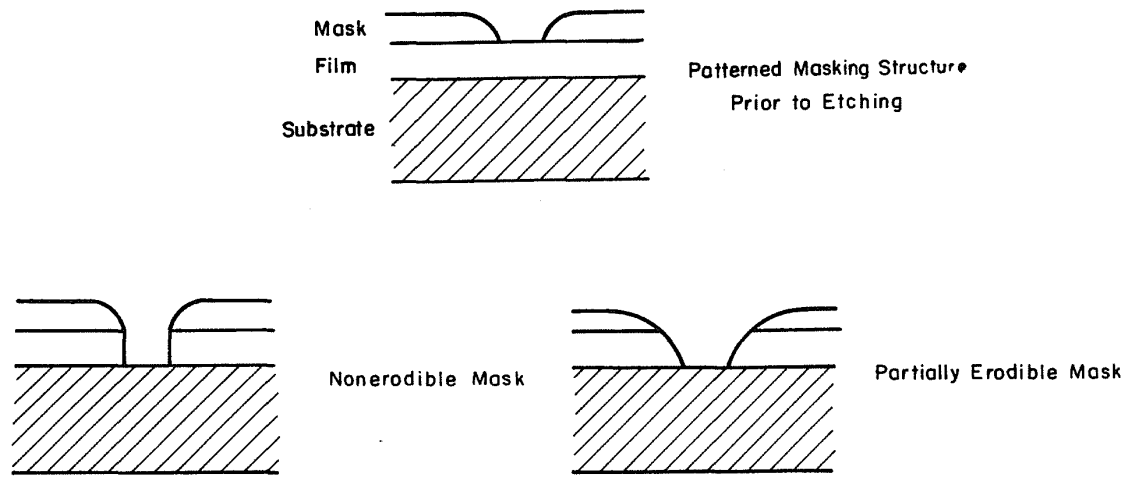

Rotating and redeposition

Typical configuration for tilting and rotating, as well as an example of redeposition in a high aspect ratio device. By tilting and rotating a sample during ion beam etching, better etching profiles can be obtained. The walls exposed to ion beam etching exhibit combined etching and redeposition while the unexposed walls are partially shadowed; rotation averages these effects out.

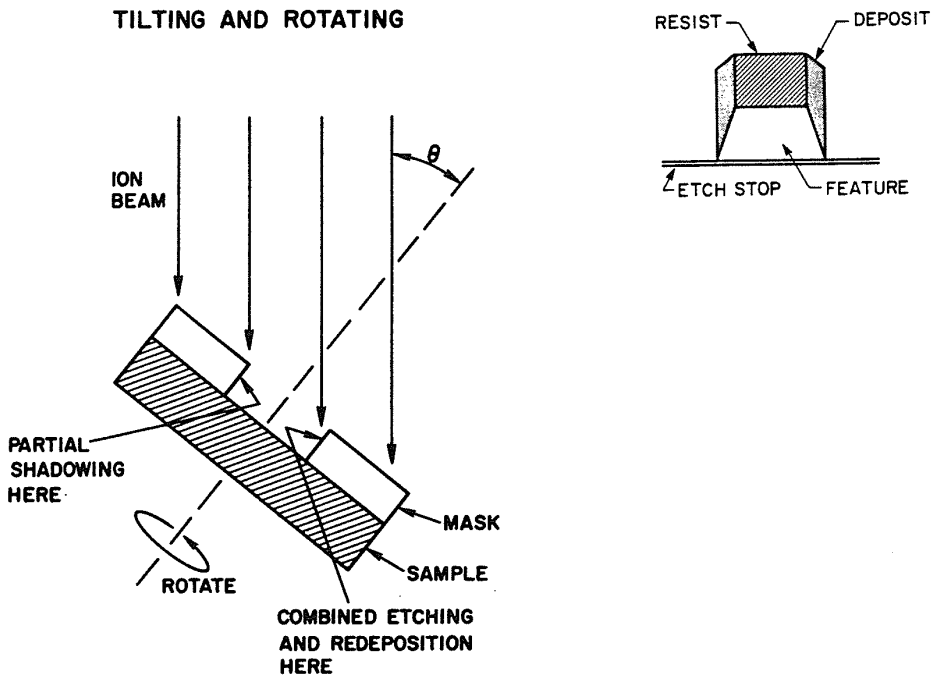

equipment one should look for in dealing with micromachining applications.

Backscattering is a form of redeposition again associated with involatile etch products. A fraction of the sputtered and involatile species from the surface is backscattered onto the substrate after several collisions with gas-phase species. This indirect redeposition may involve contaminants from the walls and fixtures in the vacuum chamber. Backscattering fixes the upper pressure limit for ion-enhanced etching. Significant redeposition can take place at pressures as low as 10 mTorr.

Physical Etching Summary

In physical etching, ion-etching or sputtering, and ion-beam milling, argon or other inert ions extracted from the glow discharge region are accelerated in an electrical field towards the substrate, where etching is purely impact controlled. Sputtering is inherently nonselective because large ion energies compared to the differences in surface bond energies and chemical reactivities are involved in ejecting substrate material. The method is slow compared to other dry etching means, with etch rates limited to several hundreds of angstroms per minute compared to thousands of angstroms per minute and higher for chemical and ion-assisted etching (as high as 6 μm/min!). Sputter etching tends to form facets, ditches, and hourglass-shaped trenches and redeposits material frequently in high aspect ratio (>2:1) features. Electrical damage from ion bombardment and implantation to the substrate can be problematic. Some of the reversible plasma damage can be removed by a thermal anneal. With the continuing increase in device complexity, which includes layers of different chemical composition, inert ion etching and ion-beam sputtering continues to find applications.

Dry Chemical Etching

Introduction

In reactive plasma etching, reactive neutral chemical species such as chlorine or fluorine atoms and molecular species generated in the plasma diffuse to the substrate where they form volatile products with the layer to be removed (Figure 2.5B). The only role of the plasma is to supply gaseous, reactive etchant

species. Consequently, if the feed gas were reactive enough, no plasma would be needed. At pressures of $>10^{-3}$ Torr, the neutrals strike the surface at random angles, leading to isotropic, rounded features. A dry chemical etching regime can be established by operating at low voltages, eliminating impingement of high-energy ions on the sample, and facilitating surface etching almost exclusively by chemically active, neutral species formed in the plasma. The reaction products, volatile gases, are removed by the vacuum system. The volatility of the formed reaction product introduces a major difference with sputtering, where involatile fragments are ejected billiard ball wise and may be redeposited close by.

Reactor Configurations

Reactive plasma etching follows the same process we encountered when discussing dry stripping. The different popular configurations for plasma etching (barrel reactor, downstream etcher, and parallel plate system) are shown in Figure 1.23. In the case of resist etching, one refers to the process as ashing. Depending on the configuration, high energy ion bombardment of the substrate can be prevented and plasma-induced device damage avoided. For example, in a barrel reactor the substrates are shielded by a perforated metal shield to reduce substrate exposure to charged high energetic species in the plasma. In a downstream stripper, the geometry of the reactor allows reactant generation and stripping to take place in two physically separated zones (triode-type configuration with a remote plasma). In parallel plate strippers, the substrates are placed inside the plasma source which leads to higher ion damage compared to the two previous methods. The diode-like, parallel plate stripper is called a reactive ion etcher (RIE), although ions rarely reactively 'eat' away the substrate.

Reaction Mechanism

The plasma etching process can be broken down into as many as six primary steps as illustrated in Figure 2.12. The first step is the production of the reactive species in the gas-phase (1). In a glow discharge a gas such as CF_4 dissociates to some degree by impact with energetic particles such as plasma electrons with an average energy distribution between 1 and 10 eV. In the dissociation reactive species such as CF_3^+, CF_3, and F are formed. This step is vital, because most of the gases used to etch thin films do not react spontaneously with the film, e.g., CF_4 does not etch silicon. In a second step, the reactive species diffuse to the solid (2) where they become adsorbed (3), diffuse over the surface, and react with the surface (4). Finally, the reaction products leave the surface by desorption (5) and diffusion (6). As in a parallel resistor combination, the total resistance is determined by the smallest resistance, the reaction with the smallest rate constant determines the overall reaction rate.

Some of the six reaction steps listed occur in the gas-phase and are termed homogeneous reactions, while others occur at the surface and are called heterogeneous reactions. For the homogeneous reactions, the plasma only plays the role of creating highly reactive species from the plasma gas. Radicals are more abundant in a glow discharge than ions because they are generated at a lower threshold energy (e.g., <8 eV), which leads to a higher generation rate. Moreover the uncharged radicals have a longer lifetime. The low-energy ions rarely act as the reactant themselves; instead, neutrals are responsible for most reactive etching (chemical etching) at pressures above 0.001 to 0.005 Torr. Radicals and molecules formed in the plasma are not inherently more chemically reactive than ions, but they are present in significantly higher concentrations. Heterogeneous reactions display even more complexity than the homogeneous reactions just described. In

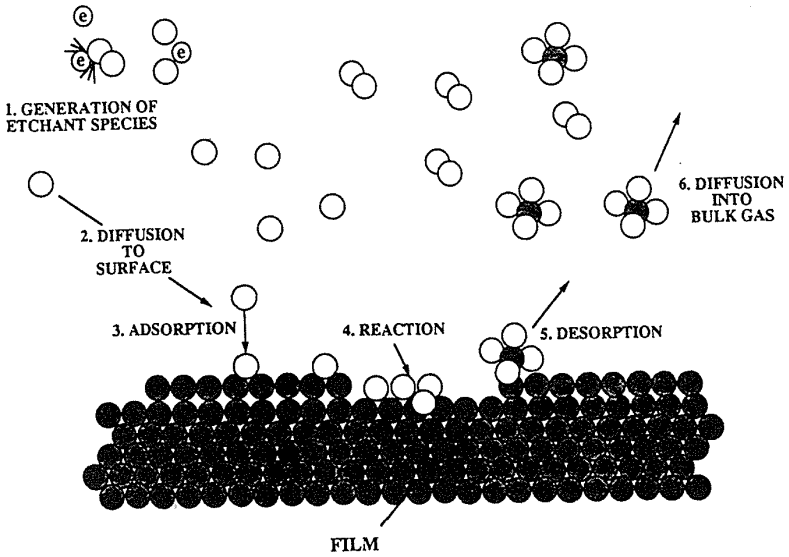

FIGURE 2.12 Primary process occurring in a plasma etch process.

principle, all the species generated in the plasma may influence the reaction rate; nonreactive species may decrease the reaction rate by blocking surface sites, and adsorption of radicals may enhance the reaction rate. Radicals and other neutrals reach the surface by diffusion, whereas ions are accelerated towards the surface by the negative potential on the substrate electrode. Besides chemically active species and ions, the effect of electron bombardment and irradiation by visible and UV radiation emanating from the plasma requires consideration. Chemical etching occurs at low bias and since, in principle, no highly energetic ions bombard the surface, sputtering itself is not an important surface-removal mechanism and radiation damage to the substrate is reduced. The term 'reactive ion etching' unfortunately is used indiscriminately for all chemical dry etching, even when ions themselves are not the major reactive species. Radicals and molecules also serve as the primary depositing species for all types of films in plasma-enhanced chemical vapor deposition (PECVD) (see Chapter 3). Ions directly participate in chemical etching only in reactive ion beam etching (RIBE), where ion reactions at very low pressures can etch at modest rates of less than 400 Å/min. RIBE is an example of physical-chemical dry etching where the same ion has both a physical component (ion impact) and a chemical component (reactive etching). Working with a remote plasma in a triode-type system (e.g., a downstream stripper) facilitates further ion bombardment reduction of and current flux to the wafer. The steps of reactant generation and actual etching are separated efficiently because charged species (mainly electrons and positive O_2^+ ions in case of a pure oxygen plasma used for stripping resist) suffer a much higher loss than reactive neutrals such as atomic oxygen due to the presence of plasma excitation.

In the absence of crystallographic effects (typically seen with III-V compounds but not with Si), chemical dry etching leads to isotropic profiles only when ions do not assist the reaction. In the case where ions do assist the chemical reaction, anisotropy is induced. Isotropic etching of the reactive species leads to mask undercutting. In some cases mask undercutting is required, for example in device fabrication involving 'lift-off' or when layers on sidewalls must be cleared.

Because of the chemical nature of the etching process, a high degree of control over the relative etch rates of different materials (i.e., selectivity) can be obtained by choosing suitable reactive gases. During photoresist stripping, an oxygen plasma removes photoresists by oxidizing the hydrocarbon material to volatile products. Fluorine compounds are used for silicon etching; many materials are susceptible to chlorine etching. For example, aluminum is etched in chlorine but not in fluorine, as aluminum chlorides are volatile and aluminum fluorides are involatile. Mixtures of gaseous compounds such as CF_4 (fluorocarbon)-O_2 assist in patterning silicon, silicon dioxide, silicon nitride, etc.

Loading Effects/Uniformity and Nonuniformity

In dry etching the number of radicals in the plasma is in proportion to the number of atoms to be removed, contrary to wet etching where the number of etchant molecules might be 10^5 times higher than the number of atoms. A so-called loading effect occurs as the result of gas phase etchant being depleted by reaction with the substrate material. The more purely chemical the etching, the bigger the loading effect. With lower pressures the loading effect becomes smaller. Conventional plasmas can sustain enough radicals to etch at a rate of 1000 Å/min. With more effective power sources such as a cyclotron or magnetron 10^4 Å/min can be achieved.

The loading effect brings an important limitation of dry etching to light; as the etch rate becomes dependent on wafer loading, uniformity is jeopardized. If the supply of reactant limits the etch rate, small variations in flow rate or gas distribution uniformity may indeed lead to etch rate nonuniformities. The gas flow is the most important parameter to control in this regard. The symmetry of the gas flow, i.e., the relative position of gas inlet and pumping port, has to be optimized for the given reactor configuration. Hence, a minimum flow rate of the reactant gas prevents the process from being limited by reactant supply. A utilization factor, U, i.e., the ratio of rate of formation of etch product to the rate of etch gas flow, may be defined and $U > 0.1$ is suggested for uniform etching. To illustrate: a 500-Å/min etch rate of a 3-in Si wafer in a CF_4 plasma corresponds to a removal rate of 5×10^{19} Si atoms per min, or a SiF_4 evolution rate of approximately 2 sccm. This means that the CF_4 flow rate should reach at least 20 sccm.[26]

The loading effect is a function of the number of wafers in the chamber and may also change while etching different features on one wafer (local loading or microloading effect). For example, after clearing an etching film from the planar regions of a surface, less residual material remains, and more etchant is available to etch the remaining material residue, say on the sidewalls of a trench.

Etching uniformity also is impacted by the relative reactivity of the wafer surface with respect to the cathode material used. Resulting nonuniformities in this case are referred to as bull's-eyes because circular interference patterns show on an etched wafer. If an aluminum electrode is used for Si or poly-Si etching in an SF_6 plasma, a very pronounced bull's-eye effect is evident. The striking nonuniformity in etching pattern results from a lower consumption of reactant species above the aluminum electrode, as aluminum only mildly reacts with reactive species formed by SF_6. By applying an electrode material that consumes the fluorine reactive species as fast as Si itself (e.g., a Si cathode), concentration gradients of reactant species at the edge of the wafer are avoided, resulting in uniform etching (see Figure 2.13).[26]

To further avoid nonuniformities, wafers should be positioned away from the edges of electrodes to eliminate edge effects caused by changing sheath thickness as well as varying angles of incidence. A good thermal contact between wafers and cathode also is important. Local temperature variations due to nonuniform heat-sinking can lead to large etch nonuniformities, particularly in chemically dominated processes.[26]

Another example of nonuniformity is the 'grass' structure sometimes observed at the bottom of a Si trench. The 'grass' consists of pillars of silicon also called 'black silicon'; Hasper speculates that the reason for the 'grass' is Al_2O_3 contamination from the mask and/or reactor walls.[27] In more recent work 'grass' formation during RIE was explained as a consequence of the sharpening of the ion angular distribution with the increasing aspect ratio of the trench during etching.[24]

Ion Energy vs. Pressure Relationship in a Plasma

In general, three factors control the etch rate in a plasma reactor: the neutral atom and free radical concentration, the ion concentration, and the ion energy. The ion and radical concentrations control the reaction rate, while the ion energy provides the necessary activation and controls the degree of anisotropy. The respective contribution to chemical and physical action of a plasma can be manipulated by varying voltage and gas pressure. For good critical dimension control, anisotropy is required and positive ions need to be formed at low pressures ($<10^{-2}$ Torr) to strike the surface at normal incidence. Etching at low pressures, with a long mean free path length of the ions, λ_i, is inherently more anisotropic, i.e., directional and less contaminating because etch reaction by-products show more volatility at lower pressures and are easier to remove, but at these lower pressures the ion density drops off quickly, causing a lower etch rate and lower wafer throughput. Increasing the power or wafer bias will increase the etch rate as the remaining ions will become more energetic. Higher ion energies can cause additional problems in terms of device damage. Really needed is a plasma source operating at low pressure with very high ion density. Operating at low pressures also reduces the effects of chemically induced loading (i.e., the total amount of material to be removed depletes the reactant chemicals) and microloading (e.g., etch-rate dependence on feature size). High plasma ion densities are created, for example, by magnetic coils increasing the electron path length in a magnetron sputtering machine. Just as the ionospheric van Allen belts are confined by the Earth's dipole field, the plasma remains confined within the magnetic envelope. This magnetic envelope also prevents electron loss to plasma exposed surfaces. With a high pressure, short λ_i, and a low voltage one gets isotropic chemical etching. The pressure-voltage relationship for a plasma is schematically represented in Figure 2.14[29] and summarized in Table 2.4. Sputtering and dry chemical etching thus represent the two extremes of a ***continuous dry-etching spectrum*** with physical etching by sputtering with inert argon ions at one end and chemical etching with reactive neutral species at the other end.

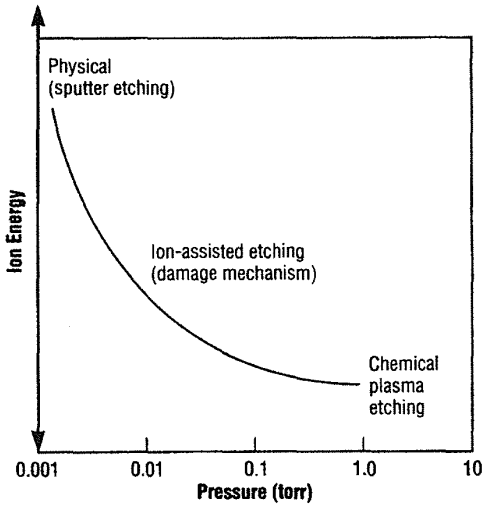

FIGURE 2.14 Ion energy vs. pressure for a plasma. (From Flamm, D. L., *Solid State Technol.*, 35, 37–39, 1991. With permission.)

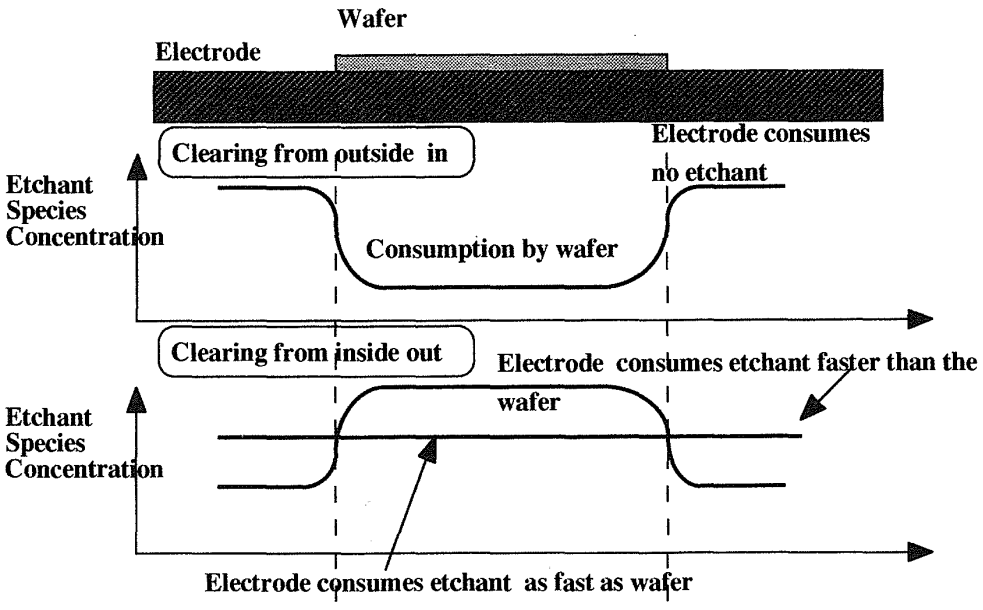

FIGURE 2.13 Chemical and physical effects leading to nonuniform etching across a wafer (bull's-eye-effect). (After Elwenspoek, et al., Universiteit Twente, *Micromechanics*, 1994.)

Gas Phase Etching without Plasma (XeF_2)

Isotropic etching of Si with xenon difluoride (XeF_2) does not require a plasma to generate the etching species. Xenon difluoride (XeF_2) is a white solid with a room temperature vapor pressure of about 4 Torr which reacts readily with Si. The Si etch occurs in the vapor phase at room temperature and at pressures between 1 and 4 Torr established by a vacuum pump throttled to the right pressure. Hoffman et al.[30] observed silicon etch rates as high as 10 μm per minute but worked at more typical rates of 1 to 3 μm. The extreme selectivity of XeF_2 to silicon over silicon dioxide and silicon nitride are well documented, but Hoffman et al.[30] have shown that XeF_2 also displays extreme etching selectivity over aluminum and photoresist. A 50-nm Al mask or a single layer of hardbaked photoresist suffice as excellent deep etch masks. The simplicity of the process, the fast etch rate as well as the resistance of even very thin layers of oxide, nitride, and Al metal make this etching process a possible choice for etching micromachined structures in the presence of CMOS electronics (in a so-called post-CMOS procedure). In Figure 2.15A, an aluminum hinge (5 μm wide and 1.1. μm thick) holding an oxide plate (200 μm square) suspended over a Si etch pit is shown. The etch pit underneath the suspended plate (not shown in Figure 2.15A) is nearly isotropic and exhibits a surface roughness of several microns. The conductivity of the Al metal was unaffected by the XeF_2 etch. The hinge contacts a polysilicon strain gauge, sandwiched between oxide layers, to protect it from the XeF_2 etchant (see Figure 2.15B). The flexible hinge enables rotation of the oxide plate out of the plane of the wafer. Hoffman et al. suggest that this contraption might function as a piezoresistive accelerometer, with the hinges providing mechanical support and electrical connectivity between the strain gauges embedded in the oxide plate proof mass and the wafer (see Figure 2.15C).

Plasma Jet Etching

Plasma jet etching is an atmospheric variant of plasma etching capable of producing very high etch rates without substrate damage. In plasma jet etching reactive chemical species are generated in a DC arc between two electrodes in a noble gas such

TABLE 2.4 Plasma Reactions

	Energy of Ions (Pressure, Torr)	
Reactive Gas	Low (0.1–10)	High (0.001–0.1)
Volatile	Plasma etching Plasma ashing	Reactive sputtering Reactive ion etching
Involatile	Plasma anodization	Reactive sputtering

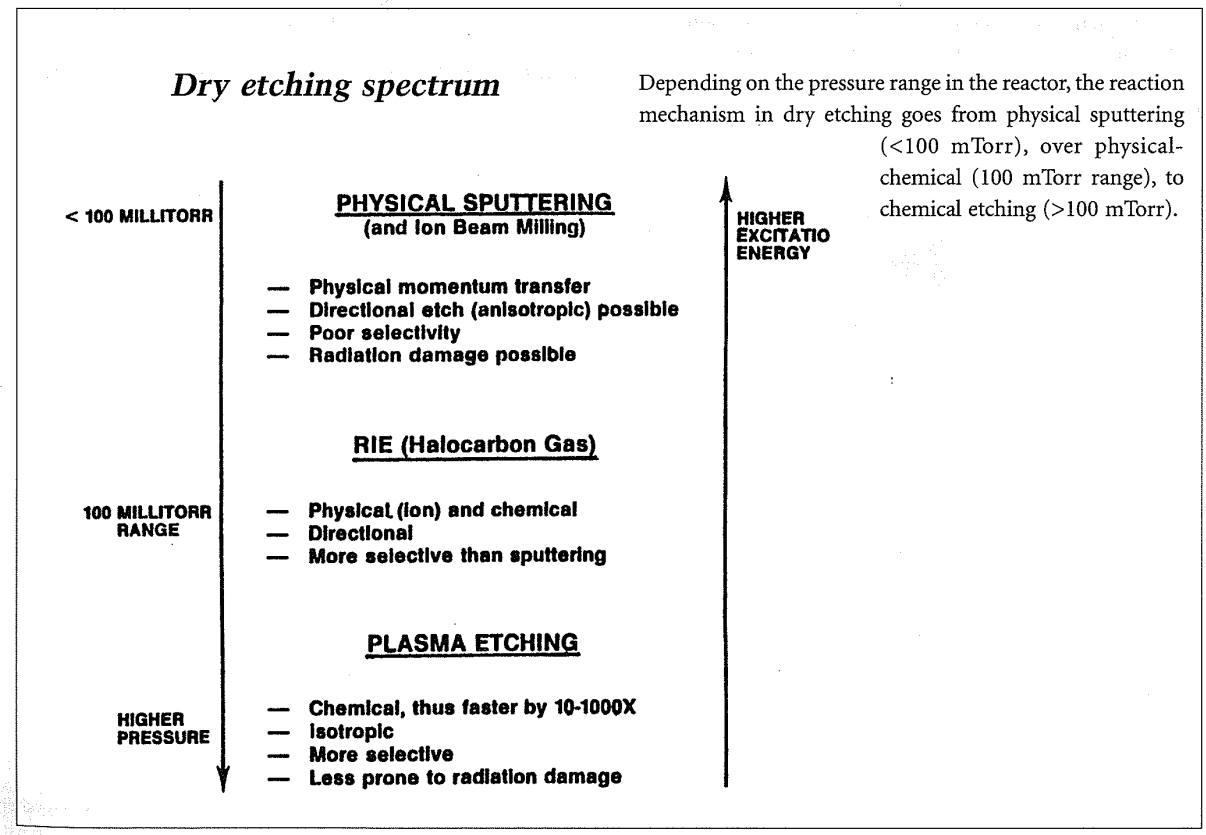

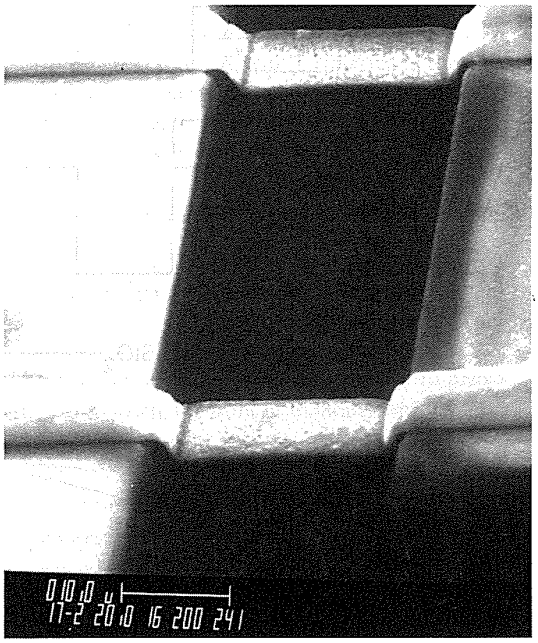

A

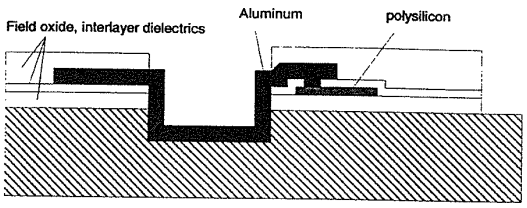

B

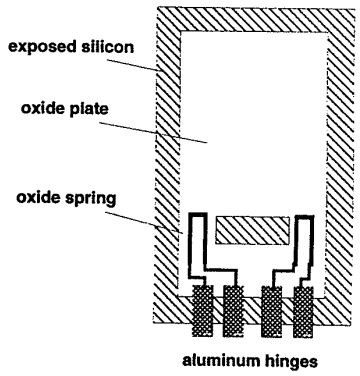

C

FIGURE 2.15 (A) Al hinge (5 μm wide and 1.1 μm thick) holding a suspended oxide plate (plate is on the right side of the photograph). The Si is etched from underneath the Al hinge and oxide plate by XeF_2. The suspended oxide plate is 200 μm square. (Courtesy of Dr. Kris Pister.) (B) Al hinge contacts a poly-Si piezoresistor embedded in the oxide plate to protect it from the XeF_2 etchant. (C) The piezoresistive accelerometer design shown enables rotation of the oxide plate out of the plane to detect orthogonal acceleration. (From Hoffman et al., MEMS '95, 288–293, 1995. With permission.)

as argon at atmospheric pressure. A stream of reactant gas (the gas jet) such as CF_4 is then flowed into the arc and onto the wafer which is located up to 12 inches away to avoid damage.[31] The technology may improve the performance and reduce the cost of bulk material removal operations such as mechanical grinding, lapping, and wet chemical etching.

Physical-Chemical Etching

Introduction

The most useful plasma etching is neither entirely chemical nor physical. By adding a physical component to a purely chemical etching mechanism, the shortcomings of both sputter-based and purely chemical dry etching processes can be surmounted.

In physical-chemical techniques, the following four types of ion-surface interactions may promote dry etching. A first is found in reactive ion beam etching (RIBE), a rather exceptional case where ions are reactive and etch the surface directly (Figure 2.16). The more general case presents itself in three types of ion-assisted etching. In one type, ion bombardment induces a reaction by making the surface more reactive for the neutral plasma species, for example, by creating surface damage (i.e., energy driven anisotropy). In another type, ions clear the surface of film-forming reaction products, allowing etching with reactive neutrals to proceed on the cleared areas (inhibitor-driven anisotropy). Finally, ion bombardment may supply the energy to drive surface reactions. Defining which step primarily causes enhanced etching is often hard to determine.

Energy-Driven Anisotropy

During energy-driven anisotropy or ion-assisted etching, bombardment by ions (<1000 eV) disrupts an unreactive substrate and causes damage such as dangling bonds and dislocations, resulting in a substrate more reactive towards etchant species (electrons or photons also can induce surface activation) (see Figure 2.5C). Vacuum pumping removes the volatile reaction products. This type of etching is referred to as reactive ion etching (RIE), when it involves reactive chemicals in a diode type reactor, and as chemically assisted ion-beam etching (CAIBE) when it involves chemical reactants (e.g., Cl_2) introduced over the substrate surface in a triode type set-up. Figure 2.8 shows the preferred set-up for RIE. Figure 2.16 represents the ideal set-up for CAIBE. We already indicated that the label RIE can cause confusion since ions are not really the dominant reactive species. In a magnetically enhanced RIE system (MERIE), a higher ion flux is obtained at lower energy through magnetic confinement of the plasma.

The etch rate reached by RIE is substantially higher than in ion etching. For example, the etch rate of Si in Ar sputtering hovers around 100 Å/ min compared to 2000 Å/min for a reactive gas such as CCl_2F_2. Chemically assisted ion etching can lead to accurate transfers of the mask pattern to the substrate and to a fair selectivity in etching different materials. The directional anisotropy ensues from operating at low pressures and high voltages. Under these conditions, the mean free path of the

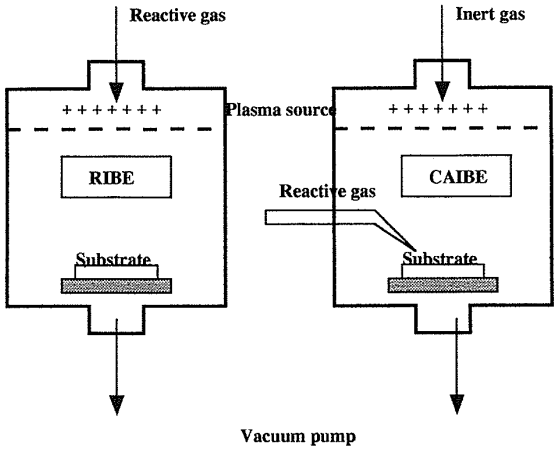

FIGURE 2.16 A chemically assisted ion beam etching system (CAIBE) compared with reactive ion beam etching system (RIBE).

reacting molecules typically grows larger than the depth to be etched, resulting in the horizontal surfaces being hit and etched by the reactive neutrals a lot more than the sidewalls. The need for energetic impinging ions, as in the case of physical etching, reduces as the complex on the surface activates more easily.

A hypothetical etch profile for Si and SiO_2 etching with a reactive gas and positive ion bombardment is shown in Figure 2.17A.[8] In the absence of ionic bombardment, the etch rate is assumed to be zero for SiO_2; consequently, the SiO_2 film etches with perfect anisotropy (vertical sidewalls). The silicon etch rate in the absence of ionic bombardment, on the other hand, is assumed finite but small; consequently, the etched feature ends up having a profile with slanted sidewalls. Mathematically, the above can be expressed in terms of etch depth, Z, undercut, X, the etch rate under bias, V_Z, and the etch rate without bias, V_X, as:

$$\frac{V_X}{V_Z} = \frac{X}{Z} \qquad 2.16$$

(See Figure 2.17B.) The anisotropy of RIE can further be enhanced by the use of helium backside cooling (as low as −120°C might be required). The low temperature suppression of chemical attack of silicon by fluorine atoms exemplifies how lower temperature further improves anisotropy and critical dimension control. While suppressing the isotropic fluorine reaction the same low temperature only slightly influences ion-assisted reactions and hence improves the anisotropy of profiles; the etch rate at $V_X = 0$ lowers or becomes zero.

With RIE, etched depths of 10 to 100 μm and beyond become within reach in a variety of materials. For example, using RIE equipment, ***through-the-wafer vias*** have been made through ***100-μm thick slices of GaAs.*** For this experiment, a GaAs wafer thinned to 100 μm was patterned with an AZ-4000 series photoresist mask 13 to 16 μm thick. The initial open area of the vias spanned 60 by 60 μm. Using a mixture of 15% Cl_2 in $SiCl_4$,

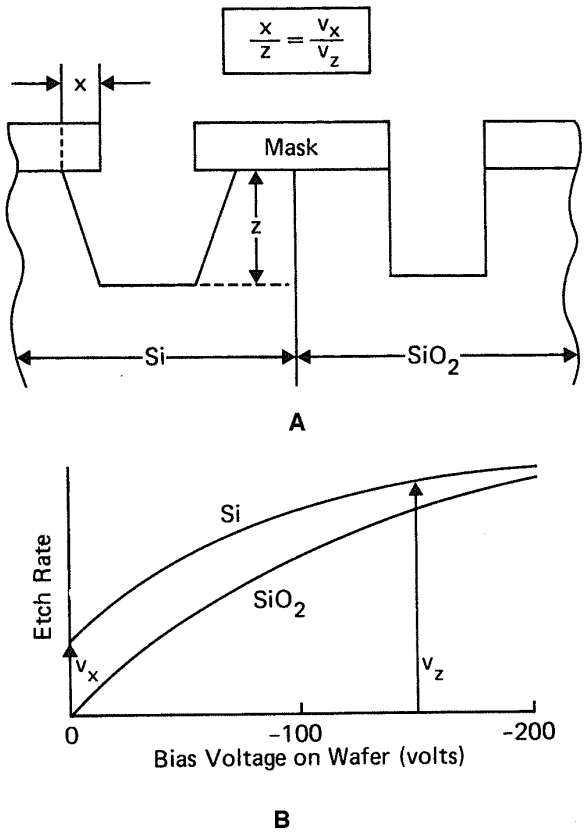

FIGURE 2.17 Relationship between the shape of the etched wall profile and the dependence of the etch rate on the wafer potential. (A) Etch profiles; (B) etch rate bias dependence. The etch rate of SiO_2 in the Z direction, V_z, increases with increasing wafer bias. Assuming no chemical etching component is present in the SiO_2 reaction, i.e., $V_X = 0$ (the etch rate equals 0 at bias = 0), an ideal vertical profile results. The etch rate of Si also is bias dependent but some reaction occurs at $V_X = 0$. In other words, a chemical component to the reaction does not need ion bombardment resulting in nonvertical walls (see text).[8]

vias were etched in the GaAs slabs.[32] For a review on etching high aspect ratio trenches in silicon by RIE, we refer to Jansen et al.[28] This article features an excellent review of possible trench shapes.

Reactive Ion-Beam Etching and Chemically Assisted Ion-Beam Etching Compared

Reactive ion-beam etching (RIBE), like CAIBE, involves chemical reactants in a triode set-up. We need to point out an important difference, though. In the case of RIBE, the reactive ions are introduced through the ion source itself; in CAIBE, the reactive gas is fed over the substrate to be etched and unreactive ions are generated in the ion source. At very low pressures in RIBE systems, reactive ions, substituting Ar ions, can sustain a modest etch rate of below 400 Å/min. In CAIBE, ion bombardment of a substrate in the presence of a reactive etchant species leads to a synergism where fast directional material removal rates greatly exceed the separate sum of chemical attack and

sputtering rates. At one point this type of etching was thought to be caused by direct chemical reactions between the ions and the surface material (as with RIBE). However, in most practical situations for etch rates ranging from 1000 to 10,000 Å/min, that possibility disappears as the ion flux is much lower than the actual surface removal rates.[8]

Via formation in GaAs slab

Through-the-wafer connections are attractive, as they improve device gain and packing density. To prepare for the via etch, the front of the wafer with the manufactured devices in place is attached to a glass substrate. The wafer is then thinned to 100 μm, and the back of the wafer is patterned with an AZ-4000 series photoresist mask that is 13 to 16 μm thick. The initial open area of the vias is 60 by 60 μm. To increase the etch resistance of the photoresist and to flow the resist to produce a sloped profile a high-temperature postbake is used. A slope sidewall is desirable to facilitate subsequent metallization. A mixture of 15% Cl_2 in $SiCl_4$ at a pressure between 150 and 300 mTorr was used.[32] (From Cooper, III, C. B., Salimian, S., and Day, M. E., *Solid State Technol.*, January, 109–112 (1989). With permission.)

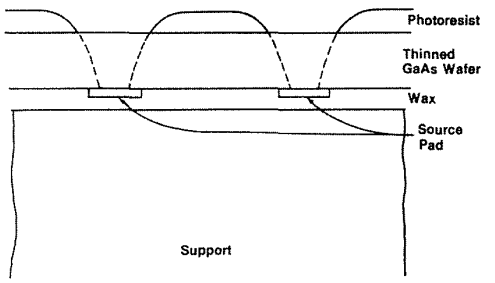

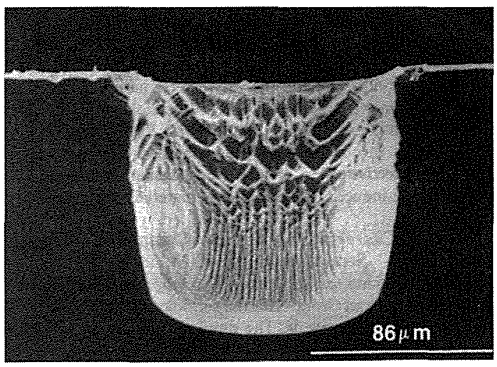

The distinction between RIBE and CAIBE is not absolute since the presence of a reactive gas in CAIBE will produce some beam ions from species that back-diffuse into the broad-beam ion source. Figure 2.16 compares a CAIBE system with a RIBE setup.

Inhibitor-Driven Anisotropy

Inhibitor-driven anisotropy embodies another example of a physical-chemical etching technique (Figure 2.5D). In this case, etching leads to the production of a surface-covering agent. Ion bombardment clears the 'passivation' from horizontal surfaces, and reaction with neutrals proceeds on these cleared surfaces only. The protective film may originate from involatile etching products or from film-forming precursors that adsorb during the etching process. Passivating gases, such as BCl_3 and some halocarbons (freons such as CCl_4 and CF_2Cl_2), are sources of inhibitor-forming species. In the latter case, the reactive gas component appears to be adsorbed on the surface, e.g., a polymer is formed, where it is subsequently dissociated by electron, ion, or photon bombardment, clearing the surface for reaction with the reactive neutrals.

An example of etch profile manipulation with inhibitor-driven chemistry using an idealized Si sample is illustrated in Figure 2.18.[8] At the top of this figure we show the Si etch rate as a function of percentage of H_2 in CF_4 for a biased and an unbiased wafer. From Figure 2.17B we remember that the Si etch rate increases as the wafer bias is increased so the etch rate curve for the biased wafer lays above the one for the unbiased wafer. If H_2 is added to a CF_4 feed gas, the Si etch rate decreases, and at some value of H_2 concentration, the nonbombarded surface etch rate decreases to zero ($V_X = 0$ at 10% H_2 in Figure 2.18) while the bombarded surface continues to etch. The decrease in etch rate stems from an increase in the amount of

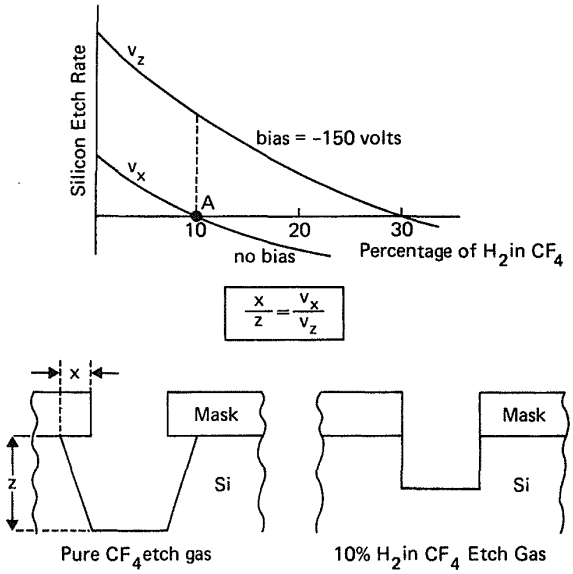

FIGURE 2.18 Trench profile manipulation by decreasing the fluorine-to-carbon ratio (through hydrogen introduction).[8]

passivating polymerization. Aggressive fluorine reacts with the hydrogen so that carbon compounds polymerize more readily. As before, Equation 2.16 can be used to calculate the ratio of underetch, X, to etch depth, Z. At $V_X = 0$, that ratio, of course, is zero.

Similarly, aluminum etching in $CCl_4 + Cl_2$ or $CHCl_3 + Cl_2$ plasmas presents a good example of an inhibitor system. Even though Cl_2 and Cl atoms formed in these plasmas are rapid chemical etchants for clean aluminum, aluminum in these plasma mixtures can afford near-vertical profiles with excellent line-width control.

Another typical example of a sidewall mechanism is the etching of phosphorous-doped Si which etches isotropically in a Cl_2 plasma but etches anisotropically when C_2F_6 is added to the source gas. Qualitatively the effect is accounted for by assuming that the two gases dissociated in the plasma are

$$C_2F_6 + e \rightarrow 2CF_3 + e$$
$$Cl_2 + e \rightarrow 2Cl + e \qquad \text{Reaction 2.1}$$

The possible surface reactions

$$xCl + Si \rightarrow SiCl_x \text{ (etching)} \qquad \text{Reaction 2.2}$$

$$CF_3 + Cl \rightarrow CF_3Cl \text{ (recombination)} \qquad \text{Reaction 2.3}$$

Reaction 2.2 results in etching of the silicon surface, and Reaction 2.3 results in recombination without material removal. Ion bombardment enhances Reaction 2.2, and Reaction 2.3 is assumed to be dominant on the sidewalls. The recombination reaction acts as a sidewall passivant.

In practice, the anisotropy brought about by the directed ion flux in a plasma allows the final etched feature to be within 10% of its dimensions in the mask and submicron resolutions become feasible. A desire to move away from sidewall passivating chemistries to avoid CD loss is prominent, especially in the IC industry. Thick sidewall coatings not only reduce CD control, they also prove difficult to strip. Processes involving little or no sidewall thickness increase are sought for tight CD control in submicron devices. In this respect wafer cooling (to as low as –120°C) presents an attractive way of obtaining sidewall protection without the need for additional chemistries. At low substrate temperatures, reaction products are involatile and can serve as very thin sidewall inhibitors. Quite generally, at lower temperatures lateral etch rate can be suppressed while using simpler chemistries. In micromachining applications where feature size is less important and aspect ratios are extreme, applying passivating chemistries is almost a necessity, but wafer cooling can help the process.

Gas Composition

Table 2.5 lists frequently used reactive gases and typical applications.[6] Oxidizing additives are added to the plasma to increase etchant concentration and to suppress polymerization. The addition of oxygen to CF_4 in Si etching typifies the procedure.[33] Oxygen, at concentrations below 16%, reacts with CF_X radicals to enhance F atom formation (increase of fluorine-to-carbon ratio F/C) and eliminate polymerization. At yet higher concentration, adsorbed oxygen on the surface depresses the etch rate.[33] Radical scavengers such as hydrogen increase the concentration of inhibitor former and reduce etchant concentration of fluorine in the etchant (decrease of F/C) (see also example in Figure 2.18). Heinecke[34] realized that the etch ratio of SiO_2/Si can be increased either by adding H_2 to the CF_4 feed gas or by employing CHF_3 or, in general, fluorocarbons displaying a smaller F/C ratio than CF_4. Adding hydrogen to fluorocarbon gases helps promote CF_X film growth (such as CF_2, C_2F_4) for selective SiO_2 etching. The carbon accumulates less on oxide surfaces than on Si surfaces, as SiO_2 surfaces directly react with the hydrogen. By adding hydrogen, the carbon blocking increases (especially on the Si) because hydrogen scavenges fluorine forming HF and preventing reaction with carbonaceous species on the surface.

The same approach helps to optimize the selectivity on other oxide/nonoxide systems (e.g., SiO_2/resist, SiO_2/Si_3N_4, Ta_2O_5/Ta, etc.). The F/C ratio should not be made smaller than two or contamination of the whole system with C_XF_Y polymer sets in. Factors that tend to control polymerization and selectivity are temperature, hydrogen concentration, pressure, and ion bombardment. Some etchants, such as Cl atoms, do not readily etch through thin native oxide films on, for instance, Si, Nb, and Al. These native oxides prevent the onset of etching unless small amounts of native oxide etchants, such as BCl_3, are added. Inert gases such as argon or helium help stabilize the plasma, enhance anisotropy, improve uniformity, or reduce the etching rate by dilution. Since helium has a high thermal conductivity, it also improves heat transfer between wafers and the supporting electrodes.[26]

TABLE 2.5 Frequently Used Reactive Plasma Gases

Etchant: Purpose	Composition (Additive-Etchant): Application
Oxide etchant: Etches through oxide to initiate etching	C_2F_6-Cl_2: SiO_2 BCl_3-Cl_2: Al_2O_3 CCl_4-Cl_2: Al_2O_3
Oxidant: Increases etchant concentration and suppresses polymerization	O_2-CF_4: Si N_2O-CHF_3: SiO_2 O_2-CCl_4: GaAs, InP
Inert gas: Stabilizes plasma, dilutes etchant, improves heat transfer	Ar-O_2: organic material removal He-CF_3Br: Ti, Nb
Inhibitor former: improves selectivity, induces anisotropy	C_2F_6-Cl_2: Si BCl_3-Cl_2: GaAs, Al H_2-CF_4: SiO_2 CHF_3-SF_6: Si O_2(50%)-SF_6: Si
Water and oxygen scavenger: prevents inhibition, improves selectivity	BCl_3-Cl_2: Al H_2-CF_4: SiO_2
Radical scavenger: increases film formation and improves selectivity	H_2-CF_4: SiO_2 CHF_3-SF_6: Si CF_3Br-SF_6: Si CF_2Cl_2-SF_6: Si

(Most data from Flamm, D. L., *Solid State Tech.*, 49–54, 1993. With permission.)

The need to eliminate the use of chlorofluorocarbons (CFCs) is changing the type of gases used for dry etching purposes. The evolution in gas mixtures is captured in Table 2.6.[17] The primary new etchant gases are SF_6, NF_3, and SiF_4 (fluorine-based etch); Cl_2, BCl_3, and $SiCl_4$ (chlorine-based etch); and Br_2 (bromine-based etch). For very aggressive etch chemistry at low pressures (e.g., to etch deep trenches in Si) HBr also gained popularity. Other new etchant gases include $SiBr_4$, HI, I_2, and even nonhalogenated gases such as CH_4 and H_2. Table 2.7 lists etchants appropriate for etching common electronic materials. Table 2.8 presents an overview of the etch rates or etch ratios for a variety of important microfabrication materials in some popular reactive gases and gas mixtures.[38] Examples are etching of photoresist on Si, SiO_2, Al, etc. in O_2 plasma and etching of Si with a metal mask (e.g., Al) in a CF_4 plasma. Metal masks influence the etch rate of Si or even SiO_2 by catalytic action of fluorinated metal surfaces, leading to excess production of free radicals. And finally, Table 2.9 reviews mask materials listing their suitability for a number of gases.[26] A plus sign in this table corresponds with a low etch rate and high selectivity. For further reading on gas composition for dry etching and stripping, see References 6, 17, 35–38.

Simplifying Rules

Some simple rules help interpret Tables 2.5 to 2.9 when specifying a choice of dry etchant and mask for a specific application. These rules are a set of semi-empirical observations; they should not be looked upon independently, and some state the same phenomenon in slightly different ways.[39]

1. *Fluorine-to-carbon (F/C) ratio:* During etching, polymerization occurs simultaneously. Etching stems from the fluorine and polymerization from the hydrocarbons. The dominant process will depend on the gas stoichiometry, reactive-gas additions, the amount of material to be etched, and the electrode potential. Adding hydrogen causes HF to form and the F/C ratio to drop, leading to more polymerization and less etching (see example in Figure 2.18). Decreasing the fluorine concentration can also occur by overloading the

TABLE 2.6 The Evolution in Gas Mixtures for Dry Etching

Material being etched	Conventional chemistry	New chemistry	Benefits
PolySi	Cl_2 or BCl_3 / CCl_4 / CF_4 / $CHCl_3$ / CHF_3 } sidewall passivating gases	$SiCl_4/Cl_2$	No carbon contamination
		BCl_3/Cl_2	
		$HBr/Cl_2/O_2$	Increased selectivity to SiO_2 and resist
		HBr/O_2	No carbon contamination
		Br_2/SF_6	
		SF_6	Higher etch rate
		CF_4	
Al	Cl_2	$SiCl_4/Cl_2$	Better profile control
	BCl_3 + sidewall passivating gases	BCl_3/Cl_2	No carbon contamination
	$SiCl_4$	HBr/Cl_2	
Al-Si (1%)-Cu (0.5%)	Same as Al	$BCl_3/Cl_2 + N_2$	N_2 accelerates Cu etch rate
Al-Cu (2%)	$BCl_3/Cl_2/CHF_3$	$BCl_3/Cl_2 + N_2 + Al$	Additional aluminum helps etch copper
W	$SF_6/Cl_2/CCl_4$	SF_6 only	No carbon contamination
		NF_3/Cl_2	Etch stop over TiW and TiN
			No carbon contamination
TiW	$SF_6/Cl_2/O_2$	SF_6 only	
WSi_2, $TiSi_2$, $CoSi_2$	CCl_2F_2	CCl_2F_2/NF_3	Controlled etch profile
		CF_4/Cl_2	No carbon contamination
Single crystal Si	Cl_2 or BCl_3 + sidewall passivating gases	CF_3Br	Higher selectivity trench etch
		HBr/NF_3	
SiO_2 (BPSG)	CCl_2F_2	CCl_2F_2	CFC alternatives
	CF_4	CHF_3/CF_4	
	C_2F_6	CHF_3/O_2	
	C_3F_8	CH_3CHF_2	
Si_3N_4	CCl_2F_2	CF_4/O_2	CFC alternatives
	CHF_3	CF_4/H_2	
		CHF_3	
		CH_3CHF_2	
GaAs	CCl_2F_2	$SiCl_4/SF_6$ /NF_3 /CF_4	Florine provides etch stop on AlGaAs
InP	None	CH_4/H_2	Clean etch
		HI	Higher etch rate than with CH_4/H_2

(From Peters, L., *Semicon. Intl.*, 66–70, 1992. With permission.)

TABLE 2.7 Plasma Etchants for Microelectronic Materials

Material	Common Etch Gases[a]	Dominant Reactive Species	Product	Comment	Vapor Pressure (Torr at 25°C)
Aluminum	Chlorine-based	Cl, Cl_2	$AlCl_3$	Toxic gas and corrosive gases	7×10^{-5}
Copper	Forms low pressure compounds	Cl, Cl_2	$CuCl_2$	Toxic gas and corrosive gases	5×10^{-2}
Molybdenum	Fluorine-based	F	MoF_6	—	530
Polymers of carbon and photoresists (PMMA and polystyrene)	Oxygen	O	H_2O, CO, CO_2	Explosive hazard	H_2O = 26, CO, CO_2 > 1 atm
III-V and II-VI compounds	Alkanes	—	—	Flammable gas	—
Silicon	Fluorine- or chlorine-based	F, Cl, Cl_2	SiF_4, $SiCl_4$	Toxic gas	SiF_4 > 1 atm, $SiCl_4$ = 240
SiO_2	CF_4, CHF_3, C_2F_6, and C_3F_6	CF_X	SiF_4, CO, CO_2	—	SiF_4 > 1 atm, CO, CO_2 > 1 atm
Tantalum	Fluorine-based	F	TaF_3	—	3
Titanium	Fluorine- or chlorine-based	F, Cl, Cl_2	TiF_4, TiF_3, $TiCl_4$	—	$TiF_4 = 2.10^{-4}$, $TiCl_4$ = 16
Tungsten	Fluorine-containing	F	WF_6	—	1000

[a] Common chlorine containing gases: BCl_3, CCl_4, Cl_2, and $SiCl_4$. Common fluorine containing gases: CF_4, SF_4, and SF_6. (After References 6, 26, 38, and 39.)

TABLE 2.8 Frequently Used Reactive Plasma Gases, Reported Etch Rates, and Etch Ratios

Film/Underlayer (F/U)	Etch Ratios-F/U
Si_3N_4 over AZ-2400 resist	CF_4-10
SiO_2 over AZ-1350 resist	CF_4/H_2-10
Poly Si over PBS resist	CF_4-15
PSG over AZ-1350	SF_6-10
SiO_2 over Si underlayer	CF_3 Cl-30
Si_3N_4 over SiO_2 underlayer	NF_3-50
Poly-Si over SiO_2 underlayer	CCl_4-10
Si over SiO_2 underlayer	SF_6-30
Etchant	**Material and Etch Rate (Å/min)**
Ar	Si-124, Al-166, resist-185, quartz-159
CCl_2F_2	Si-2200, Al-1624, resist-410, quartz-533
CF_4	Si-900, PSG-200, thermal SiO_2-50, CVD SiO_2-75
C_2F_6-Cl_2	Undoped Si-600, thermal SiO_2-100
CCl_3F	Si-1670

Source: Moreau, *Semiconductor Lithography* (Plenum Press, New York, 1988). With permission.

TABLE 2.9 Mask Materials in Dry Etching

Mask Material	SF_6	CHF_3	CF_4	O_2	N_2
Si	–	+/–	–	+	+
SiO_2	+/–	–	+/–	+	+
Si_3N_4	+/–	–	+/–	+	+
Al/Al_2O_3	+	+	+	+	+
W	–	–	–	+	+
Au	+	+	+	+	+
Ti	–	–	–	+	+
Resist	+/–	+/–	+/–	–	+
CFs	+	+	+	+	–

Source: After Elwenspoek et al., Universiteit Twente, *Micromechanics,* (1994).

reactor, leading to overconsumption of fluorine and favoring of polymerization. Adding oxygen to a fluorine carbon mixture leads to formation of CO and CO_2 reaction products, increasing F/C and thus the etch rate while decreasing the polymerization tendency. In other words, the addition of oxygen to a gas mixture reduces the tendency of Freons™ to polymerize and increases the concentration of halogen etchants ensuing from these gases. Adding oxygen to improve the F/C ratio leads to aggressive resist etching. Gases such as NF_3 and ClF_3 allow high fluorine concentrations (for aggressive Si etching) without the addition of oxygen, thus avoiding resist attack.

2. *Selective vs. unselective dry etching:* The polymerizing point of the gas (i.e., the composition of the gas where polymerization takes over) primarily determines selectivity. The closer one works to the polymerization point the better the selectivity. Factors that have a tendency to increase polymerization rate increase selectivity: decreased temperature, high hydrogen concentration, low power, high pressure, and high monomer concentration all increase polymerization and thus selectivity. Typical unselective etchants for Si and polysilicon, used for noncritical etching are CF_4 and CF_4-O_2. Less toxic gases such as CF_4 and SF_6 get preference over fluorine and are more selective, leading to polymerization. The most commonly used gases for selective Si etching are Cl_2, CCl_4, CF_2Cl_2, CF_3Cl, Br_2, and CF_3Br, along with

mixtures such as Cl_2-C_2F_6. Small additions of halogens significantly increase the selectivity of fluorine-based etchants, especially the selectivity of Si over silicon dioxide. For pure chlorine, the etch rate of SiO_2 is so low that even a native oxide can prevent the Si from etching. The high selectivity of SiO_2/Si is a major objective of many plasma processes to mimic the wet HF etch.

3. *Substrate bias:* A negative bias on a surface exposed to the plasma increases, at a constant F/C ratio, the etching behavior over polymerization tendency. This effect is caused by the enhanced energy of the ions striking the surface, resulting in polymer sputtering.

4. and 5. *Dry etching of III-V compounds:* Group III halides, particularly fluorides, tend to be involatile. As a result, F plasmas are usually substituted for chlorine-containing plasmas and elevated substrate temperatures are used to further help volatize the chlorides (fourth rule). The chemical composition (Ga/As ratio) of the different atomic planes in GaAs vary, and crystallographic etch patterns are observed under etch conditions in which chemical processes dominate (fifth rule). The latter establishes a major difference with dry Si etching where crystallography does not play a role.

6. *Metal etching:* Chlorocarbons and fluorocarbons typically are used to etch metal films since they can reduce native metal oxides chemically. Oxygen and water vapor must be rigorously excluded during etching because of the high stability of the metal-oxide bond. Also, because of the stability of that bond, ion bombardment is essential. Since AlF_3 is not volatile, chlorine-containing gases are preferred for Al etching, while tungsten can be etched in fluorine (SF_6 or NF_3/chlorine).

7. *Organic films:* To retain an organic mask while etching away materials such as SiO_2 and Si_3N_4 one must work in etching conditions close to the polymerization point so that some loss of resist is compensated by condensation of reaction product, e.g., CF_4-C_2H_4 and CF_4-H_2. We already discussed that CF_4-O_2 plasmas severely degrade resist materials.

8. *Carbon-containing additives:* Carbon-containing additives generally degrade the selectivity of Cl- and Br-based inorganic chemistries for polysilicon etching over SiO_2. The Br atom attack on SiO_2 is thermodynamically unfavorable, whereas reactions between carbon halogen bonded species and SiO_2 are exothermic. It was shown that with HBr a polysilicon over silicon dioxide selectivity of 300:1 can be achieved when completely avoiding carbon containing gases or photoresists; the presence of resists or carbon traces in gases severely diminishes this ratio.

New Plasma Sources

New plasma sources keep emerging. More recently introduced plasma sources are based on ***microwave electron cyclotron resonance*** (ECR)[40] sources and ***inductively coupled plasma (ICP) technology,***[7] both producing very high-density plasmas.

In ECR reactors, a magnetically enhanced source is driven by microwave excitation resonating at the orbital frequency where electrons circle in the magnetic field. The 2.45-GHz microwave frequency is generated by a magnetron and injected into an etching chamber, enclosed by a quartz bell-jar, through a waveguide. A magnetic field generated by solenoid coils is applied to the chamber. The interaction of the magnetic field and the microwaves result in an intense, high-density plasma maintainable at low pressure (usually 10^{-5} to 10^{-2} Torr). In many ECR systems the wafers are placed downstream of the plasma to further limit their exposure to this intense discharge. Wafers can also be biased to control ion bombardment energy. Like MERIE, ECR produces higher plasma densities with low energy density, reducing charge-up damage. Using ECR, Juan et al.[41] demonstrated that the n^{++} Si etch increases, but the p^{++} Si etch rate decreases with respect to lightly doped Si. It was thus established that with a high microwave power, high RF power, and an increased temperature a large difference in etch rates of p^{++} and n^{++} Si results.

In an ICP source, a plasma is driven inductively with a power source operating at the standard 13.56 MHz. Such ICP sources create high-density, low-pressure, low-energy plasmas by coupling ion-producing electrons to the magnetic field arising from the RF voltage. In ICP sources, one shields the plasmas from the electric field of the RF to avoid capacitive coupling which tends to create high-energy ions. The Alcatel radio frequency (RF) inductively coupled plasma source has recently been advanced as an ideal source for deep anisotropic Si etching.[7] This equipment, using fluorine based gases, etches silicon at rates of 6 μm/min with an etch uniformity better than +/– 5% while maintaining a Si:SiO_2 selectivity of more than 150:1 (wafer at –100°C). Etch depths greater than 250 μm and profile angles of +/– 1 degree were demonstrated while aspect ratios of 9:1 were achieved (e.g. a 4 μm wide and 35 μm deep trench). The electron density in this plasma source reaches $>10^{12}/cm^3$ in argon.

The ideal dry etching technology of the future will have high plasma densities ($>10^{11}/cm^3$) in order to achieve a high etch rate while operating at a low pressure (1 to 20 m Torr). Low pressure increases ion directionality and discourages microloading. The source also needs to produce ions uniformly in energy and distribution while keeping the ions' energy low. For building high aspect ratio micromachines, cryogenic cooling of the substrate will gain importance and might, for certain applications, become a less expensive means to build molds than the LIGA technique (see Chapter 6).

Dry Etching Models — *In Situ* Monitoring

A serious impediment to more effective use of plasma etching is the large number of parameters that affect the process.[42] Just consider pressure and temperature. Pressure influences the ion-to-neutral ratio and fluxes of these particles, the sheath potentials and energy of the ions bombarding surfaces, the electron energy, and the relative rate of chemical kinetics. Temperatures, both gas and surface, have a profound influence on discharge chemistry as well. Only the surface temperature is really controllable and influences selectivity, etch rates, degradation of

Microwave electron cyclotron resonance (ECR)

(From Editorial, *Semicon. Intl.*, 72–76, 1992. With permission.)

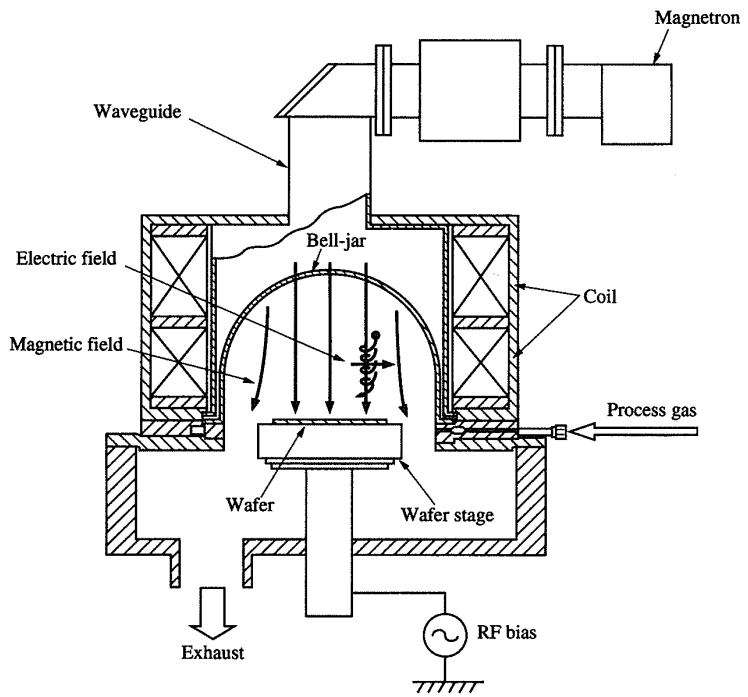

resist masks, and surface roughness (higher temperature leads to a rougher surface).

Also, electrode area ratio, RF frequency, and power will alter plasma and electrode potentials, thereby changing the ion energies. At lower frequencies, where ions can respond directly to the oscillating field, ions can attain the maximum energy corresponding to the maximum field across the sheath. As a result, for a constant sheath potential, ion bombardment energies are higher at lower frequencies (lower than 50 kHZ). Nonuniformity can be caused by gradients in etchant concentration. Such gradients are responsible for the dreaded bull's-eye etching pattern, where the etch rate decreases monotonically from the wafer periphery to its center (see above). Pressure, power, and gas flow must be adapted until the specified uniformity is obtained.

Predicting the exact relation between the flux and the energy of particles striking a wafer surface and the actual etch rate still is not state of the art, largely because no equilibrium is attained in these dry etching reactors and the kinetics are not known for most reactions.[8] Consequently, *in situ* monitoring of the plasma to improve etching uniformity is an important area for further research.[43,44] Besides measuring these controlling parameters, techniques such as optical emission spectroscopy (OES) to map *in situ* etchant concentration are coming to the foreground as sensitive and effective endpoint detectors. Emissions can emanate from etchants, etch products, or their fragments. An optical spectrometer is set to the line of a reaction product of interest and one follows its intensity during an etch cycle. Laser interferometry (for thin transparent films such as polysilicon, silicon dioxide, and silicon nitride) and laser spot reflectance (for opaque, highly reflecting metal films) are used to monitor film thickness and film disappearance, respectively. Also, the ***temperature of the wafer*** during reactive ion etching affects process quality in terms of photoresist integrity, selectivity, etch rate, and etch residues. An *in situ* temperature monitor enables one to improve the performance during the plasma etch.[45]

Comparing Wet and Dry Etching

In bulk micromachining, requiring more extreme topologies (more z-axis) than classical IC devices, wet etching of crystalline Si still dominates the state of the art. Wet anisotropic etching of Si results in atomically smooth planes and atomically

Inductively-coupled plasma

This electrostatic, shielded, inductive-coupled plasma source produces electric field lines from helical resonator combined with an electrostatic shield to produce electric field lines that are circumferential in response to the axial RF magnetic field.

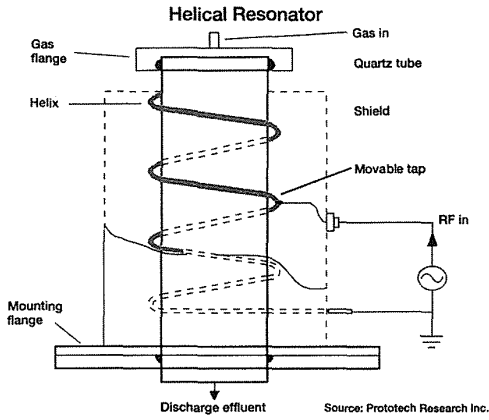

Wafer temperature

Noncontact temperature monitoring of wafer temperature during plasma etch. The monitor relies on the temperature dependence of intrinsic optical properties of silicon, as detected from the back surface of a wafer. (From Duek et al., *Semicon. Intl.*, 208–210, 1993. With permission.)

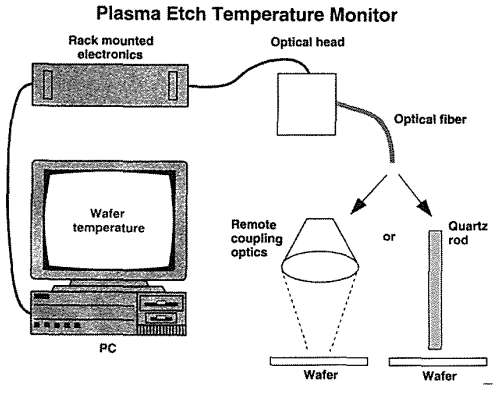

sharp edges, properties which are hard to obtain with dry etching.

Dry etching already is predominately used in the IC manufacture, and, with higher aspect ratio devices and better materials selectivity being attained the same is happening now in micromachining. Besides selectivity and aspect ratio, problems with and concerns about the slow dry etch rate and high sensitivity to operating parameters are being addrressed. Etch rates as high as 6 μm/min have become possible and operation is much more automated. A more recent concern is the search for alternative chemistries since production of chlorofluorocarbons (CFCs) were banned after 1995. According to the Montreal Protocol, all ozone-depleting CFCs must be eliminated by the year 2000. This includes etchants such as $CFCl_3$, CCl_2F_2, CF_3Cl, C_2F_5Cl, and CF_3Br.[46] Environmental issues dictated a switch from wet to dry etching for most IC applications. Another more decisive concern was the need for better CD control. A lot more research and development are needed to establish new dry etching schemes that outperform the wet anisotropic etch performances.

Surface micromachining relies on both wet and dry etchants, with processes similar to the ones used in the IC industry. For example, wet etchants are employed to etch away sacrificial layers (e.g., HF to etch CVD phosphosilicate glass) while dry etching helps to define polysilicon structural elements (e.g., in a NF_3-O_2 plasma). A combination of wet and dry techniques presently makes up the majority of Si micromachining work. Table 2.10 compares the characteristics of dry vs. wet etching techniques.

See Appendix B for Dry Etching URL's.

Dry Etching Micromachining Examples

Examples of dry etched micromachines are presented below. They involve dry etching in single crystal Si (SCS), single crystal GaAs and polyimide, and combined wet/dry etching. In the IC industry deep trenches for device isolation and narrow contact holes also require higher and higher aspect ratios. Dry etching requirements for future IC development are presented, as well.

Example 1. Silicon Single Crystal Reactive Etching and Metallization (SCREAM)

As a first example of dry etching in micromachining we will follow some of the work by the Cornell Nanofabrication Laboratory in making laterally driven micromachines.[47,48] In laterally driven micromachines, beams and structures of various shapes should be of a construction often narrow and thick, that can move freely and in parallel to the supporting substrate while rigidly held above it. Increased thickness of beams permits greater driving power for a given voltage and increases stiffness of the device perpendicular to the plane of motion. Thin suspended beams about 2 μm thick can be made with combinations of dry and wet etching in poly-Silicon (surface micromachining, see Chapter 5), but thick single crystal beams, >20 μm, in materials such as quartz, Si, and GaAs, can best be

TABLE 2.10 Comparison of Dry vs. Wet Etching Techniques[a]

Parameter	Dry Etching	Wet Etching
Directionality	Can be highly directional with most materials (aspect ratio of 25 and higher)	Only directional with single crystal materials (aspect ratio of 100 and higher).
Production-line automation	Good	Poor
Environmental impact	Low	High
Masking film adherence	Not as critical	Very critical
Cost chemicals	Low	High
Selectivity	Poor	Can be very good
Materials that can be etched	Only certain materials can be etched (not, e.g., Fe, Ni, Co)	All
Radiation damage	Can be severe	None
Process scale-up	Difficult	Easy
Cleanliness	Good under the right operational conditions	Good to very good
Critical dimension control	Very good (<0.1 μm)	Poor
Equipment cost	Expensive	Inexpensive
Submicron features	Applicable	Not applicable
Typical etch rate	Slow (0.1 μm/min) to fast (6 μm/min)	Fast (1μm/min, anis.)
Theory	Very complex, not well understood	Better understood (see Chapter 4)
Operating parameters	Many	Few
Control of etch rate	Good in case of slow etching	Difficult

[a] See also Chapter 4.

made with dry etching the single crystalline materials, especially since thick lateral moving microstructures, given the crystallographic limitations, are very difficult to realize using wet bulk micromachining (Chapter 4). A Cornell dry etching process that obtains such laterally driven, single crystal micromachines is called SCREAM (single crystal reactive etching and metallization). This technology uses reactive ion etching both to define and release structures. SCREAM portrays a relatively new micromachining approach and represents an important new technique from several points of view. It is a self-aligned, single mask process, run at low-temperatures (<300°C), and completed in less than 8 hours that can be carried out in the presence of integrated circuitry on the same chip. The SCREAM example given here is the fabrication of single crystal, silicon-released beam structures (see Figure 2.19).[49]

As starting substrate an arsenic-doped, 0.005-Ωcm, n-type (100) silicon wafer is used. A masking layer of plasma-enhanced chemical vapor-deposited silicon dioxide (PECVD), 1 to 2 μm thick, is coated with resist (step 1 and 2). Photolithography on the photoresist layer creates the desired pattern (step 2) to be transferred onto the silicon dioxide using CHF_3-based, magnetron reactive ion etching (MERIE) (step 3). The photoresist is then stripped in an oxygen barrel etcher (step 4). The silicon dioxide mask pattern subsequently is transferred to the silicon substrate using a Cl_2/BCl_3 plasma etch. The etch depth, depending on the intended micromachine, ranges between 4 and 20 μm (step 5). Following the silicon etch, silicon dioxide is conformably deposited using plasma-enhanced chemical vapor deposition (PECVD). This oxide will serve as a protection for the sidewalls during release at a thickness of 0.3 μm (step 6). The next step is very interesting and crucial to the process. The objective is to remove the oxide from the bottom and the top of the structure without removing the oxide from the sidewalls. This selective clearing of oxide materializes in an anisotropic CF_4/O_2 etch at 10 mT. It removes 0.3 μm from the mesas and the trench bottoms while leaving the sidewalls oxides intact (step 7). In the next step, a second deep Si etch (BCl_3/Cl_2) deepens the trench further (3 to 5 μm deeper) so as to expose some Si sidewall underneath the oxide-covered part (step 8). This exposed Si will be removed during release. The release is accomplished with a SF_6 isotropic etch at 90 mT. The RIE step etches the Si out from underneath the beams, releasing them in the process (step 9). An etchant such as SF_6 hardly etches the oxide and gives good selectivity to the process. A layer of aluminum is then sputter-deposited using DC magnetron sputter deposition (see Chapter 3) (step 10). The Al can be contacted and used as drive electrodes in micromechanical resonator structures. Resonator elements with beam elements of 0.5 to 5 μm and aspect ratios >10 have been achieved using this Si SCREAM process.

The measurement of the resonant frequency variation of small resonator devices made this way (see Figure 2.19B) can be used to measure monolayer mass changes, as well as pressure, temperature, acceleration, etc. In the measurement of mass, for example, the sensitivity of the device is a function of resonant frequency and mass of the resonating structure:

$$\text{Sensitivity} \sim \frac{\text{Resonant frequency}}{\text{Mass}} \qquad 2.17$$

To build the most sensitive detector, the mass must be minimized and the resonant frequency maximized. The mechanical resonant frequency of an ideal resonator is given by:

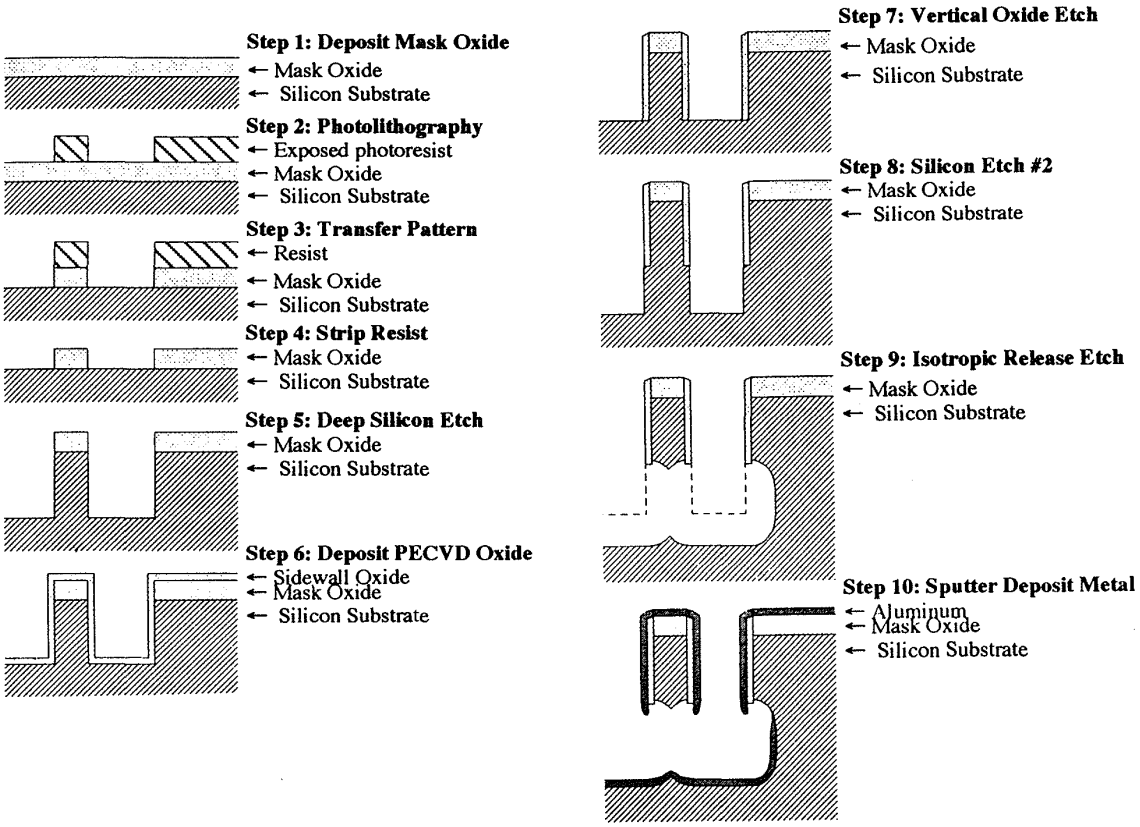

FIGURE 2.19 (A) Si-SCREAM process. Cross-section of a typical beam made using the SCREAM process. These figures show a beam and its associated parallel plate capacitor. The released beam is free to move while the plate on the right is static and can be used to measure the motion of the beam. (From Shaw, K. A. et al., *Sensors and Actuators A*, 40, 63–70 (1994). With permission.) (B) A representative SCREAM structure: SEM micrograph of a Si x,y stage with parallel plate capacitive drives and sinuous springs. (From Yao, J. J. et al., *J. Microelectromech. Syst.*, 1, 14–22 (1992). With permission.)

$$f_r = \left(\frac{k}{m}\right)^{\frac{1}{2}} \qquad 2.18$$

with k the force constant and m its mass (stiffness/mass)$^{1/2}$. A large spring stiffness must be designed and m minimized to make f_r as high as possible. For some of the very stiff, low mass structures made at Cornell, f_r was 5 MHz, with k = 55 N/m and m = 2.0×10^{-13} kg. The above simple considerations illustrate the power of micromachining in enabling more sensitive detectors.

Lateral resonant structures as shown in Figure 2.17B can also be used to make sets of comb electrodes, for example to drive precision x-y microstages for positioning or as comb-drives in accelerometers. Scanning tunneling microscopes (STM), 40×40 μm in size, have been manufactured using the SCREAM technology.[49] In the latter case, field emitter tips were integrated on an x-y stage with moving beams with nominal cross-sectional dimensions of 250 nm in width and 1000 nm in height. Displacements in the x-y directions through parallel plate capacitive drives measured ±200 nm for an applied voltage in the 50 V range.

Example 2. GaAs-SCREAM

Figure 2.20A outlines the SCREAM process steps in the case of a GaAs-based device.[48] Specifically, the process sequence for the fabrication of a cantilever beam structure identical to the Si one in Figure 2.19A is shown here again.[50] Considering two identical structures enables us to better compare the degree of complexity of micromachining in those two materials. Single crystal GaAs, in some respects, is an attractive material for micromechanics because of its optoelectronic properties. With this kind of material one can envision the possibility of vertically etched mirrors, lenses, detectors, waveguides, and semiconductor lasers, all adding up to the possibility of a totally integrated optical bench on GaAs. On the other hand, in comparison to silicon, GaAs possesses a low fracture strength (its yield strength is considerably lower: 2 vs. 7 GPa) and is more difficult to passivate than Si as its own oxides are either leaky or chemically unstable. The process example illustrates the difficulty in passivating GaAs vs. passivating Si (a dual layer dielectric is required to passivate GaAs). A more complete comparison of Si vs. GaAs in micromachining is presented in Chapter 8.

For the simple movable beam in Figure 2.20A, chemically assisted ion beam etching (CAIBE) produces deep vertical trenches, and reactive ion etching (RIE) laterally undercuts and releases the vertically etched structures from the GaAs substrate.[50] This process produces aspect ratios of 25:1 with trenches of 20 μm vertical depth to 400 nm lateral width. Plasma-enhanced chemically vapor-deposited SiN_X:H (200 nm) and a second layer of SiO_X:H (150 nm) are used to mask the GaAs substrate (Figure 2.20A,a). PECVD-SiN_X:H on GaAs easily results in structural buckling and layer cracking, but nevertheless is preferred as a conformable layer because the surface of PECVD-SiO_X:H on GaAs is rough due to the diffusion of gallium into PECVD-SiO_X:H. The PECVD-SiN_X:H deposition temperature of 100°C is selected to obtain simultaneously good dielectric properties and low residual stress in the film. To further protect the GaAs during etching, an additional sacrificial

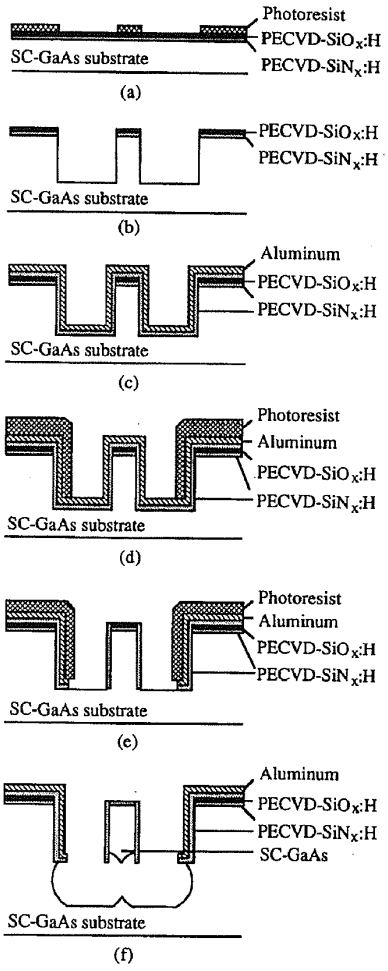

A

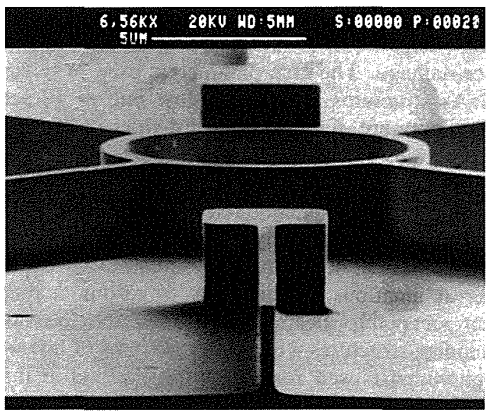

B

FIGURE 2.20 (A) Formation of a SC-GaAs cantilever beam with aluminum electrodes adjacent to each side of the beam using PECVD-SIN_x: H for insulation and for the top and sidewall etch mask. (From Zhang, et al., *MEMS '92*, 72–77. With permission.) (B) SEM micrography showing SC-GaAs circular and angled straight-line features after the CAIBE step. (From Zhang, Z. L., *J. Microelectromechanical Systems*, Vol. 2, No. 2, June 1993, 66–73. With permission.)

PECVD-SiO_X:H is deposited. The thermal expansion mismatch between the two dielectrics is less than between either dielectric and the GaAs. The pattern producing freestanding beams in GaAs is then printed in a photoresist layer on top of the bilayer dielectric. Plasma etching with CHF_3/O_2 transfers this image into the dielectric layer. The pattern in the dielectric stack subsequently is transferred to the single crystal GaAs by CAIBE (Figure 2.20A,b) using a 500-eV, 0.1-mA/cm² Ar ion beam and a Cl_2 flow of 10 ml/min. After the CAIBE process, the remaining photoresist is stripped in an oxygen plasma and a 300 nm PECVD layer of SiN_X:H is conformably deposited. Subsequently, using DC magnetron sputtering, a 400-nm layer of aluminum is deposited (Figure 2.20A,c). Photoresist is spun on the Al layer and the aluminum side-electrode pattern is printed in the resist, developed (Figure 2.20A,d), and then transferred to the Al by a Cl_2/BCl_3 etch. The latter step removes the Al from the areas that have been cleared of resist. Prior to the aluminum deposition, contact windows are formed to allow electrical contact to both the GaAs substrate and the movable GaAs beams. To clear the PECVD-SiN_X:H (from the second deposition of this compound) from the bottom of the trenches and to retain the dielectric elsewhere, a highly anisotropic CHF_3/O_2 is applied (Figure 2.20A,e). Finally, the GaAs structures are released from the substrate using a chlorine-based RIE (Figure 2.20A,f). The top and sidewalls of the GaAs structure remain protected by the PECVD-SiN_X:H and PECVD-SiO_X:H mask. At the end of the beam-releasing etch, the PECVD-SiO_X:H is consumed, i.e., it acts as a sacrificial mask. Finally, the photoresist for the Al patterning is stripped in oxygen. In a simplification of the process described in Figure 2.20A, Zhang et al.[48] recently discovered an improved PECVD-SiN_xH_y conformal coating enabling a single dielectric mask for the GaAs SCREAM process. Figure 2.20B demonstrates circular and angled straight-line features in SC-GaAs produced with the simplified process.

Example 3. Dry Etching of Polymeric Materials

Electron Cyclotron Resonance to Etch Polyimide

Juan et al.[51] use electron cyclotron resonance (ECR) to etch polyimide molds for the fabrication of electroplated microstructures in one of several reported 'pseudo-LIGA' processes (see also Chapter 6). A fast polyimide etch rate of 0.91 μm/min and a high selectivity over a Ti etch mask of 3150:1 was reached in an oxygen plasma. Polyimide (Dupont Pyralin® PI-2611) was spun on in multiple coatings and cured at 380°C for one hour. According to these authors, etching with an ECR source is 10 times faster and six times more selective than conventional RIE. The combination of magnetic confinement and microwave power, leading to an order of magnitude greater dissociation efficiency at much lower pressures than RIE, reduces scattering of reactive species and promotes vertical profiles and smooth surface morphology. Cooling down to –130°C helps maintain a vertical etch profile by suppressing spontaneous chemical reactions. This way, lateral resonator elements, 32 μm thick with a 1-μm gap, have been fabricated in polyimide, and electroplated Ni accelerometers, with an aspect ratio of 11:1 were formed from these polyimide molds. Compared to LIGA, where the average wall roughness is below 50 nm, the walls produced in this process still appear rough, but for many applications they might be good enough.

MERIE to Etch Polyimide

To obtain the optimum anisotropy in high aspect ratio devices, one cools the substrate, uses high RF power density, works at the lowest possible pressure, utilizes high flow rate, and relies on sidewall-passivating additives. We quote more examples of the anisotropic power of magnetically enhanced reactive ion etching, very similar to the preceding example except for the microwave power, by Murakami et al.[52] and Furuya et al.[53]

Murakami et al.[52] investigated the etching of silicon and polyimide (Kapton H film) with an RIE cathode stage where the temperature could be controlled between 0 and –140°C. To offset the cooling effect on etching, the etch rate was increased by magnetic plasma confinement, a narrow 1-cm gap between the electrodes, and high flow rates. With Si a maximum etch rate of 1.6 μm/min was achieved with normalized side etching (defined as the ratio of the lateral etch to the vertical etch depth) of less than 0.02 at a temperature of –120°C. Etching selectivity for Si over a mask of 0.2-μm Al and 2 μm of Ni went beyond 900 with SF_6 at a power density of 4 W/cm². This work also nicely illustrates the so-called micro-loading effect discussed above. Figure 2.21 shows the relationship between the etch depth in Si and the opening width of the mask pattern.[52] High aspect ratio grooves prevent active species from reaching the bottom of the grooves while reaction products cannot diffuse out from the grooves. For polyimide, the normalized side etch reached less than 0.01 at an etch rate of 0.7 μm/min at –100°C in an oxygen plasma. A 0.3-μm sputtered Al mask was hardly

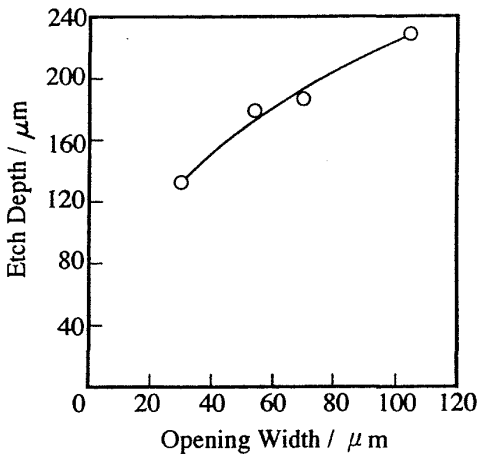

FIGURE 2.21 Micro-loading. Relationship between the etch depth and the opening width of the mask pattern (pressure 2.7 Pa, temperature –120°C, RF-power density 2.0 W/cm²). (From Murakami, K. et al., Cryogenic Dry Etching for High Aspect Ratio Microstructures, *Micro Electromechanical Systems* (Institute of Electrical and Electronics Engineers, Hilton Head, SC 1994), pp. 82–85. With permission.)

etched by the oxygen plasma. The cryogenic temperatures suppress radical reactions on sidewalls while the bottom parts are cleared by ion bombardment.

Furuya et al. at NTT[53] made a fluorinated polyimide micro-grid (Figure 2.22) by using MERIE in an oxygen plasma. The grid elements consist of 18 pole-shaped, gold-covered electrodes connected at the base by a common electrode. Individual poles measure 15 μm in diameter and 100 μm high. The micro-grid is formed by pairs of grid elements facing each other. A voltage can be applied between opposing electrodes of the grid-element pairs. A micro-grid like this, the authors suggest, can be used in an electrostatic ion drag micro-pump and in micro-electrophoresis devices. The fluorinated polyimide used in this study etches rapidly (3 to 5 μm/min) and with high selectivity (2600 over a Ti mask) because MERIE produces a high-density, low energy plasma and because the fluorine in the polimide produces a high concentration of oxygen radicals in the plasma. From the F/C rule, presented above, we predict that a fluorocarbon/oxygen atmosphere leads to a more aggressive and less selective etch. In the current case, by adding the fluorine to the polyimide instead of to the etchant gas, a faster etch rate occurs without losing the high selectivity.

The morphology of the fluorinated polyimide surface, as revealed by atomic force microscopy, is smooth at high etching rate, i.e., at high magnetic fields. The NTT fluorinated polyimide is chemically stable and the fluorine content makes the material extremely transparent, so it can be used to make optical components such as optical waveguides and lenses. The optical quality (and the high aspect ratio of the produced polyimide structures) could make this fabrication technology a competitive technology for many X-ray lithography-based LIGA structures.

Example 4. Combination Wet and Dry Etching

Brugger et al.[54] developed an elegant micromachining process, combining wet and dry etching, to fabricate a meander type cantilever with an integrated high aspect ratio tip for microprobe applications. The crucial part of an atomic force microscope (AFM) or scanning tunneling microscope (STM) microprobe is the tip, which for some applications (e.g., IC trench probing) should have a curvature radius ideally in the range of 50 Å or less, an angle of aperture of about 5°, and a height of 10 μm. The meander structure and integrated tip are presented in Figure 2.23 and the process sequence in Figure 2.24.

First a 30-μm thin Si membrane is anisotropically etched in a double-sided polished 280-μm thick Si wafer (Figure 2.24A). The etching occurs at the back side with 40% KOH at 60°C through an opening etched with BHF in a 1.5 μm thermal oxide. During the KOH etch, the front side is protected by a mechanical chuck. The front side oxide is patterned into a two-step profile using two lithographic and two BHF etching steps. The 0.75-μm thick oxide in the two-step profile acts as the mask for the cantilever and a 1.5-μm thick oxide serves as the mask for the tip (Figure 2.24A). The topside is etched with 15-μm deep RIE using chlorine/fluorine gas mixtures (C_2ClF_5/SF_6) to preshape the cantilevers (Figure 2.23B). By adjusting the RIE parameters, vertical sidewalls of the cantilever can be obtained. The 0.75-μm thick oxide that covered the cantilever is completely removed afterwards and the remaining oxide cap, formerly 1.5 μm and now 0.75 μm thick, serves as a mask for the tip etching. Then a C_2ClF_5/SF_6 gas mixture is applied again to RIE the tip (Figure 2.24C). In the final step (Figure 2.24D) an isotropic HNO_3:HF:CH_3COOH etch lasting 2 minutes forms the tips (using the oxide cap as mask), releases the cantilever by etching through the remaining Si membrane, smoothes the dry-etched rough surface and cleans the remainder of organic photoresist. Mixtures of HNO_3, HF, with CH_3COOH and/or water etch the silicon isotropically and exhibit high etch rates (10 to 300 μm/min). The SiO_2 mask withstands the three successive etch steps: cantilever RIE etching, tip RIE etching, and 1- to 2-min wet etching with HF:HNO_3:CH_3COOH sharpening the tip. Tip heights up to 20 μm with opening angles of approximately 5 to 10° and tip radii estimated to be 40 nm can be obtained this way.

A postoxidation process yielding Si tips with curvature radius of less than 10 nm by several consecutive oxidation and HF etching steps, exploiting an anomaly of the oxidation behavior at regions with high geometric curvature, has been demonstrated by Marcus et al.[55,56] and by our own group at TSDC.[57] By applying this oxidation sharpening technique to the tips produced in the current example, further sharpening would result. A rigid cantilever structure rather than a meander structure as shown in Figure 2.23A would also be of more use in a practical STM.[57]

Example 5. Dry Etching Applications In IC Technology

One area where requirements for high aspect ratio in the IC industry are quite extreme is in the etching of deep Si trenches. Trenches in Si can be used to isolate devices in CMOS and bipolar circuitry. Vertical capacitors and transistors are actually constructed inside these trenches. The latter enables denser packing of devices.[24] A width of 1 μm and a depth of 6 to 15 μm might be required. Care needs to be taken that the mask will survive the etching; for example, a 10-μm trench will need 2 μm of SiO_2 if the selectivity is 5:1. In micromachining, we might want to etch to a depth of several hundreds of microns, requiring even more selectivity. In Table 2.11 the typical requirements for trench etching and selectivity in the IC industry are provided.

TABLE 2.11 Typical Process Specifications for IC Etch Requirements[18]

	16 Mb	256 Mb
Poly-Si vs. SiO_2	>25:1 (must)	120:1 (target)
Gate CD	0.6 μm	0.22 μm
Trench size	0.6 × 3 μm	0.3 × 5 μm
Aspect ratio	3:1	>5:1
SiO_2 vs. poly-Si	>18:1 (must)	>35:1 (target)
Profile control	86°	88°

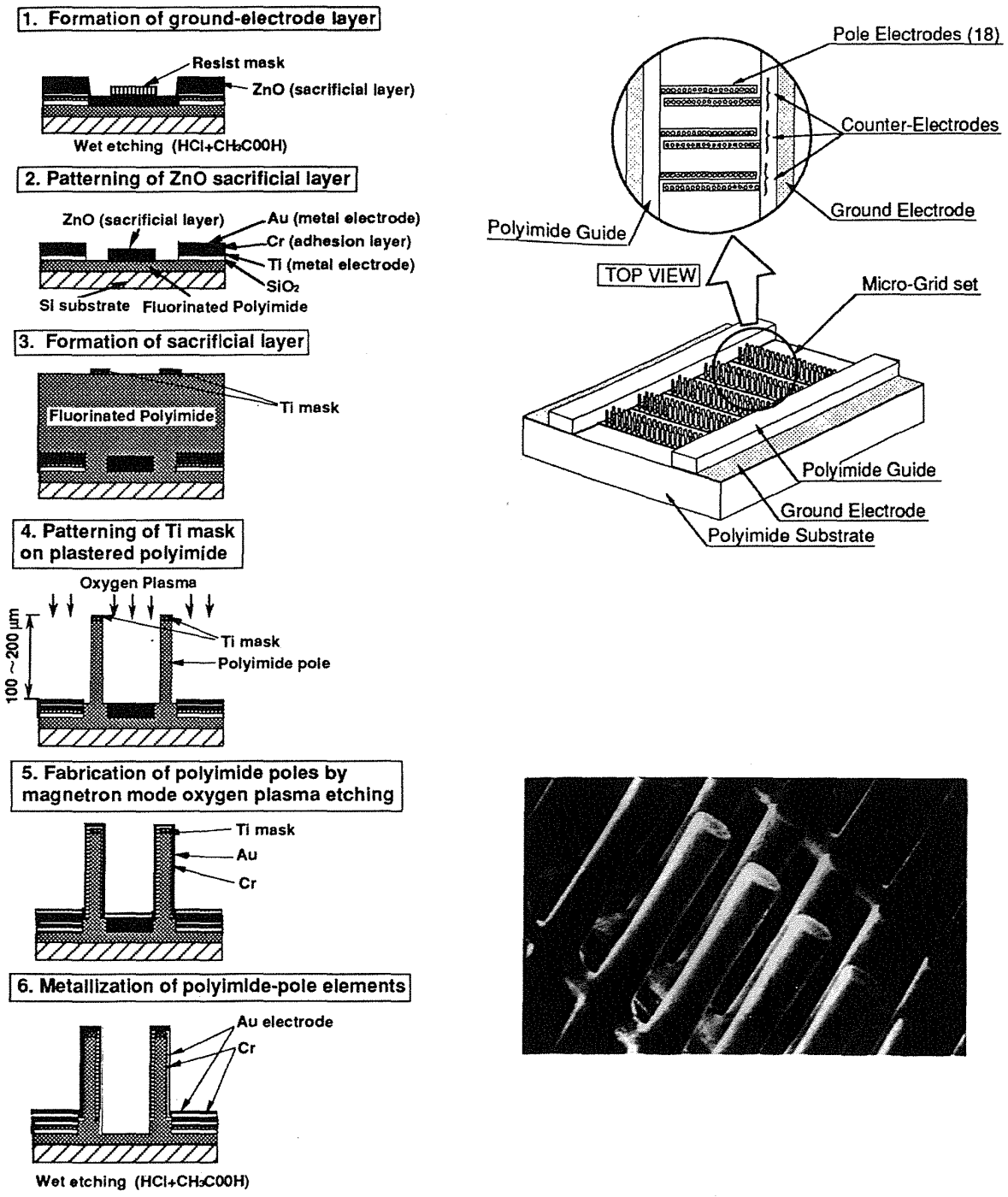

FIGURE 2.22 An array of polyimide posts made by crogenic MERIE. (From Furuya, A. et al., Micro-Grid Fabrication of Fluorinated Polyimide by using magnetically enhanced reactive ion etching (MERIE), *Micro Electromechanical Systems* (Institute of Electrical and Electronics Engineers, Ft. Lauderdale, FL, 1993, pp. 59–64. With permission.)

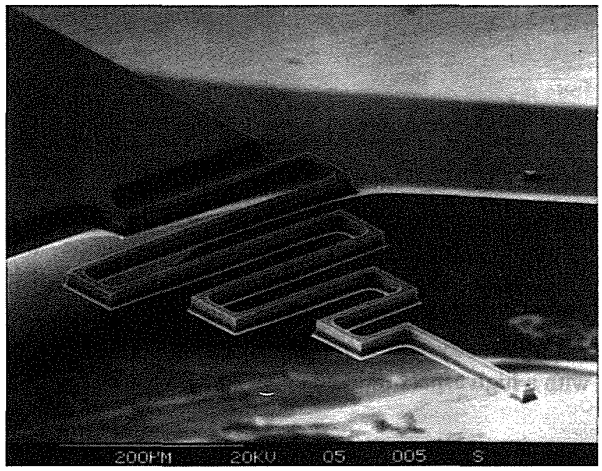

A

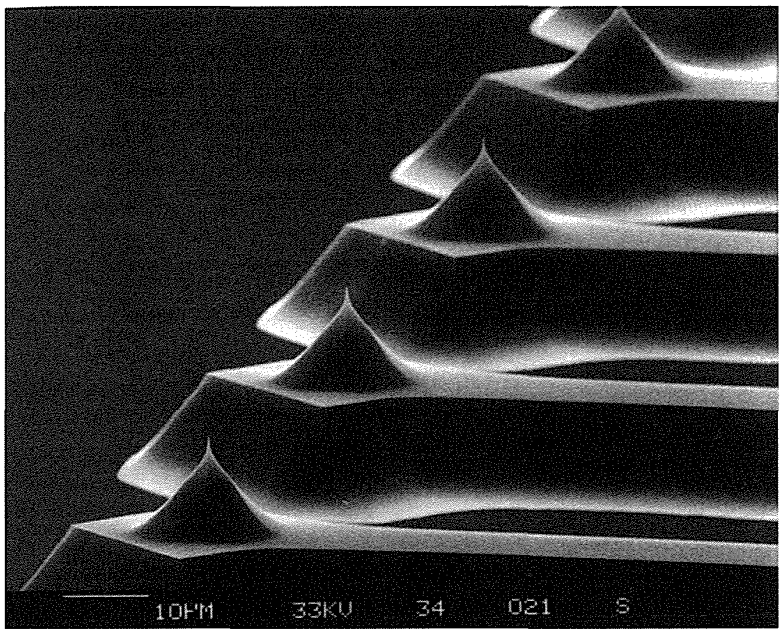

B

FIGURE 2.23 Si-cantilever with square cross-section, designed as a meander shape. (From Brugger, et al., *Sensors & Actuators,* A34, 193–200, 1992. With permission.)

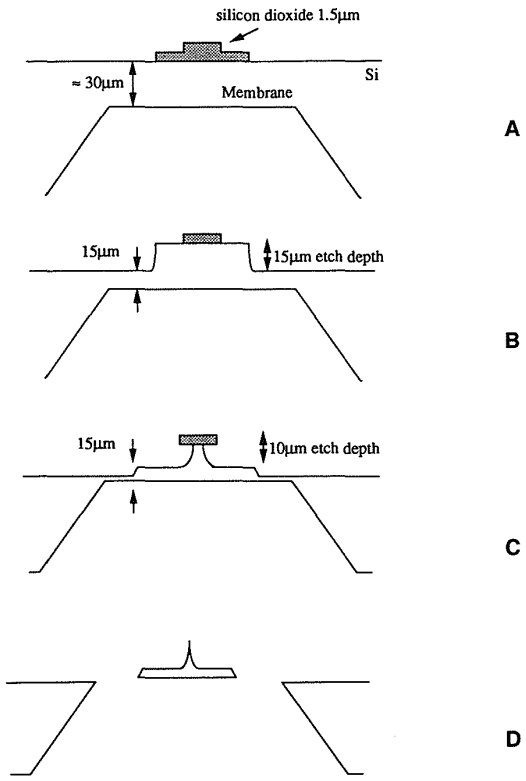

FIGURE 2.24 Fabrication process for a silicon meander beam with integrated tip. (A) Patterning of oxide mask onto pre-processed 30-μm thin membrane. (B) Dry etching of rough cantilever shape. (C) Dry etching the tip. (D) Final wet etching step releasing the cantilever, forming the tip and smoothing the surface. (From Brugger, J. et al., *Sensors & Actuators*, A34, 193–220 (1992). With permission.)

References

1. Kern, W. and C. A. Deckert, "Chemical Etching", in *Thin Film Processes*, Vossen, J. L. and Kern, W., Eds., Academic Press, Orlando, 1978.
2. Jackson, T. N., M. A. Tischler, and K. Wise, D., "An Electrochemical P-N Junction Etch-Stop for The Formation of Silicon Microstructures", *IEEE Electron Device Lett.*, EDL-2, 44-45, 1981.
3. Meek, R. L., "Electrochemically Thinned N/N+ Epitaxial Silicon-Method and Applications", *J. Electrochem. Soc.*, 118, 1240-1246, 1971.
4. Yoshida, T., T. Kudo, and K. Ikeda, "Photo-Induced Preferential Anodization for Fabrication of Monocrystalline Micromechanical Structures", *Proceedings. IEEE Micro Electro Mechanical Systems, (MEMS '92)*, Travemunde, Germany, 1992, p. 56-61.
5. Watanabe, Y., Y. Arita, T. Yokoyama, and Y. Igarashi, "Formation and Properties of Porous Silicon and Its Applications", *J. Electrochem. Soc.*, 122, 1351-1355, 1975.
6. Flamm, D., L., "Feed Gas Purity and Environmental Concerns in Plasma Etching-Part 1", *Solid State Technol.*, October, 49-54, 1993.
7. Pandhumsoporn, T., M. Feldbaum, P. Gadgil, M. Puech, and P. Maquin, "High Etch Rate, Anisotropic Deep Silicon Plasma Etching for the Fabrication of Microsensors", *Micromachining and Microfabrication Process Technology II*, Austin, Texas, USA, 1996, p. 94-102.
8. Manos, D. M. and D. L. Flamm, Eds., *Plasma Etching, an Introduction*, Academic Press, Boston, 1989.
9. Vasile, M. J., C. Biddick, and S. Schwalm, A., "Microfabrication by Ion Milling : The Lathe Technique", *J. Vac. Sci. Technol.*, B12, 2388-2393, 1994.
10. Chryssolouris, G., *Laser Machining*, Springer Verlag, New York, 1991.
11. Moreland, M. A., "Ultrasonic Machining", in *Engineered Materials Handbook*, Schneider, S. J., Ed., ASM International, Metals Park, OH, 1992, p. 359-362.
12. Kalpajian, S., *Manufacturing Processes for Engineering Materials*, Addison-Wesley, Reading, MA, 1984.
13. DeVries, W. R., *Analysis of Material Removal Processes*, Springer-Verlag, New York, 1992.
14. Lehmann, H. W., "Plasma-Assisted Etching", in *Thin Film Processes II*, Vossen, J. L. and Kern, W., Eds., Academic Press, Inc., Boston, 1991, p. 673-748.
15. Singer, P., "Trends in Plasma Sources: The Search Continues", *Semicond. Int.*, July, 52-56, 1992.
16. Singer, H., P., "ECR: Is the Magic Gone?", *Semicond. Int.*, July, 46-48, 1991.
17. Peters, L., "Plasma Etch Chemistry: The Untold Story", *Semicond. Int.*, May, 66-70, 1992.
18. Singer, P., "Meeting Oxide, Poly and Metal Etch Requirements", *Semicond. Int.*, April, 50-54, 1993.
19. Comello, V., "ICP Etchers Start to Challenge ECR", *R&D Magazine*, 79-80, 1993.
20. Flamm, D. L., "Trends in Plasma Sources and Etching", *Solid State Technol.*, March, 47-50, 1991.
21. Burke, R. R. and C. Pomot, "Microwave Multipolar Plasma for Etching and Deposition", *Solid State Technol.*, February, 67-71, 1988.
22. Brodie, I. and J. J. Muray, *The Physics of Microfabrication*, Plenum Press, New York, 1982.
23. Wolf, S. and R. N. Tauber, *Silicon Processing for the VLSI Era*, Lattice Press, Sunset Beach, 1987.
24. Schutz, R. J., "Reactive Plasma Etching", in *VLSI Technology*, Sze, S. M., Ed., McGraw-Hill Book Company, New York, 1988, p. 184-232.
25. Arnold, J. C. and H. H. Sawin, "Charging of Pattern Features During Plasma Etching", *J. Appl. Phys.*, 70, 5314, 1991.
26. Elwenspoek, M., H. Gardeniers, M. de Boer, and A. Prak, "Micromechanics", University of Twente, Report No. 122830, Twente, Netherlands, 1994.
27. Hasper, A., Ph.D. Thesis, University of Twente, 1987.

28. Jansen, H., M. de Boer, and M. Elwenspoek, "The Black Silicon Method VI: High Aspect Ratio Trench Etching for MEMS Applications", *Proceedings. IEEE Micro Electro Mechanical Systems (MEMS '96)*, San Diego, California, USA, 1996, p. 250-257.
29. Flamm, D. L., "Dry Plasma Resist Stripping Part I: Overview of Equipment", *Solid State Technol.*, 35, 37-39, 1992.
30. Hoffman, E., B. Warneke, E. Kruglick, J. Weigold, and K. S. J. Pister, "3D Structures with Piezoresistive Sensors in Standard CMOS", *Proceedings. IEEE Micro Electro Mechanical Systems, (MEMS '95)*, Amsterdam, Netherlands, 1995, p. 288-93.
31. Editorial, Introducing Plasma Jet Etching, IPEC Precision, Inc., 1996.
32. Cooper III, C. B., S. Salimian, and M. E. Day, "Dry Etching for the Fabrication of Integrated Circuits in III-V Compound Semiconductors", *Solid State Technol.*, January, 109-112, 1989.
33. Mogab, C. J., A. C. Adams, and D. L. Flamm, "Plasma Etching of Si and SiO_2-the Effect of Oxygen Additions to CF4 Plasmas", J. Appl. Phys., 49, 3796-803, 1979.
34. Heinecke, R., H., "Control of Relative Etch Rates of SiO2 and Si in Plasma Etching", *Solid State Electron.*, 18, 1146-7, 1975.
35. Flamm, D. L., "Dry Plasma Resist Stripping Part II: Physical Processes", *Solid State Technol.*, 35, 43-48, 1992.
36. Flamm, D., L., "Feed Gas Purity and Environmental Concerns in Plasma Etching-Part 2", *Solid State Technol.*, November, 43-50, 1993.
37. Flamm, D., L., "Dry Plasma Resist Stripping Part III: Production Economics", *Solid State Technol.*, 35, 43-48, 1992.
38. Moreau, W. M., *Semiconductor Lithography*, Plenum Press, New York, 1988.
39. Hess, D. W. and D. B. Graves, "Plasma-Enhanced Etching and Deposition", in *Microelectronics Processing: Chemical Engineering Aspects*, Hess, D. W. and Jensen, K. F., Eds., American Chemical Society, Washington, DC, USA, 1989, p. 377-440.
40. Editorial, "Microwave Plasma Etching System", *Semiconductor International*, 1992, 72-76.
41. Juan, W. H., J. W. Weigold, and S. W. Pang, "Dry Etching and Boron Diffusion of Heavily Doped, High Aspect Ratio Si Trenches", *Proceedings. SPIE-The International Society for Optical Engineering*, Austin, Texas, USA, 1996, p. 45-55.
42. Mucha, J., A. and D. W. Hess, "Plasma Etching", in Introduction to Microlithography, Thompson, L. F., Willson, C. G. and Bowden, M. J., Eds., *ACS Symposium Series*, Washington D.C., 1983.
43. Economou, D., E. S. Aydil, and G. Barna, "In Situ Monitoring of Etching Uniformity in Plasma Reactors", *Solid State Technol.*, 34, 107-111, 1991.
44. Elta, M., "Developing 'Smart' Controllers for Semiconductor Processes", *Res. & Dev.*, February, 69-70, 1993.
45. Duek, R., N. Vofsi, M. Haemek, S. Mangan, and M. Adel, "Improving Plasma Etch With Wafer Temperature Readings", *Semicond. Int.*, July, 208-210, 1993.
46. Mocella, M. T., "The CFC-Ozone Issue in Dry Etch Process Development", *Solid State Technol.*, April, 63-64, 1991.
47. Zhang, L. Z. and N. C. MacDonald, "An RIE Process for Submicron, Silicon Electromechanical Structures", 6th International Conference on Solid-State Sensors and Actuators (Transducers '91), San Francisco, CA, 1991, p. 520-523.
48. Zhang, Z. L. and N. C. MacDonald, "Fabrication of Submicron High-Aspect-Ratio GaAs Actuators", *J. Microelectromech. Syst.*, 2, 66-73, 1993.
49. Yao, J. J., S. C. Arney, and N. C. MacDonald, "Fabrication of High Frequency Two-Dimensional Nanoactuators for Scanned Probe Devices", *J. Microelectromech. Syst.*, 1, 14-22, 1992.
50. Zhang, Z. L., G. A. Porkolab, and N. C. MacDonald, "Submicron, Movable Gallium Arsenide Mechanical Structures and Actuators", *Proceedings. IEEE Micro Electro Mechanical Systems (MEMS '92)*, Travemunde, Germany, 1992, p. 72-77.
51. Juan, W., H., S. W. Pang, A. Selvakumar, M. W. Putty, and K. Najafi, "Using Electron Resonance (ECR) Source to Etch Polyimide Molds For Fabrication of Electroplated Microstructures", Technical Digest of the 1994 Solid State Sensor and Actuator Workshop., Hilton Head Island, SC, 1994, p. 82-85.
52. Murakami, K., Y. Wakabayashi, K. Minami, and M. Esashi, "Cryogenic Dry Etching for High Aspect Ratio Microstructures", *Proceedings. IEEE Micro Electro Mechanical Systems, (MEMS '93)*, Fort Lauderdale, FL, 1993, p. 65-70.
53. Furuya, A., F. Shimokawa, T. Matsuura, and R. Sawada, "Micro-grid Fabrication of Fluorinated Polyimide by Using Magnetically Controlled Reactive Ion Etching (MC-RIE)", *Proceedings. IEEE Micro Electro Mechanical Systems, (MEMS '93)*, Fort Lauderdale, FL, 1993, p. 59-64.
54. Brugger, J., R. A. Buser, and N. F. de Rooij, "Silicon Cantilevers and Tips for Scanning Force Microscopy", *Sensors and Actuators A*, A34, 193-200, 1992.
55. Marcus, B. R. and T. S. Ravi, "Method for Making Tapered Microminiature Silicon Structures", in US Patent 5,201,992, Bell Communications Research, Inc., 1993.
56. Marcus, R. B., T. S. Ravi, T. Gmitter, K. Chin, D. Liu, W. J. Orvis, D. R. Ciarlo, C. E. Hunt, and J. Trujillo, "Formation of Silicon Tips With <1 nm Radius", *Appl. Phys. Lett.*, 56, 236-238, 1990.
57. Editorial, Tips for STM, TSDC (Teknekron), Menlo Park, CA, USA, 1991.

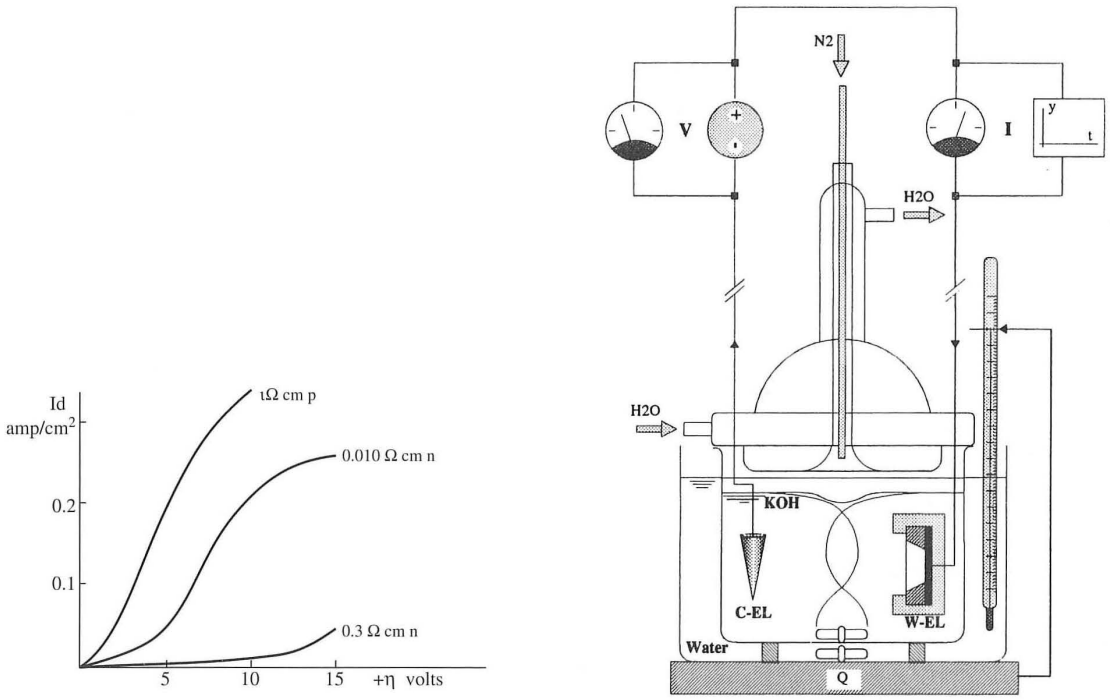

FIGURE 4.25 Electrochemical etching apparatus. W-EL: working electrode (Si), C-EL: counter electrode (e.g. Pt, Q = heat supplied. Inset: Current-voltage (I_d/η) curves in electrochemical etching of Si of various doping. Etch rate dependence on dopant concentration for HF-anodic etching of silicon. (From van Dijk, H.J.A. and de Jonge, J., *J. Electrochem. Soc.*, 117, 553–554, 1970. With permission.)

Anisotropic Etching

Introduction

Anisotropic etchants shape, also 'machine', desired structures in crystalline materials. When carried out properly, anisotropic etching results in geometric shapes bounded by perfectly defined crystallographic planes. Anisotropic wet etching techniques, dating back to the 1960s at the Bell Laboratories, were developed mainly by trial and error. Going over some experimental data, before embarking upon the models, seems fitting. Moreover, we must keep in mind that for higher index planes most models fail.

Figure 4.1 shows a cross-section of a typical shape formed using anisotropic etching. The thinned membranes with diffused resistors could be used for a piezoresistive pressure sensor or an accelerometer. In the usual application, the wafer is selectively thinned from a starting thickness of 300 to 500 μm to form a diaphragm having a final thickness of 10 to 20 μm with precisely controlled lateral dimensions and a thickness control of the order of 1 μm or better. A typical procedure involves the steps summarized in Table 4.8.[42]

The development of anisotropic etchants solved the lateral dimension control lacking in isotropic etchants. Lateral mask geometries on planar photoengraved substrates can be controlled with an accuracy and reproducibility of 0.5 μm or better, and the anisotropic nature of the etchant allows this accuracy to be translated into control of the vertical etch profile. Different etch stop techniques, needed to control the membrane thickness, are available. The invention of these etch stop techniques truly made items as shown in Figure 4.1 manufacturable.

While anisotropic etchants solve the lateral control problem associated with deep etching, they are not without problems. They are slower, even in the fast etching <100> direction, with etch rates of 1 μm/min or less. That means that etching through a wafer is a time-consuming process: to etch through a 300-μm thick wafer one needs 5 hours. They also must be run hot to achieve these etch rates (85 to 115°C), precluding many simple masking options. Like the isotropic etchants, their etch rates are temperature sensitive; however, they are not particularly agitation sensitive, considered to be a major advantage.

Anisotropic Etchants

A wide variety of etchants have been used for anisotropic etching of silicon, including alkaline aqueous solutions of KOH, NaOH, LiOH, CsOH, NH_4OH, and quaternary ammonium hydroxides, with the possible addition of alcohol. Alkaline organics such as ethylenediamine, choline (trimethyl-2-hydroxyethyl ammonium hydroxide) or hydrazine with additives such as pyrocathechol and pyrazine are employed as well. Etching of silicon occurs without the application of an external voltage and is dopant insensitive over several orders of magnitude, but in a curious contradiction to its suggested chemical nature, it has been shown to be bias dependent.[82,83] This contradiction will be explained with the help of the chemical models presented below.

TABLE 4.7 Isotropic and Preferential Defect Etchants and Their Specific Applications

Etchant	Application	Remark
HF: 8 vol%, HNO_3: 75 vol%, and CH_3COOH: 17 vol%	n- and p-type Si, all planes, general etching	Planar etch; e.g., 5 μm/min at 25°C
1 part 49% HF, 1 part of (1.5 *M* CrO_3) (by volume)	Delineation of defects on (111), (100), and (110) Si without agitation	Yang etch[a]
5 vol parts nitric acid (65%), 3 vol parts HF (48%), 3 vol parts acetic acid (96%), 0.06 parts bromine	Polishing etchant used to remove damage introduced during lapping	So-called CP4 etchant; Heidenreich, U.S. Patent 2619414
HF	SiO_2	Si etch rate for 48% HF at 25°C is 0.3 Å/min with n-type 2 Ω cm (111) Si
1HF, 3HNO_3, 10CH_3COOH (by volume)	Delineates defects in (111) Si; etches p^+ or n^+ and stops at p^- or n^-	Dash etch; p- and n-Si at 1300 Å/min in the [100] direction and 46 Å/min in the [111] direction at 25°C[b]
1HF, 1(5 *M* CrO_3) (by volume)	Delineates defects in (111); needs agitation; does not reveal etch pits well on (100) well	Sirtl etch[c]
2HF, 1(0.15 *M* $K_2Cr_2O_7$) (by volume)	Yields circular (100) Si dislocation etch pits; agitation reduces etch time	Secco etch[d]
60 ml HF, 30 ml HNO_3, 30 ml (5 *M* CrO_3), 2 g $Cu(NO_3)_2$, 60 ml CH_3COOH, 60 ml H_2O	Delineates defects in (100) and (111) Si; requires agitation	Jenkins etch[e]
2HF, 1 (1 *M* CrO_3) (by volume)	Delineates defects in (100) Si without agitation; works well on resistivities 0.6–15.0 Ωcm n- and p-types)	Schimmel etch[f]
2HF, 1 (1 *M* CrO_3), 1.5 (H_2O) (by volume)	Works well on heavily doped (100) silicon	Modified Schimmel[f]
$HF/KMnO_4/CH_3COOH$	Epitaxial Si	
H_3PO_4	Si_3N_4	160–180°C
KOH + alcohols	Polysilicon	85°C
$H_3PO_4/HNO_3/HC_2H_3O_2$	Al	40–50°C
HNO_3/BHF/water	Si and polysilicon	0.1 μm min^{-1} for single crystal Si

[a] Yang, K.H., *J. Electrochem. Soc.*, 131, 1140 (1984).

[b] Dash, W.C., *J. Appl. Phys.*, 27, 1193 (1956).

[c] Sirtl, E. and Adler, A., *Z. Metallkd.*, 52, 529 (1961).

[d] Secco d'Aragona, F., *J. Electrochem. Soc.*, 119, 948 (1972).

[e] Jenkins, M.W., *J. Electrochem. Soc.*, 124, 757 (1977).

[f] Schimmel, D.G., *J. Electrochem. Soc.*, 126, 479 (1979).

Alcohols such as propanol and isopropanol butanol typically slow the attack on Si.[84,85] The role of pyrocathechol[86] is to speed up the etch rate through complexation of the reaction products. Additives such as pyrazine and quinone have been described as catalysts by some;[87] but this is contested by other authors.[88] The etch rate in anisotropic etching is reaction rate controlled and thus temperature dependent. The etch rate for all planes increases with temperature and the surface roughness decreases with increasing temperature, so etching at the higher temperatures gives the best results. In practice, etch temperatures of 80 to 85°C are used to avoid solvent evaporation and temperature gradients in the solution.

Arrhenius Plots for Anisotropic Etching

A typical set of Arrhenius plots for <100>, <110>, and <111> silicon etching in an anisotropic etchant (EDP, or ethylene-diamine/pyrocathechol) is shown in Figure 4.26.[90] It is seen that the temperature dependence of the etch rate is quite large and is less dependent on orientation. The slope differs for the different planes, i.e., (111) > (100) > (110). Lower activation energies in Arrhenius plots correspond to higher etch rates. The anisotropy ratio (AR) derived from this figure is

$$AR = (hkl)_1 \text{ etch rate}/(hkl)_2 \text{ etch rate} \qquad 4.29$$

The AR is approximately 1 for isotropic etchants and can be as high as 400/200/1 for (110)/(100)/(111) in 50 wt% KOH/H_2O at 85°C. Generally, the activation energies of the etch rates of EDP are smaller than those of KOH. The (111) planes always etch slowest but the sequence for (100) and (110) can be reversed (e.g., 50/200/8 in 55 vol% ethylenediamine ED/H_2O; (also at 85°C). The (110) Si plane etches 8 times faster and the (111) 8 times slower in KOH/H_2O than in ED/H_2O, while the (110) etches at the same rate.[89] Working with alcohols and other organic additives often changes the relative etching rate of the different Si planes. Along this line, Seidel et al.[88,90] found that the decrease in etch rate by adding isopropyl alcohol to a KOH solution was 20% for <100>, but almost 90% for <110>. As a result of the much stronger decrease of the etch rate on a (110) surface, the etch ratio of (100):(110) is reversed.

TABLE 4.8 Summary of the Process Steps Required for Anisotropic Etching of a Membrane[42]

Process	Duration	Process Temperature (°C)
Oxidation	Variable (hours)	900–1200
Spinning at 5000 rpm	20–30 sec	Room temperature
Prebake	10 min	90
Exposure	20 sec	Room temperature
Develop	1 min	Room temperature
Post-bake	20 min	120
Stripping of oxide (BHF:1:7)	±10 min	Room temperature
Stripping resist (acetone)	10–30 sec	Room temperature
RCA1 (NH_3(25%) + H_2O + H_2O_2:1:5:1)	10 min	Boiling
RCA2 (HCl + H_2O + H_2O_2:1:6:1)	10 min	Boiling
HF-dip (2% HF)	10 sec	Room temperature
Anisotropic etch	From minutes up to one day	70–100

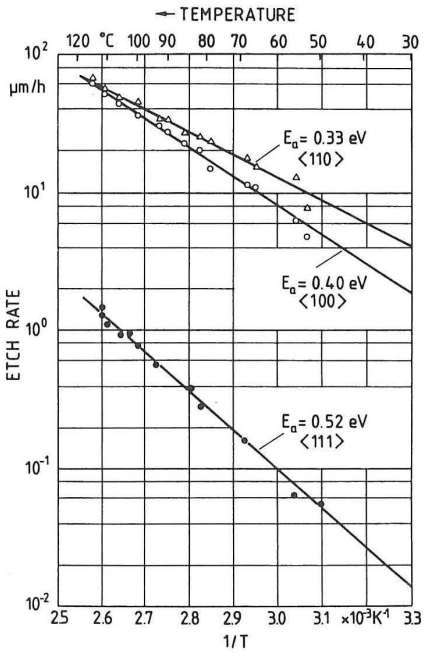

FIGURE 4.26 Vertical etch rates as a function of temperature for different crystal orientations: (100), (110), and (111). Etch solution is EDP (133 ml H_2O, 160 g pyrocatechol, 6 g pyrazine, and 1 l ED). (From Seidel, H. et al., *J. Electrochem. Soc.*, 137, 3612–3626, 1990. With permission.)

Important Anisotropic Etchant Systems

In choosing an etchant, a variety of issues must be considered:

- Ease of handling
- Toxicity
- Etch rate
- Desired topology of the etched bottom surface
- IC-compatibility
- Etch stop
- Etch selectivity over other materials
- Mask material and thickness of the mask

The principal characteristics of four different anisotropic etchants are listed in Table 4.9. The most commonly used are KOH[11-24,88-94,96-98] and ethylene-diamine/pyrocatechol + water (EDP);[86,87,99] hydrazine-water rarely is used.[100,101] More recently, quaternary ammonium hydroxide solutions such as tetraethyl ammonium hydroxide (TEAH) have become more popular.[102,103] Each has its advantages and problems. NaOH is not used much anymore.[95]

Hydrazine-water is explosive at high hydrazine concentrations (rocket fuel) and is a suspected carcinogen. Its use should be avoided for safety reasons. A 50% hydrazine/water solution is stable, though, and, according to Mehregany,[101] excellent surface quality and sharply defined corners are obtained in Si. Also on the positive side, the etchant has a very low SiO_2 etch rate and will not attack most metal masks except for Al, Cu, and Zn. According to Wise, on the other hand, Al does not etch in hydrazine either, but the etch produces rough Si surfaces.[104]

Ethylenediamine in EDP reportedly causes allergic respiratory sensitization, and pyrocathechol is described as a toxic corrosive. The material is also optically dense, making end-point detection harder, and it ages quickly; if the etchant reacts with oxygen, the liquid turns to a red-brown color, and it loses its good properties. If cooled down after etching, one gets precipitation of silicates in the solution. Sometimes one even gets precipitation during etching, spoiling the results. When preparing the solution, the last ingredient added should be the water, since water addition causes the oxygen sensitivity. All of the above make the etchant quite difficult to handle. But, a variety of masking materials can be used in conjunction with this etchant and it is less toxic than hydrazine. No sodium or potassium contamination occurs with this compound and the etch rate of SiO_2 is slow. The ratio of etch rates of Si and SiO_2 using EDP can be as large as 5000:1 (about 2 Å/min of SiO_2 compared to 1 μm/min of Si) which is much larger than the ratio in KOH (about 400:1).[105] Importantly, the etch rate slows down at a lower boron concentration than with KOH. A typical fastest-to-slowest hierarchy of Si etch rates with EDP at 85°C according to Barth[106] is (110) > (411) > (311) > (511) > (211) > (100) > (331) > (221) > (111).

The simple KOH water system is the most popular etchant. A KOH etch, in near saturated solutions (1:1 in water by weight) at 80°C, produces a uniform and bright surface. Nonuniformity of etch rate gets considerably worse above 80°C. Plenty of bubbles are seen emerging from the Si wafer while etching in KOH. The etching selectivity between Si and SiO_2 is not very good in KOH, as it etches SiO_2 too fast. KOH is also incompatible with the IC fabrication process and can cause blindness when it gets in contact with the eyes. The etch rate for low index planes is maximal at around 4 *M* (see Figure 4.27A[41] and Lambrechts et al.[107]). The

TABLE 4.9 Principal Characteristics of Four Different Anisotropic Etchants[a]

Etchant/Diluent/Additives/ Temperature	Etch Stop	Etch Rate (100) (μm/min)	Etch Rate Ratio (100)/(111)	Remarks	Mask (Etch Rate)
KOH/water, isopropyl alcohol additive, 85°C	$B > 10^{20}$ cm^{-3} reduces etch rate by 20	1.4	400 and 600 for (110)/(111)	IC incompatible, avoid eye contact, etches oxide fast, lots of H_2 bubbles	Photoresist (shallow etch at room temperature); Si_3N_4 (not attacked); SiO_2 (28 Å/min)
Ethylene diamine pyrocatechol (water), pyrazine additive, 115°C	$\geq 5 \times 10^{19}$ cm^{-3} reduces the etch rate by 50	1.25	35	Toxic, ages fast, O_2 must be excluded, few H_2 bubbles, silicates may precipitate	SiO_2 (2–5 Å/min); Si_3N_4 (1 Å/min); Ta, Au, Cr, Ag, Cu
Tetramethyl ammonium hydroxide (TMAH) (water), 90°C	$>4 \times 10^{20}$ cm^{-3} reduces etch rate by 40	1	From 12.5 to 50	IC compatible, easy to handle, smooth surface finish, few studies	SiO_2 etch rate is 4 orders of magnitude lower than (100) Si LPCVD Si_3N_4
N_2H_4/(water), isopropyl alcohol, 115°C	$>1.5 \times 10^{20}$ cm^{-3} practically stops the etch	3.0	10	Toxic and explosive, okay at 50% water	SiO_2 (<2 Å/min) and most metallic films; does not attack Al according to some authors[104]

[a] Given the many possible variables, the data in the table are only typical examples.

surface roughness continuously decreases with increasing concentration as can be gleaned from Figure 4.27B. Since the difference in etch rates for different KOH concentrations is small, a highly concentrated KOH (e.g., 7 *M*) is preferred to obtain a smooth surface on low index planes.

Except at very high concentrations of KOH, the etched (100) plane becomes rougher the longer one etches. This is thought to be due to the development of hydrogen bubbles, which hinder the transport of fresh solution to the silicon surface.[108] Average roughness, R_a, is influenced strongly by fluid agitation. Stirring can reduce the R_a values over an order of magnitude, probably caused by the more efficient removal of hydrogen bubbles from the etching surface when stirring.[109] The silicon etch rate as a function of KOH concentration is shown in Figure 4.27C.[90]

Herr[110] found that the high-index crystal planes exhibit the highest etch rates for 6 *M* KOH and that for lower concentrations the etch bottoms disintegrate into microfacets. In 6 *M* KOH, the etch-rate order is (311) > (144) > (411) > (133) > (211) > (122). These authors could not correlate the particular etch rate sequence with the measured activation energies. This is in contrast to lower activation energies corresponding to higher etching rates for low index planes as shown in Figure 4.26. Their results obtained on large open area structures differ significantly from previous ones obtained by underetching special mask patterns. The vertical etching rates obtained here are substantially higher than the underetching rates described elsewhere, and the etch rate sequence for different planes is also significantly different. These results suggest that crevice effects may plan an important role in anisotropic etching.

Besides KOH,[111] other hydroxides have been used, including NaOH,[82,95] CsOH,[112] and NH_4OH.[113] A major disadvantage of KOH is the presence of alkali ions, which are detrimental to the fabrication of sensitive electronic parts. Work is under way to find anisotropic etchants that are more compatible with CMOS processing and that are neither toxic nor harmful. Two examples are ammonium hydroxide-water (AHW) mixtures[113] and tetramethyl ammonium hydroxide-water (TMAHW) mixtures (Tabata et al.[103] and Schnakenberg et al.[113]). TMAHW solutions do not decompose at temperatures below 130°C, a very important feature from the viewpoint of production. They are nontoxic and can be handled easily. TMAHW solutions also exhibit excellent selectivity to silicon oxide and silicon nitride. At a solution temperature of 90°C and 22 wt% TMAH, a maximum (100) silicon etch rate of 1.0 μm/min is observed, 1.4 μm/min for (110) planes (this is higher than those observed with EDP, AHW, hydrazine water, and tetraethyl ammonium hydroxide (TEA), but slower than those observed for KOH) and an anisotropy ratio, AR(100)/(111), of between 12.5 and 50.[114] From the viewpoint of fabricating various silicon sensors and actuators, a concentration above 22 wt% is preferable, since lower concentrations result in larger roughness on the etched surface. However, higher concentrations give a lower etch rate and lower etch ratio (100)/(111). Tabata[115] also studied the etching characteristics of pH-controlled TMAHW. To obtain a low aluminum etching rate of 0.01 μm/min, pH values below 12 for 22 wt% TMAHW were required. At those pH values the Si(100) etching rate is 0.7 μm/min.

Surface Roughness and Notching

Anisotropic etchants frequently leave too rough a surface behind, and a slight isotropic etch is used to 'touch-up'. A distinction must be made between ***macroscopic*** and ***microscopic roughness.*** Macroscopic roughness, also referred to as notching or pillowing, results when centers of exposed areas etch with a seemingly lower average speed compared with the borders of the areas, so that the corners between sidewalls and (100)

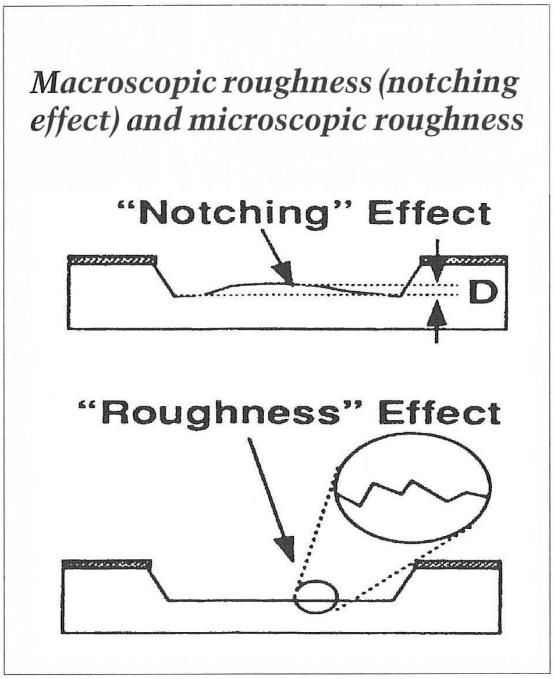

ground planes are accentuated. Membranes or double-sided clamped beams (microbridges) therefore tend to be thinner close to the clamped edges than in the center of the structure. This difference can be as large as 1 to 2 μm, which is quite considerable if one is etching 10 to 20 μm thick structures. Notching increases linearly with etch depth but decreases with higher concentrations of KOH. The microscopic smoothness of originally mirror-like polished wafers can also be degraded into microscopic roughness. It is this type of short-range roughness we referred to in discussing Figure 4.27B above. For more background on metrology techniques to measure surface roughness, see Appendix A.

Masking for Anisotropic Etchants

Etching through a whole wafer (400 to 600 μm) takes several hours (a typical wet anisotropic etch rate being 1.1 μm/min), definitely not a fast process. When using KOH, SiO_2 cannot be used as a masking material for features requiring that long an exposure to the etchants. The SiO_2 etch rate as a function of KOH concentration at 60°C is shown in Figure 4.28. There is a distinct maximum at 35 wt% KOH of nearly 80 nm/hr. The shape of this curve will be explained further below on the basis of Seidel et al.'s model. Experiments have shown that even a 1.5-μm thick oxide is not sufficient for the complete etching of a 380-μm thick wafer (6-hours) because of pinholes in the oxide.[107] The etch rate of thermally grown SiO_2 in KOH-H_2O somewhat varies and apparently depends not only on the quality of the oxide, but also on the etching container and the age of the etching solution, as well as other factors.[44] The Si/SiO_2 selectivity ratio at 80°C in 7 *M* KOH is 30 ± 5. This ratio increases with decreasing temperature; reducing the temperature from 80 to 60°C increases the selectivity ratio from 30 to 95 in 7 *M* KOH.[43] Thermal oxides are under strong compressive stress due to the fact that in the oxide layer one silicon atom takes nearly twice as much space as in single crystalline Si (see also Chapter 3). This might have severe consequences; for example, if the oxide mask is stripped on one side of the wafer, the wafer will bend. Atmospheric pressure chemical vapor deposited (APCVD) SiO_2 tends to exhibit pinholes and etches much faster than thermal oxide. Annealing of APCVD oxide removes the pinholes but the etch rate in KOH remains greater by a factor of 2 to 3 than that of thermal oxide. Low pressure chemical vapor deposited (LPCVD) oxide is a mask material of comparable quality as thermal oxide. The etch rate of SiO_2 in EDP is smaller by two orders of magnitude than in KOH.

For prolonged KOH etching, a high density silicon nitride mask has to be deposited. A low pressure chemical vapor deposited (LPCVD) nitride generally serves better for this purpose than a less dense plasma deposited nitride.[116] With an etch rate of less than 0.1 nm/min, a 400-Å layer of LPCVD nitride suffices to mask against KOH etchant. The etch selectivity Si/Si_3N_4 was found to be better than 10^4 in 7 *M* KOH at 80°C. The nitride also acts as a good ion-diffusion barrier, protecting sensitive electronic parts. Nitride can easily be patterned with photoresist and etched in a CF_4/O_2-based plasma or, in a more severe process, in H_3PO_4 at 180°C (10 nm/min).[117] Nitride films are typically under a tensile stress of about 1×10^9 Pa. If in the overall processing of the devices, nitride deposition does not pose a problem, KOH emerges as the preferential anisotropic wet etchant. For dopant dependent etching, EDP is the better etchant and generally better suited for deep etching since its oxide etch rate is negligible (<5 Å/min).

Oxide and nitride are masking for anisotropic etchants to varying degrees with both mask types being used. When these layers are used to terminate an etch in the [100] direction, a low etch rate of the mask layer allows overetching of silicon, to compensate for wafer thickness variations. A KOH solution etches SiO_2 at a relatively fast rate of 1.4 to 3 nm/min so that Si_3N_4 or Au/Cr must be used as a mask against KOH for deep and long etching.

Backside Protection

In many cases it is necessary to protect the backside of a wafer from an isotropic or anisotropic etchant. The backside is either mechanically or chemically protected. In the mechanical method the wafer is held in a holder, often made from Teflon. The wafer is fixed between Teflon-coated O-rings which are carefully aligned in order to avoid mechanical stress in the wafer. In the chemical method, waxes or other organic coatings are spun onto the back side of the wafer. Two wafers may be glued back to back for faster processing.

Etch Rate and Etch Stops

The Si etch rate, R, as a function of KOH concentration at 72°C, was shown in Figure 4.27C. The etch rate has a maximum at about 20% KOH. The best fit for this experimentally determined etch rate, for most KOH concentrations, is[88,90]

$$R = k[H_2O]^4[KOH]^{\frac{1}{4}} \qquad 4.30$$

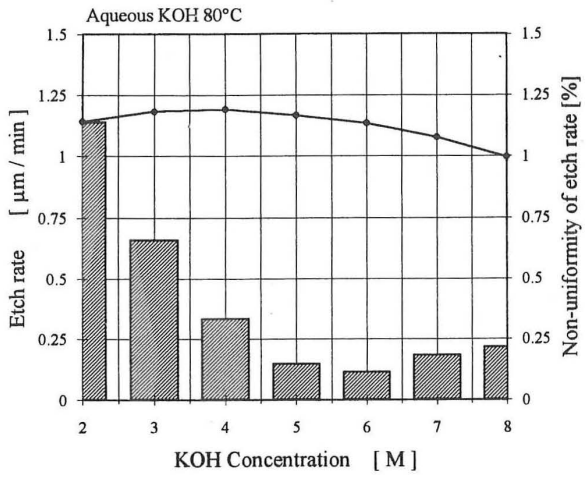

A

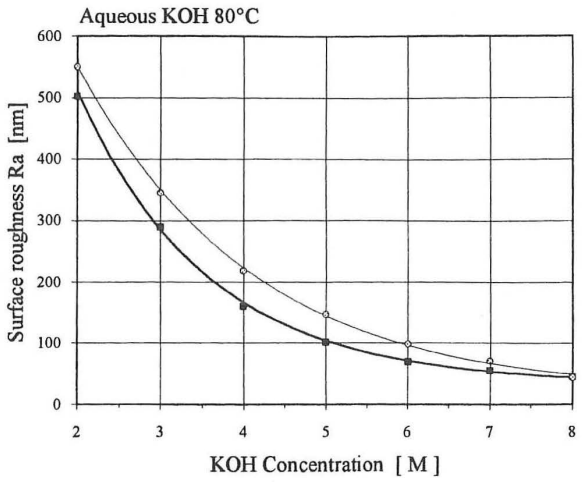

B

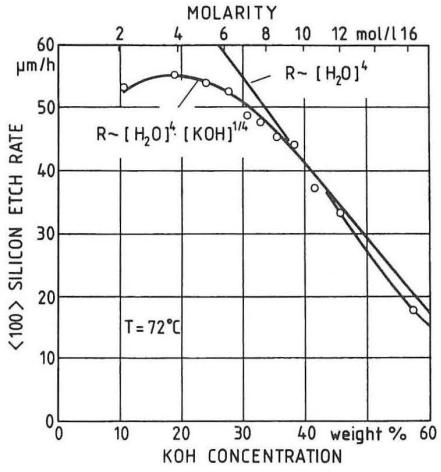

C

FIGURE 4.27 Anisotropic etching of silicon. (A) Silicon (100) etch rate (line) and nonuniformity of etch rate (column) in KOH at 80°C as a function of KOH concentration. The etch rate for all low index planes is maximal at around 4 *M*. (B) Silicon (100) surface roughness (Ra) in aqueous KOH at 80°C as a function of concentration for a 1-hour etch time (thin line) and for an etch depth of 60 µm (thick line). (C) Silicon (100) etch rate as a function of KOH concentration at a temperature of 72°C. (See also Appendix B.) (A and B from Peeters, E., Ph.D. thesis, 1996, KUL, Belgium. With permission. C from Seidel et al., *J. Electrochem. Soc.*, 137, 3612–3626, 1990. With permission.)

Any model of anisotropic etching will have to explain this peculiar dependency on the water and KOH concentration, as well as the fact that all anisotropic etchant systems of Table 4.9 exhibit drastically reduced etch rates for high boron concentrations in silicon ($\geq 5 \times 10^{19}$ cm^{-3} solid solubility limit). Other impurities (P, Ge) also reduce the etch rate, but at much higher concentrations (see Figure 4.29[90]). Boron typically is incorporated using ion implantation (thin layers) or liquid/solid source deposition (thick layers > 1 µm). These doped layers are used as very effective etch stop layers (see below). Hydrazine or EDP, which display a smaller (100) to (111) etch rate ratio (~ 35) than KOH, exhibit a stronger boron concentration dependency. The etch rate in KOH is reduced by a factor of 5 to 100 for a boron concentration larger than 10^{20} cm^{-3}. When etching in EDP, the factor climbs to 250.[118] With TMAHW solutions, the Si etch rate decreases to 0.01 µm/min for boron concentrations of about 4×10^{20} cm^{-3}.[119] The mechanism eludes us, but Seidel et al.'s model (see below) gives the most plausible explanation for now. Some of the different mechanisms to explain etch stop effects that have been suggested follow:

1. Several observations suggest that doping leads to a more readily oxidized Si surface. Highly boron- or phosphorus-doped silicon in aqueous KOH spontaneously can form a thin passivating oxide layer.[120,121] The boron-oxides and -hydroxides initially generated on the silicon surface are not soluble in KOH or EDP etchants.[34] The substitutional boron creates local tensile stress in the silicon, increasing the bond strength so that a passivating oxide might be more readily formed at higher boron concentrations. Boron-doped silicon has a high defect density (slip planes), encouraging oxide growth.
2. Electrons produced during oxidation of silicon are needed in a subsequent reduction step (hydrogen evolution in Reaction 4.2). When the hole density passes 10^{19} cm^{-3} these electrons combine with holes instead, thus

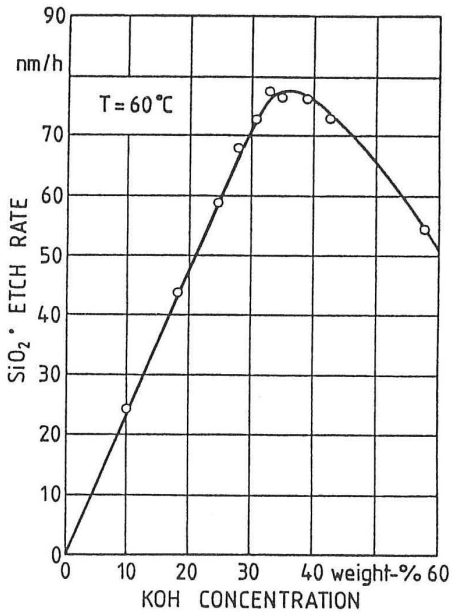

FIGURE 4.28 The SiO_2 etch rate in nm/hr as a function of KOH concentration at 60°C. (From Seidel, H. et al., *J. Electrochem. Soc.*, 137, 3612–3626, 1990. With permission.)

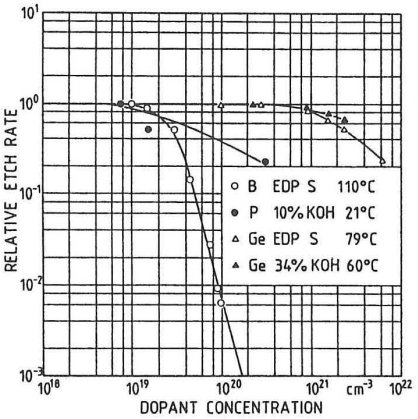

FIGURE 4.29 Relative etch rate for (100) Si in EDP and KOH solutions as a function of concentration of boron, phosphorus, and germanium. (From Seidel, H. et al., *J. Electrochem. Soc.*, 137, 3626–3632, 1990. With permission.)

stopping the reduction process.[121] Seidel et al.'s model follows this explanation (see below).

3. Silicon doped with boron is under tension as the smaller boron atoms enter the lattice substitutionally. The large local tensile stress at high boron concentration makes it energetically more favorable for the excess boron (above 5×10^{19} cm^{-3}) to enter interstitial sites. The strong B-Si bonds bind the lattice rigidly. With high enough doping the high binding energy can stop etching.[34] This hypothesis is similar to item 1, except that no oxide formation is invoked.

In what follows we review the results of some typical anisotropic etching experiments.

Anisotropically Etched Structures

Examples

In Figure 4.30 we compare a wet isotropic etch (a) with examples of anisotropic etches (b to e). In the anisotropic etching examples, a square (b and c) and a rectangular pattern (d) are defined in an oxide mask with sides aligned along the <110> directions on a <100>-oriented silicon surface. The square openings are precisely aligned (within one or two degrees) with the <110> directions on the (100) wafer surface to obtain pits that conform exactly to the oxide mask rather than undercutting it. Most (100) silicon wafers have a main flat parallel to a <110> direction in the crystal, allowing for an easy alignment of the mask (see Figure 4.5). Etching with the square pattern results in a pit with well-defined {111} sidewalls (at angles of 54.74° to the surface) and a (100) bottom.

The dimensions of the hole at the bottom of the pit, as we saw above, are given by Equation 4.2. The larger the square opening in the mask, the deeper the point where the {111}

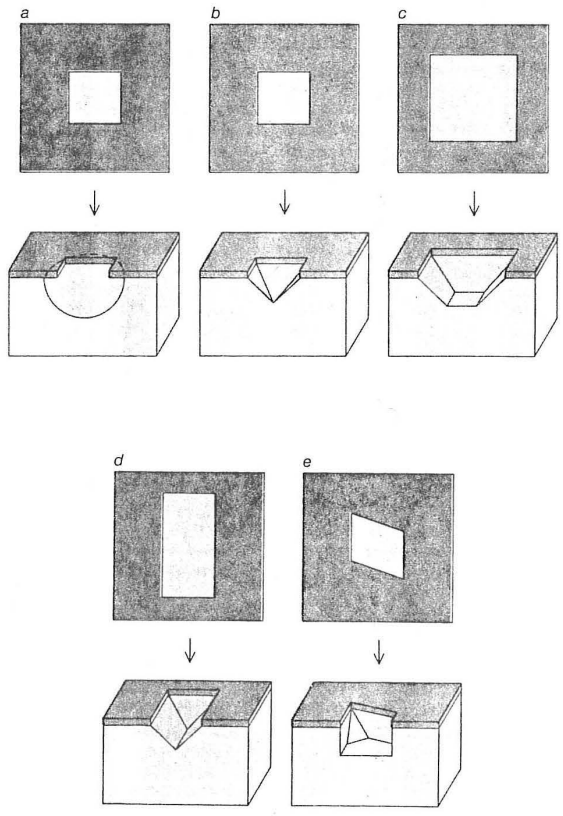

FIGURE 4.30 . Isotropic and anisotropic etched features in <100> and <110> wafers. (a) isotropic etch; (b) to (e) anisotropic etch. (a) to (d): <100> oriented wafers and (e): <110> oriented wafer.

sidewalls of the pit intersect. If the oxide opening is wide enough, i.e., $L > \sqrt{2}\,T$ (with $T = 600\ \mu m$ for a typical 6-in. wafer, this means $L_1 > 849\ \mu m$), the {111} planes do not intersect within the wafer. The etched pit in this particular case extends all the way through the wafer, creating a small square opening on the bottom surface. As shown in Figure 4.30 (b to d), no under-etching of the etch mask is observed due to the perfect alignment of the concave oxide mask opening with the <110> direction. In Figure 4.30a, an undercutting isotropic etch (acidic) is shown. Misalignment in the case of an anisotropic etch still results in pyramidical pits, but the mask will also be severely undercut. A rectangular pattern aligned along the <110> directions on a <100> wafer leads to ***long V-shaped grooves*** (see Figure 4.30d) or an open slit, depending on the width of the opening in the oxide mask.

Using a properly aligned mask on a <110> wafer, holes with four vertical walls ({111} planes) result (see Figure 4.30e and Figure 4.31 A and C). Figure 4.31B shows that a slight mask misorientation leads to all skewed sidewalls. A U-groove based on a rectangular mask with the long sides along the <111> directions and anisotropically etched in (110) silicon has a complex shape delineated by six {111} planes, four vertical and two slanted (see Figure 4.31D). Before emergence of {111} planes, the U-groove is defined by four vertical (111) planes and a horizontal (110) bottom. Self-stopping occurs when the tilted end planes intersect at the bottom of the groove. It is easy to etch long, narrow U-grooves very deeply into a <110> silicon wafer. However, it is impossible to etch a short, narrow U-groove deeply into a slice of silicon,[44] because the narrow dimension of the groove is quickly limited by slow-etching {111} planes that subtend an angle of 35° to the surface and cause etch termination. At a groove of length L = 1 mm on the top surface, etching will stop when it reaches a depth of 0.289 mm, i.e., $D_{max} = L/2\sqrt{3}$ For very long grooves, the tilted end planes are too far apart to intersect in practical cases, making the end effects negligible compared to the remaining U-shaped part of the groove.

A laser can be used to melt or 'spoil' the shallow (111) surfaces, making it possible to etch deep vertical-walled holes through a (110) wafer as shown in Figure 4.32A.[122-124] The technique is illustrated in Figure 4.32B. The absorbed energy of a Nd:YAG laser beam causes a local melting or evaporation zone enabling etchants to etch the shallow (111) planes in the line-of-sight of the laser. Etching proceeds till 'unspoiled' (111) planes are encountered. Some interesting resulting possibilities, including partially closed microchannels, are shown in Figure 4.32C.[122,125] Note that with this method it is possible to use <111> wafers for micromachining. The light of the Nd:YAG laser is very well suited for this micromachining technique due to the 1.17-eV photon energy, just exceeding the band gap energy of Si. Details on this laser machining process can be found, for example, in Alavi et al.[40,125]

Especially when machining surface structures by undercutting, the orientation of the wafer is of extreme importance. Consider, for example, the formation of a bridge in Figure 4.33A.[123] When using a (100) surface, a suspension bridge cannot form across the etched V-groove; two independent truncated V-grooves flanking a mesa structure result instead. To form a suspended bridge it must be oriented away from the <110> direction. This in contrast with a (110) wafer where a

Long V-shaped grooves in a (100) Si wafer

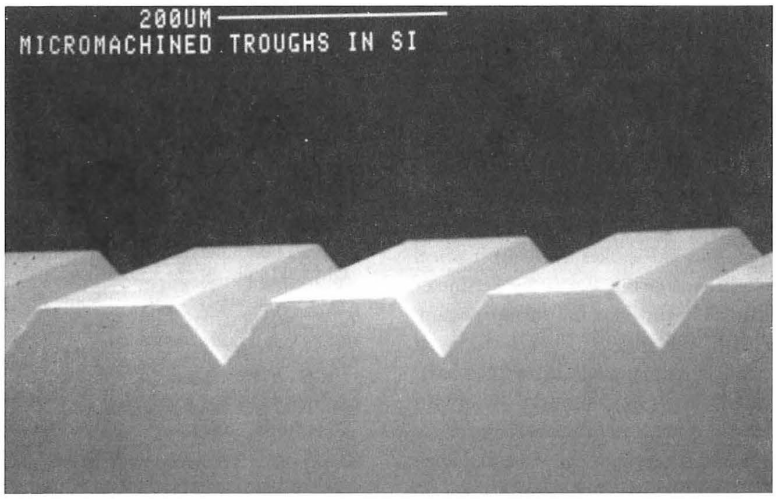

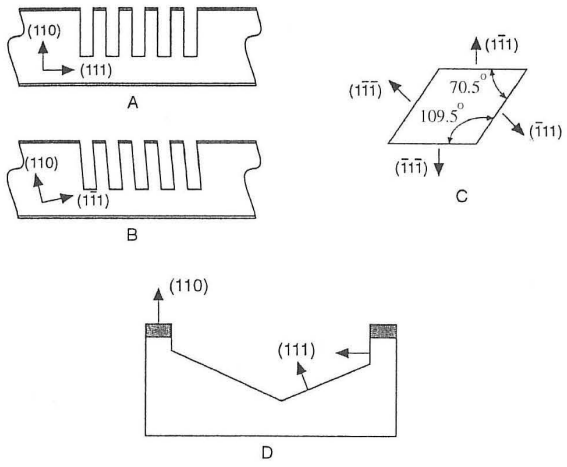

FIGURE 4.31 Anisotropic etching of <110> wafers. (A) Closely spaced grooves on correctly oriented (110) surface. (B) Closely spaced grooves on misoriented <110> wafer. (C) Orientations of the {111} planes looking down on a (110) wafer. (D) Shallow slanted (111) planes eventually form the bottom of the etched cavity.

microbridge crossing a V-groove with a 90° angle will be undercut. Convex corners will be undercut by etchant, allowing formation of cantilevers as shown in Figure 4.33B. The diving board shown forms by undercutting starting at the convex corners.

To create vertical (100) faces, as shown in Figure 4.10, in general only KOH works (not EDP or TMAHW) and it has to happen in high-selectivity conditions (low temperature, low concentration: 25 wt% KOH, 60°C). Interestingly, high concentration KOH (45 wt%) at higher temperatures (80°C) produces a smooth sidewall, controllable and repeatable at an angle of 80°. EDP produces 45° angled planes and TMAHW usually makes a 30° angle.[120]

Alignment Patterns

When alignment of a pattern is critical, pre-etch alignment targets become useful to delineate the planes of interest since the wafer flats often are aligned to ±1° only. In order to find the proper alignment for the mask, a test pattern of closely spaced lines can be etched (see Figure 4.34). The groove with the best vertical walls determines the proper final mask orientation. Along this line, Ciarlo[127] made a set of lines of 3 mm long and 8 μm wide, fanning out like spokes in a wagon wheel at angles 0.1° apart. This target was printed near the perimeter of the wafer and then etched 100 μm into the surface. Again, by evaluating the undercut in this target the correct crystal direction could be determined. Alignment with better than 0.05° accuracy was accomplished this way. Similarly, to obtain detailed experimental data on crystal orientation dependence of etch rates, Seidel et al.[90] used a wagon-wheel or star-shaped mask (e.g., made from CVD-Si_3N_4; SiH_4 and NH_3 at 900°C), consisting of radially divergent segments with an angular

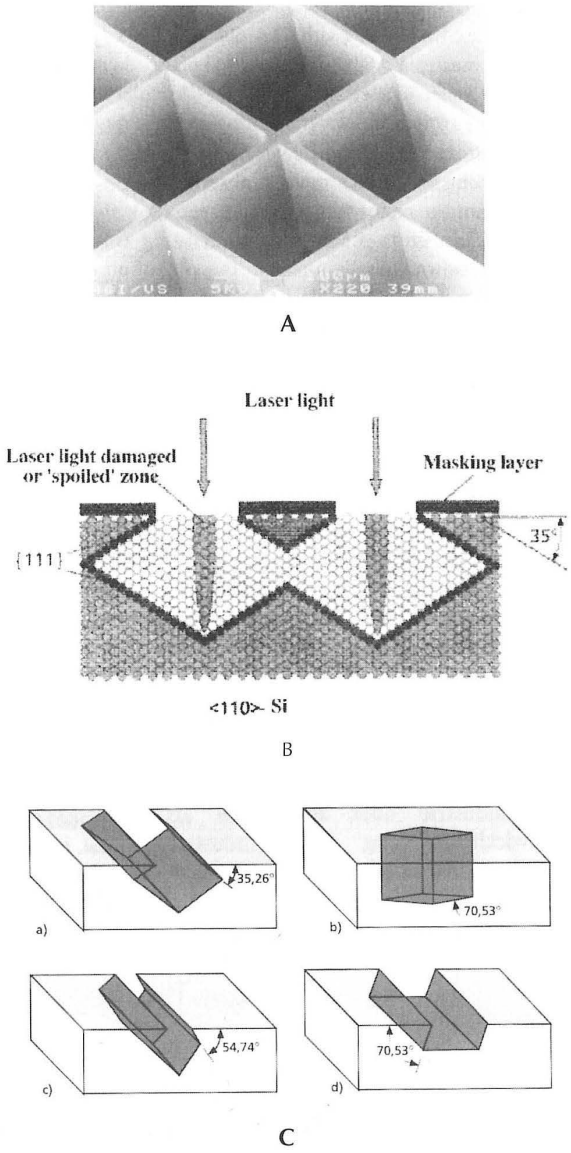

FIGURE 4.32 Laser/KOH machining. (A) Holes through a (110) Si wafer created by laser spoiling and subsequent KOH etching. The two sets of (111) planes making an angle of 70° are the vertical walls of the hole. The (111) planes making a 35° angle with the surface tend to limit the depth of the hole but laser spoiling enables one to etch all the way through the wafer (see also B (c)). (B) After laser spoiling, the line-of-sight (111) planes are spoiled and etching proceeds until unspoiled (111) planes are reached. (C) Some of the possible features rendered by laser spoiling. (From Schumacher, A. et al., *Technische Rundschau*, 86, 20–23, 1994. With permission.)

separation of one degree. Yet finer 0.1° patterns were made around the principal crystal directions. The etch pattern emerging on a <100> oriented wafer covered with such a mask is shown in Figure 4.35A. The blossom-like figure is due to the total underetching of the passivation layer in the vicinity of the

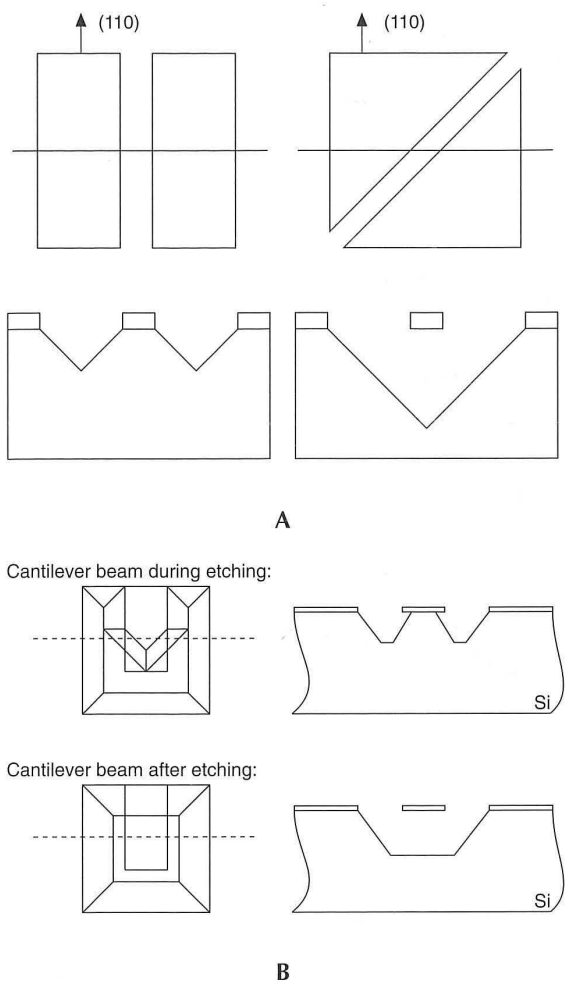

FIGURE 4.33 How to make (A) a suspension bridge from a (100) Si wafer and (B) a diving board from a (110) Si wafer.[123]

center of the wagon wheel, leaving an area of bare exposed Si. The radial extension of the bare Si area depends on the crystal orientation of the individual segments, leading to a different amount of total underetching. The observation of these blossom-like patterns was used for qualitative guidance of etching rates only. In order to establish quantitative numbers for the lateral etch rates, the width, w, of the overhanging passivation layer was measured with an optical line-width measurement system (see Figure 4.35B). Laser beam reflection was used to identify the crystal planes and ellipsometry was used to monitor the etching rate of the mask itself. Lateral etch rates determined in this way on <100>- and <110>-oriented wafers at 95°C in EDP (470 ml water, 1 1 ED, 176 g pyrocatechol) and at 78°C in a 50% KOH solution are shown in Figure 4.36. Etch-rates shown are normal to the actual crystal surface and are conveniently described in a polar plot in which the distance from the origin to the polar plot surface (or curve in two dimensions) indicates the etch rate for that particular direction. Note the deep minima at the {111} planes. It can also be seen that in KOH the peak etch rates are more pronounced. A further difference is that with EDP the minimum at {111} planes is steeper than with KOH. For both EDP and KOH, the etch rate depends linearly on misalignment. All the above observations have important consequences for the interpretation of anisotropy of an etch (see below). The difference between KOH and EDP etching behavior around the {111} minima has the direct practical consequence that it is more important for etching in EDP to align the crystallographic direction more precisely than in KOH.[42]

When determining etch rates without using underetching masks but by using vertical etching of beveled silicon samples, results are quite different than when working with masked silicon.[110] The etch rates on open areas of beveled structures are much larger than in underetching experiments with masked silicon, and different crystal planes develop. Herr et al. conclude that crevice effects may play an important role in anisotropic etching. Elwenspoek et al.'s model,[128,129] analyzed below, is the only model which predicts such a crevice effect. He explains why, when etchants are in a small restricted crevice area and are not refreshed fast enough, etching rates slow down and increase anisotropy.

Chemical Etching Models

Introduction

Lots of conflicting data exist in the literature on the anisotropic etch rates of the different Si planes, especially for the higher index planes. This is not too surprising, given the multiple parameters influencing individual results: temperature, stirring, size of etching feature (i.e., crevice effect), KOH concentration, addition of alcohols and other organics, surface defects, complexing agents, surfactants, pH, cation influence, etc. More rigorous experimentation and standardization will be needed, as well as better etching models, to better understand the influence of all these parameters on etch rates.

Several chemical models explaining the anisotropy in etching rates for the different Si orientations have been proposed. Presently we will list all of the proposed models and compare the two most recent and most detailed models (the one by Seidel et al.[88,90] and the one by Elwenspoek et al.[128,129]). Different Si crystal properties have been correlated with the anisotropy in silicon etching.

1. It has been observed that the {111} Si planes present the highest density of atoms per cm^2 to the etchant and that the atoms are oriented such that ***three bonds are below the plane.*** It is possible that these bonds become chemically shielded by surface bonded (OH) or oxygen, thereby slowing the etch rate.
2. It also has been suggested that etch rate correlates with available bond density, the surfaces with the highest bond density etching faster.[85] The available bond densities in Si and other diamond structures follow the sequence 1:0.71:0.58 for the {100}:{110}:{111} surfaces. However, Kendall[44] commented that bond density alone is an unlikely explanation because of the magnitude of etching

Appendix E

Glossary*

Abrasive: A hard and wear-resistant material (such as a ceramic) used to wear, grind, or cut away other material.

Accuracy: The degree of correctness with which the measuring system yields the "true value" of a measured quantity, where the "true value" refers to an accepted standard, such as a standard meter or volt. Typically described in terms of a maximum percentage of deviation expected based on a full-scale reading.

Affinity: A thermodynamic measurement of the strength of binding between molecules, say between an antibody and antigen. Each antibody/antigen pair has an association constant, K_a, expressed in L/mol.

Algorithm: A set of well-defined mathematical rules or operations for solving a problem in a finite number of steps.

AM 1: The air mass 1 spectrum of a light source is equivalent to that of sunlight at the earth's surface when the sun is at zenith.

Ampere (amp) [A]: Measure of electric current: 1A = 1 coulomb/second.

Amperometric Sensor: Amperometric sensors involve a heterogeneous electron transfer as a result of an oxidation/reduction of an electro-active species at a sensing electrode surface. A current is measured at a certain imposed voltage of the sensing electrode with respect to the reference electrode. Analytical information is obtained from the current-concentration relationship at that given applied potential.

Analyte: A chemical species targeted for qualitative or quantitative analysis.

Angstrom [Å]: Measure of length: 1 Å= 10^{-10} m.

Anisotropic: Exhibiting different values of a property in different crystallographic directions.

Anneal: Heat process used to remove stress, crystallize or render deposited material more uniform.

Anode: The electrode in an electrochemical cell or galvanic couple that experiences oxidation, or gives up electrons.

Arrhenius equation: The equation representing the rate constant as $k = Ae^{E_a/RT}$ where A represents the product of the collision frequency and a steric factor, and $e^{-E_a/RT}$ is fraction of collisions with sufficient energy to produce a reaction.

ASIC: Application-specific integrated circuit; an IC designed for a custom requirement.

Atomic mass unit (a.m.u.): A unit of mass used to express relative atomic masses. It is equal to 1/12 of the mass of an atom of the isotope carbon-12 and is equal to 1.66033×10^{-27}.

Atomic number (also proton number Z): The number of protons within the atomic nucleus of a chemical element.

Atomic weight: The weighted average mass of the atoms in a naturally occuring element.

Austenite: Face-centered cubic iron; also iron and steel alloys that have the FCC crystal structure.

Avogadro's number: The number of atoms in exactly 12 grams of pure ^{12}C, equal to 6.022×10^{12}.

Band gap energy (E_g): For semiconductors and insulators, the energies that lie between the valence and conduction bands; for intrinsic materials, electrons are forbidden to have energies within this range.

Bandwidth: The range of frequencies over which the measurement system can operate within a specified error range.

BAW: Bulk acoustic wave.

Bilayer lipid membrane (BLM): The structure found in most biological membranes, in which two layers of lipid molecules are so arranged that their hydrophobic parts interpenetrate, whereas their hydrophilic parts form the two surfaces of the bilayer.

Binary: Numbering system based on powers of 2 using only the digits 0 and 1, called "bits".

Biosensor: The term " biosensor" is a general designation that denotes either a sensor to detect a biological substance or a sensor which incorporates the use of biological molecules such as antibodies or enzymes. Biosensors are a subcategory of chemical sensors.

Bipolar-junction transistor: Transistor with n-type and p-type semiconductors having base-emitter and collector-base junctions.

Bit: see binary.

Body-centered cubic (BCC): A common crystal structure found in some elemental metals. Within the cubic unit cell, atoms are located at corner and cell center positions.

Brazing: A metal joining technique that uses a molten filler metal alloy having a melting temperature greater than about 425°C (800°F).

Breakdown: Failure of a material resulting from an electrical overload. The resulting damage may be in the form of thermal damage (melting or burning) or electrical damage (loss of polarization in piezoelectric materials).

Bus: Transmission medium for electrical or optical signals that perform a particular function, such as computer control.

* See also Lexicon of Semiconductor Terms: http://rel.semi.harris.com/docs/lexicon-old/

Intrinsic: Characterizes pure undoped semiconductor; electrical conductivity depends only on temperature and the band gap energy.

I/O: Input/output information transfer between computer and peripherals such as keyboard or printer.

Ionic bond: A coulombic interatomic bond existing between two adjacent and oppositely charged ions.

Ionophore: A macro-organic molecule capable of specifically solubilizing an inorganic ion of suitable size in organic mediums.

ISE (Ion selective electrode): Ions in solution are quantified by measuring the change in voltage (i.e. potentiometric) resulting from the distribution of ions (by ion exchange controlled by the ion exchange current i_o) between a sensing membrane (the ion selective membrane) and the solution. This potential is measured at zero current with respect to a reference electrode which is also in contact with the solution. The potential measured is proportional to the logarithm of the analyte concentration. The oldest and best known ISE is the pH sensor based on a glass membrane. More recently, polymeric membranes have been formed incorporating ionophores (see ionophore) rendering the membrane specific to certain ions only.

ISFET: Ion Sensitive Field Effect Transistor: a logical extension of ISE's. They can be conceptualized by imagining that the lead from an ion-selective electrode, attached via a cable to a FET in the high impedance input stage of a voltmeter, is made shorter until no lead exists and the selective membrane is attached directly to the FET. For an ISFET, the property measured is the lateral conductivity between two opposing doped regions (the source and drain) surrounding the active area. The underlying change is a change in flat-band voltage.

Isomorphous: Having the same structure. In the phase diagram sense, isomorphicity means having the same crystal structure or complete solid solubility for all compositions.

Isothermal: At a constant temperature. In an isothermal process heat is, if necessary, supplied or removed from the system at just the right rate to maintain constant temperature.

Isotropic: Having identical values of a property in all crytallographic directions.

Kilobyte (kB): 2^{10} (= 1024, or about one thousand) bytes of information.

Kilohertz (kHz): One thousand cycles per second (see also "frequency").

Kinetic molecular theory: A model that assumes that an ideal gas is composed of tiny particles (molecules) in constant motion.

Label or marker: A problem endemic in immunoassays is the absence of a chemical signal created by the antibody-antigen binding, in contrast with an enzyme-substrate binding reaction which produces a chemical reaction product. As a result of this absence, the use of a label or marker is usually required to detect the bound antibody-antigen complex. Several markers have been established for use in immunoassays. Examples of such markers are:

- Particles (e.g. latex, gold particles, erythrocytes)
- Metal and dye sols (e.g. Au, Palanil® Luminous Red G)
- Chemiluminescent and bioluminescent compounds (e.g. Luciferase/luciferins, Luminol and derivatives, Acridinium esters, Peroxidase)
- Electrochemical active species (ions, redox species, ionophores)
- Fluorophores (e.g. Dansyl chloride DANS, Rare earth metal chelates, Umbelliferones)
- Chromophores
- Enzymes (e.g. Alkaline phosphatase, β-D-Galactosidase, Peroxidase), substrates, cofactors
- Liposomes
- Iodine-125, tritium, ^{14}C, ^{75}Se, ^{57}Co.

Laser: Light Amplification by the Stimulated Emission of Radiation — quantum device that produces coherent light.

Laser trimming: A method for adjusting the value of thin- or thick-film resistors by using a computer-controlled laser system.

LCD: Liquid Crystal Display — display device employing light source and electrically alterable optically active thin film.

LED: Light-Emitting diode — semiconducting diode that produces visible or infrared radiation.

Leakage: The loss of all or parts of a useful agent, as of the electric current that flows through an insulator or the magnetic flux that passes outside useful flux circuits.

Lewis acid: An electron-pair acceptor.

Lewis base: An electron-pair donor.

Life (lifetime): The length of time the sensor can be used before its performance changes.

Linear coefficient of thermal expansion: see thermal expansion coefficient, linear.

Linearity: The degree to which the calibration curve of a device conforms to a straight line.

Limit of detection: The smallest measurable input. This differs from resolution, which defines the smallest measurable change in input. For a temperature measurement, this would provide an indication of the lowest temperature a sensor could generate an output in response to.

Lipids: Water-insoluble substances than can be extracted from cells by nonpolar organic solvents.

Luminescence: defined as the mission of light from a substance in an electronically excited state. Depending on whether the excited state is singlet or triplet, the emission is called fluorescence (less than one second decay) or phosphorescence (longer than 1 second decay). Depending on the source, molecules get the needed extra energy from different types of luminescence are distinguished: radioluminescence, photoluminescence (in the same category are fluorescence and phosphorescence), chemiluminescence and bioluminescence, electrochemiluminescence, sonochemi-luminescence and thermoluminescence.

Magnetic field strength (designated by H) [A/m]: Magnetic field produced by a current, independent of the presence of magnetic material. The units of H are ampere-turns per meter, or just amperes per meter.

Magnetic flux density or magnetic induction (designated by B): The magnetic field produced in a substance by an